

# Tests for a Strong Electroweak Sector at Future $e^+e^-$ High Energy Colliders

Daniele Dominici

Dipartimento di Fisica, Università di Firenze and Sezione di Firenze, INFN  
largo E.Fermi 2, I-50125 Firenze, Italy

## Abstract

The study of the scattering at high energy of the gauge bosons  $W$  and  $Z$ , in particular longitudinally polarized  $W$  and  $Z$ , can clarify the mechanism of spontaneous symmetry breaking in the Standard Model of the electroweak interactions. Different models of strong electroweak sector, based on the effective lagrangian approach are briefly reviewed. They include models with no resonance, with scalar resonance, additional vector and axial-vector resonances. The effective Lagrangians are derived from the chiral symmetry of the symmetry breaking sector. Limits on these models from existing measurements, mainly LEP and Tevatron, are considered. We study also direct and indirect effects of the new interactions at high energy future  $e^+e^-$  linear colliders, through  $WW$  scattering and the direct production of these new vector gauge bosons.

# Contents

<b>1</b>	<b>Introduction</b>	<b>4</b>
<b>2</b>	<b>Electroweak symmetry breaking</b>	<b>6</b>
<b>3</b>	<b>No resonance models</b>	<b>7</b>
<b>4</b>	<b>Scalar resonance models</b>	<b>12</b>
4.1	The chirally coupled model . . . . .	12
4.2	$O(N)$ model . . . . .	13
<b>5</b>	<b>A vector resonance model</b>	<b>13</b>
5.1	Masses and fermion couplings of the gauge bosons . . . . .	17
<b>6</b>	<b>Vector axial-vector resonance models</b>	<b>20</b>
6.1	Masses and couplings of the new resonances . . . . .	24
6.2	Low energy limits . . . . .	28
6.3	Comparison with technicolor theories . . . . .	28
<b>7</b>	<b>Generalizations</b>	<b>32</b>
<b>8</b>	<b><math>e^+e^- \rightarrow f^+f^-</math> channel</b>	<b>33</b>
8.1	Observables . . . . .	34
<b>9</b>	<b><math>e^+e^- \rightarrow WW</math> channel</b>	<b>35</b>
9.1	Observables . . . . .	36
<b>10</b>	<b>Results for the BESS model</b>	<b>38</b>
<b>11</b>	<b>Results for the Degenerate BESS</b>	<b>45</b>
<b>12</b>	<b>Final state rescattering</b>	<b>47</b>
<b>13</b>	<b>Anomalous trilinear gauge boson couplings</b>	<b>50</b>
<b>14</b>	<b>Fusion subprocesses and vector resonances</b>	<b>52</b>
<b>15</b>	<b>Fusion: comparison of models</b>	<b>55</b>
<b>16</b>	<b>Measuring chiral parameters</b>	<b>58</b>
<b>17</b>	<b>Comparison LC - LHC</b>	<b>59</b>
<b>18</b>	<b>Conclusions</b>	<b>63</b>



# 1 Introduction

The Standard Model (SM) of the electroweak interactions is in good agreement with all current experimental results from LEP, SLC and Tevatron. However the mechanism which is responsible for gauge boson and fermion masses is still lacking of experimental confirmation. It is usually assumed that a scalar field, acquiring vacuum expectation value, induces a spontaneous breaking of the symmetry, generating the masses. The Higgs field is the remnant of such a mechanism.

Direct search of the Higgs at LEPI and LEP II has already put a lower limit on its mass,  $M_H \geq 77 \text{ GeV}$  [1]. There are also upper limits from lattice calculations of the order  $M_H \sim 700 \text{ GeV}$  [2], tree level unitarity [3]  $M_H \sim 1000 \text{ GeV}$  and Landau pole  $M_H \sim 200 - 1000 \text{ GeV}$  depending on the new physics cutoff [4].

The known mechanism for spontaneous symmetry breaking suffers of the so-called hierarchy problem. Quantum corrections to the Higgs mass are naturally of the order of the highest scale of the theory, then requiring a fine tuning of the parameters in absence of some symmetry protecting the Higgs mass. An appealing solution to this problem is offered by supersymmetry, because of the cancellation among scalar and fermion loop-corrections.

An alternative approach is suggested in dynamical symmetry breaking schemes like technicolor [5, 6]; the Higgs is substituted by a fermion condensate and the SM is thought of as an effective theory valid up to the new scale. In this approach the hierarchy problem is solved by the natural cutoff given by the new theory. These two different philosophies require therefore two different approaches; while predictions of supersymmetric theories are mainly based on renormalizable Lagrangians, the predictions of dynamical breaking theories are based on non perturbative approaches like effective Lagrangians or strong interaction methods. Existing measurements already exclude the simply QCD rescaled version of technicolor and suggest that only extensions of the SM which smoothly modify it are still conceivable.

The physics of  $e^+e^-$  linear colliders has been the subject of intensive work during the last years in all its aspects [7, 8, 9, 10, 11, 12, 13, 14]. The properties of top quark (mass and decay), the self couplings of  $W$  bosons can be studied with great accuracy. The Higgs particle and supersymmetric particles can be explored and therefore we can gain insight in beyond the SM.

In this report we are going to review the general phenomenology at future  $e^+e^-$  linear colliders (LC's) of the strong interactions associated to the electroweak symmetry breaking problem. These predictions are derived from models of dynamical breaking which are based just on the symmetry structure of the electroweak breaking or its extensions but irrespectively of the underlying theory which is responsible for the breaking. Technicolor with a chiral symmetry flavor  $SU(2) \otimes SU(2)$  is the simplest example for such dynamical breaking. This is a limited point of view. However it allows to get predictions which are general enough at least in a class of models of dynamical breaking.

Model dependent predictions can be obtained when one deals also with the problem of fermion masses and theories like extended technicolor [15], walking technicolor [16], top-

color assisted technicolor [17] or noncommuting extended technicolor [18] are considered.

The study of  $WW$  scattering and in particular of longitudinal  $W$  can clarify the mechanism of spontaneous symmetry breaking since we know from the Equivalence Theorem [19] that this process is equivalent at high energy to the corresponding Goldstone boson scattering. We expect an energy threshold at which  $WW$  scattering will become strong [3, 20] and in principle resonances ( $WW$  or technifermion bound states like techni- $\rho$  or techni- $\omega$ ) can appear. Models for  $WW$  interactions have been proposed, using in particular the chiral lagrangian technique, taking into account the spontaneous breaking of the global symmetry of the Higgs sector  $SU(2) \otimes SU(2)$  to  $SU(2)$ . Effective Lagrangians without new resonances have been built by considering the SM in the  $M_H \rightarrow \infty$  limit [21, 22] or in the context of technicolor theories based on the same symmetry breaking scheme or its generalizations like  $SU(8) \otimes SU(8)$  to  $SU(8)$  [23].

Models for scalar bound states in the  $W^+W^-$ ,  $ZZ$  channels, after the pioneering papers [3, 20], were first considered in [24, 25], studying the  $O(4)$  linear scalar model, by replacing it with the  $O(N)$  model, studied in the limit of large  $N$  for all values of the fourlinear coupling  $\lambda$ . This is particularly convenient, when considering the large Higgs mass regime of the Higgs sector.

A model describing a new triplet of vector resonances in the  $W^+W^-$ ,  $ZZ$  and  $W^\pm Z$  channels was also proposed [26]. It was derived from the non-linear  $\sigma$ -model, based on the manifold  $SU(2) \otimes SU(2)/SU(2)$  and introducing the vector resonances by means of the hidden gauge symmetry approach [27, 28] which is equivalent to the method used by Weinberg to describe the  $\rho$  particle in chiral Lagrangians [29]. The model was also generalized to include axial-vector bound states [30].

In the following we will review all these different models based on the same chiral symmetry but with a different spectrum of resonances.

Two classes of different processes will be considered at future LC's. The annihilation processes  $e^+e^- \rightarrow f^+f^-$  and  $e^+e^- \rightarrow W^+W^-$  will be in particular relevant if a new vector resonance mixed with  $Z$  is present. These channels are already important at a LC of a center of mass energy of 500  $GeV$ . In principle if LHC has already discovered such a new vector boson one can tune the LC energy to study its properties and decays. Otherwise the LC can give bounds on its couplings and masses. The other process is the fusion, for example  $e^+e^- \rightarrow \bar{\nu}\nu W^+W^-$ , and can be used to study  $WW$  scattering also in absence of new resonances but, as we will see, it requires much higher energy (of the order 1.5  $TeV$ ) and luminosity.

Finally let us mention that, as already noticed, the symmetry group can be larger than  $SU(2)_L \times SU(2)_R$  like in the one family technicolor model based on the chiral symmetry  $SU(8)_L \times SU(8)_R$  [6]. In this review we do not extend the phenomenological analysis to such models. These models have a rich particle spectrum with new pseudo-Goldstone bosons which in principle could be produced at future LC's [31].

We do not consider here the study of  $WW$  scattering at  $\gamma\gamma$ ,  $\gamma e^-$  and  $e^-e^-$  options of the machine (we refer to [32, 33] for recent reviews).

The contents of the paper is the following. We briefly review the features of the electroweak symmetry breaking in Section 2. In Section 3 we discuss the chiral lagrangian

approach to the electroweak symmetry breaking, considering different models, built in terms of the Goldstone fields, and, using the Equivalence Theorem, we study also the corresponding amplitudes for the scattering of longitudinal bosons. In Section 4 we discuss models containing in addition to the Goldstone fields, a scalar bound state which could arise from the new strong underlying interaction. In Section 5 we review an effective parametrization of the strong electroweak breaking with a new triplet of vector bosons. The model is extended in Section 6 to describe also axial-vector bound states. Limits on these models from LEP, SLC, Tevatron measurements are also studied. In Section 7 models with scalar, vector and axial-vector bound states are presented. We then study the different processes and observables which can be used at future LC's  $e^+e^-$ , starting with the channel  $e^+e^- \rightarrow f^+f^-$  in Section 8 and  $e^+e^- \rightarrow W^+W^-$  in Section 9. The limits that can be obtained from these processes, by considering the virtual effects of new vector resonances are presented in Sections 10 and 11. In Section 12 the strong effects from electroweak symmetry breaking are included in  $e^+e^- \rightarrow W^+W^-$  through final state rescattering and the corresponding limits on  $W_L W_L$  scattering amplitudes are derived. In Section 13 we review the effective parametrization for trilinear gauge boson couplings and their bounds at future LC's. In Section 14 we consider the study of  $WW$  scattering through the fusion processes  $e^+e^- \rightarrow W^+W^-e^+e^-$  and  $e^+e^- \rightarrow W^+W^-\bar{\nu}\nu$ . The results for various models of strong sector are compared in Section 15 and 16. In Section 17 we perform a comparison of reach of LC and LHC for different models and in Section 18 we make some general conclusive comments. In the Appendix we briefly review the technique of non linear realization of a symmetry group  $G$  which spontaneously breaks to a subgroup  $H$ .

## 2 Electroweak symmetry breaking

Perhaps the most important subject of research which has generated a lot of theoretical activities and models beyond the SM is the electroweak symmetry breaking. Gauge bosons, quarks and leptons get their masses from this breaking. One of the basic feature of the standard Higgs sector is the global symmetry of the Higgs potential, which is invariant, neglecting the gauge interactions, under the following transformation

$$M = (v + H) \exp(i\pi^a \tau^a / v) \rightarrow g_L M g_R^\dagger \quad (1)$$

with  $g_{L,R} \in SU(2)_{L,R}$ ,  $v = 246 \text{ GeV}$  and  $\tau^a$  ( $a = 1, 2, 3$ ) the Pauli matrices. The vacuum expectation value  $\langle M \rangle = v$  breaks the symmetry  $SU(2)_L \otimes SU(2)_R$  to  $SU(2)_{L+R}$ . A second feature of the Higgs Lagrangian is, in the standard approach but also in the supersymmetric one, the renormalizability of the theory in the conventional sense.

Most of the non supersymmetric extensions of the SM assume that this breaking  $SU(2)_L \otimes SU(2)_R$  to  $SU(2)_{L+R}$  is generated by a new confining strong interaction (technicolor, metacolor...) and the usual Higgs field is replaced by a bound state fermion-antifermion. In theories like technicolor one has a  $SU(2)_L \otimes SU(2)_R$  chiral symmetry acting on the technifermion fields and a technifermion condensate induces a breaking to

$SU(2)_{L+R}$ . This dynamical breaking produces three Goldstones  $\pi^a$  such that

$$< 0 | J_A^{a\mu} | \pi^b > = i \delta^{ab} v p^\mu \quad (2)$$

where  $J_A^{a\mu}$  denote the axial currents. By computing the lowest order vacuum polarization for the gauge bosons one gets the usual mass matrix in the basis  $(W_1, W_2, W_3, Y)$

$$M^2 = \frac{1}{4} v^2 \begin{pmatrix} g^2 & & & \\ & g^2 & & \\ & & g^2 & -gg' \\ & & -gg' & g'^2 \end{pmatrix} \quad (3)$$

This solves only the problem of gauge boson masses and some new mechanism is necessary for fermion masses.

We do not discuss here the problem of fermion masses, and therefore we will consider an effective field theory parametrization of the symmetry breaking  $SU(2)_L \otimes SU(2)_R \rightarrow SU(2)_{L+R}$ . In this case the effective field theory approach is the most convenient for working out the consequences of this breaking without knowing the new underlying interaction; the Higgs sector is now a theory valid up to the scale characterized by the new interaction and renormalizability is no longer a requirement for the Lagrangian. Effective Lagrangians can be derived using the global symmetry  $G = SU(2)_L \times SU(2)_R$  and an expansion in the energy [34, 35, 36]. Goldstones are described by a unitary field  $U(x) = \exp(i\pi^a(x)\tau^a/v)$ , transforming under  $G$  as  $(2, 2)$  or  $U \rightarrow g_L U g_R^\dagger$ . The most general chiral Lagrangian is a sum of an infinite number of terms with an increasing number of derivatives or equivalently in terms of increasing powers of energy or momentum. These Lagrangians allow for a description of the physics below a cutoff scale  $\Lambda$ , related to the new underlying interaction. Effective field theories are not renormalizable in the usual sense (finite number of primitive divergences). However at a finite order in the momentum expansion only a finite number of parameters is necessary to get a finite result; therefore at low energy only the first terms in the expansion are retained and one has definite predictions in terms of few parameters (for a recent proof of renormalizability in “modern” sense of effective field theory see [37]).

Applications to the electroweak sector have been considered by different authors [21, 22, 23, 38].

### 3 No resonance models

In this Section we review the chiral lagrangian approach which allows to study the symmetry breaking sector of the SM. In fact, by making use of the Equivalence Theorem [19], one can work taking as degrees of freedom the Goldstone bosons, equivalent to the longitudinal components of  $W$  and  $Z$ .

Experiments, like the measurement of the  $\rho$  parameter at LEPI, suggest the existence of a custodial symmetry  $SU(2)$  [39], which guarantees, at tree level,

$$\rho = \frac{M_W^2}{M_Z^2 \cos^2 \theta_W} = 1 \quad (4)$$

Therefore chiral Lagrangians can be built as non linear  $\sigma$ -models assuming the spontaneous breaking  $SU(2)_L \otimes SU(2)_R \rightarrow SU(2)_{L+R}$ . A brief review of the non linear group realizations of a group  $G$  which breaks spontaneously to a subgroup  $H$  [40] can be found in Section 19.

At the lowest order, the Lagrangian is given by

$$\mathcal{L} = \frac{v^2}{4} \text{Tr} \partial_\mu U^\dagger \partial^\mu U = \frac{1}{2} \partial_\mu \pi^a \partial^\mu \pi^a + \frac{1}{6v^2} [(\pi^a \partial_\mu \pi^a)^2 - \pi^a \pi^a (\partial_\mu \pi^a)^2] + \dots \quad (5)$$

Here and in the following we make the identification  $v^2 = 1/(\sqrt{2}G_F)$ ,  $G_F$  being the Fermi constant.

This already allows, using the Equivalence Theorem, to calculate the scattering amplitudes for  $W^\pm, Z$  gauge bosons at high energy,  $\sqrt{s} \gg M_W, M_Z$ , by considering the scattering of the corresponding Goldstone bosons  $\pi^\pm, \pi^3$ .

We have (symmetry factors for identical particles are not included in the amplitudes)

$$\begin{aligned} M(W_L^+ W_L^- \rightarrow Z_L Z_L) &= A(s, t, u) \\ M(W_L^+ W_L^- \rightarrow W_L^+ W_L^-) &= A(s, t, u) + A(t, s, u) \\ M(Z_L Z_L \rightarrow Z_L Z_L) &= A(s, t, u) + A(t, s, u) + A(u, t, s) \end{aligned} \quad (6)$$

with

$$A(s, t, u) = s/v^2 \quad (7)$$

where  $s = (p_1 + p_2)^2$ ,  $t = (p_1 - p_3)^2 = -s(1 - \cos \theta)/2$  and  $u = (p_1 - p_4)^2 = -s(1 + \cos \theta)/2$  are the Mandelstam variables. Using the crossing property we have also

$$\begin{aligned} M(W_L^\pm Z_L \rightarrow W_L^\pm Z_L) &= A(t, s, u) \\ M(W_L^\pm W_L^\pm \rightarrow W_L^\pm W_L^\pm) &= A(t, s, u) + A(u, t, s) \end{aligned} \quad (8)$$

These amplitudes violate unitarity. In fact, if we define the generic partial wave  $a_l^I$ ,

$$a_l^I = \frac{1}{64\pi} \int_{-1}^1 P_l(\cos \theta) T^I d \cos \theta \quad (9)$$

where  $T^I$  is the generic isospin amplitude and the Legendre polynomials are normalized as

$$\int_{-1}^1 P_l(\cos \theta) P_m(\cos \theta) d \cos \theta = \frac{1}{m + 1/2} \delta_{lm} \quad (10)$$

we find that partial wave unitarity is violated at  $\sqrt{s} = 1.7 \text{ TeV}$  by requiring  $|a_0^0| \leq 1$  (at  $\sqrt{s} = 1.2 \text{ TeV}$  by requiring  $|a_0^0| \leq 1/2$ ) [3].

The isospin amplitudes are given by

$$\begin{aligned} T^0 &= 3A(s, t, u) + A(t, s, u) + A(u, t, s) \\ T^1 &= A(t, s, u) - A(u, t, s) \\ T^2 &= A(t, s, u) + A(u, t, s) \end{aligned} \quad (11)$$



The most general  $SU(2)_L \times SU(2)_R$  invariant Lagrangian with custodial  $SU(2)$ , up to the order  $p^4$ , contains two additional invariant terms and correspondingly two more parameters  $\alpha_4$  and  $\alpha_5$ :

$$\begin{aligned}\mathcal{L}' &= \frac{v^2}{4} \text{tr} \partial_\mu U^\dagger \partial^\mu U \\ &+ \alpha_4 \text{tr}(\partial_\mu U^\dagger \partial_\nu U) \text{tr}(\partial^\mu U^\dagger \partial^\nu U) \\ &+ \alpha_5 \text{tr}(\partial_\mu U^\dagger \partial^\mu U) \text{tr}(\partial_\nu U^\dagger \partial^\nu U)\end{aligned}\quad (12)$$

The parameters  $\alpha_4$  and  $\alpha_5$  are related to the analogous parameters  $L_1$  and  $L_2$  (in the notation in [36]) by

$$\alpha_4 = \frac{L_2}{16\pi^2} \quad \alpha_5 = \frac{L_1}{16\pi^2} \quad (13)$$

This allows to compute the amplitudes at tree level at the order  $p^4$

$$A(s, t, u) = \frac{s}{v^2} + \alpha_4 \frac{4(t^2 + u^2)}{v^4} + \alpha_5 \frac{8s^2}{v^4} \quad (14)$$

However terms of order  $p^4$  are also generated when one uses the Lagrangian at one-loop level.

The corresponding result is a sum of the tree and one-loop amplitudes

$$\begin{aligned}A(s, t, u) &= \frac{s}{v^2} + \frac{1}{v^4} \left( 4\alpha_4(\mu)(t^2 + u^2) + 8\alpha_5(\mu)s^2 \right) \\ &+ \frac{1}{16\pi^2 v^4} \left[ -\frac{t}{6}(s + 2t) \log\left(-\frac{t}{\mu^2}\right) - \frac{u}{6}(s + 2u) \log\left(-\frac{u}{\mu^2}\right) \right. \\ &\left. - \frac{s^2}{2} \log\left(-\frac{s}{\mu^2}\right) \right]\end{aligned}\quad (15)$$

where  $\alpha_4(\mu)$  and  $\alpha_5(\mu)$  are the renormalized coefficients.

All these amplitudes violate partial wave unitarity. One can however unitarize them by using for instance the  $K$  matrix prescription [41] (see [42] for applications to  $WW$  scattering)

$$a_l^K = \frac{a_l}{1 - ia_l} \quad (16)$$

or a different method like Padé approximant [43] (see [44] for applications to  $WW$  scattering) or  $N/D$  technique. In the Padé technique the unitarized partial wave is built using the tree level amplitude  $a^{(0)}$  and the one-loop one  $a^{(1)}$ , as

$$a_l^P = \frac{a_l^{(0)}}{1 - a_l^{(1)}/a_l^{(0)}} \quad (17)$$

Both the Padé method and  $N/D$  can generate a resonant behaviour. Therefore the choice of the unitarization procedure introduces some arbitrariness in the predictions in terms of unitarized chiral amplitudes.

For a review of different techniques of unitarization see [45].

If we allow violations of the custodial symmetry, then the Lagrangian at the lowest order becomes

$$\mathcal{L} = \frac{v^2}{4} \text{Tr} \partial_\mu U^\dagger \partial^\mu U + \frac{v^2}{2} \frac{1-\rho}{\rho} [\text{Tr} \frac{\tau_3}{2} U^\dagger \partial^\mu U]^2 \quad (18)$$

and contains  $\rho$  as a new parameter.

When the gauging of  $SU(2)_L \otimes U(1)_Y$  is considered, one has a correction to the  $\rho$  parameter; the existing measurements of this parameter give  $1 - \rho = -\Delta\rho = -(4.1 \pm 1.2) \times 10^{-3}$  [46].

The symmetry group is now  $SU(2) \otimes U(1)_Y$ , breaking to  $U(1)_{em}$ . From this Lagrangian one gets the following scattering amplitudes at the lowest order [47]

$$\begin{aligned} M(W_L^+ W_L^- \rightarrow Z_L Z_L) &= (4 - \frac{3}{\rho}) \frac{s}{v^2} \\ M(W_L^+ W_L^- \rightarrow W_L^+ W_L^-) &= \frac{1}{\rho} \frac{u}{v^2} \\ M(Z_L Z_L \rightarrow Z_L Z_L) &= 0 \end{aligned} \quad (19)$$

The remaining amplitudes can be obtained via crossing.

If one is interested in the physics of the symmetry breaking sector at energies of the order of the mass of the gauge vector bosons then the complete gauge chiral Lagrangians have to be used, since the Equivalence Theorem is not applicable. The Lagrangian is now built using the Goldstone bosons and the  $SU(2)_L \otimes U(1)_Y$  gauge vector bosons.

The corresponding Lagrangian is equivalent to a nonlinear gauged  $\sigma$ -model, obtained simply substituting the usual derivatives with corresponding covariant ones [21, 22]

$$D_\mu U = (\partial_\mu + \frac{i}{2} g W_\mu^a \tau^a) U - \frac{i}{2} g' U Y_\mu \tau^3 \quad (20)$$

and adding all the terms consistent with the symmetry at a given order in the energy expansion. The model so obtained is also equivalent at the tree and one-loop level to the SM in the limit of infinite  $M_H$ .

Recent review of chiral Lagrangians can be found in [48, 49].

The chiral Lagrangian up to order  $p^2$ , invariant under  $SU(2)_L \otimes U(1)$ , is given by (we follow here [50])

$$\mathcal{L} = \frac{v^2}{4} \text{Tr} (D_\mu U)^\dagger (D_\mu U) + \frac{1}{4} \beta_1 g^2 v^2 [\text{Tr} (T V_\mu)]^2 - \frac{1}{4} Y_{\mu\nu} Y^{\mu\nu} - \frac{1}{2} \text{Tr} W_{\mu\nu} W^{\mu\nu} \quad (21)$$

in terms of  $SU(2)_L$  covariant and  $U(1)_Y$  invariants

$$T = U \tau^3 U^\dagger \quad V_\mu = (D_\mu U) U^\dagger \quad (22)$$

and

$$\begin{aligned} Y_{\mu\nu} &= \partial_\mu Y_\nu - \partial_\nu Y_\mu \\ W_{\mu\nu} &= \partial_\mu W_\nu - \partial_\nu W_\mu + ig [W_\mu, W_\nu] \end{aligned} \quad (23)$$

The second term of eq. (21) violates the custodial  $SU(2)$ , and  $\beta_1$  is related to  $\Delta\rho$ :  $\beta_1 g^2 = \Delta\rho/2$ .

Up to  $p^4$  order the Lagrangian is given by eq. (21) and by the following expression

$$\begin{aligned}
\mathcal{L}_4 = & \frac{1}{2}\alpha_1 g g' Y_{\mu\nu} \text{Tr}(TW^{\mu\nu}) + \frac{1}{2}i\alpha_2 g' Y_{\mu\nu} \text{Tr}(T[V^\mu, V^\nu]) \\
& + i\alpha_3 g \text{Tr}(W_{\mu\nu}[V^\mu, V^\nu]) + \alpha_4 [\text{Tr}(V_\mu V_\nu)]^2 + \alpha_5 [\text{Tr}(V_\mu V^\mu)]^2 \\
& + \alpha_6 \text{Tr}(V_\mu V_\nu) \text{Tr}(TV^\mu) \text{Tr}(TV^\nu) + \alpha_7 \text{Tr}(V_\mu V^\mu) \text{Tr}(TV_\nu) \text{Tr}(TV^\nu) \\
& + \frac{1}{4}\alpha_8 g^2 [\text{Tr}(TW^{\mu\nu})]^2 + \frac{1}{2}i\alpha_9 g \text{Tr}(TW_{\mu\nu}) \text{Tr}(T[V^\mu, V^\nu]) \\
& + \frac{1}{2}\alpha_{10} [\text{Tr}(TV_\mu) \text{Tr}(TV_\nu)]^2 + \alpha_{11} g \epsilon^{\mu\nu\rho\sigma} \text{Tr}(TV_\mu) \text{Tr}(V_\nu W_{\rho\sigma})
\end{aligned} \tag{24}$$

where  $\alpha_1, \dots, \alpha_{11}$  are arbitrary parameters. All these terms are CP invariant. There are also eight CP non invariant terms [50].

There are already bounds on the lagrangian parameters coming from LEP results. These can be obtained using the  $\epsilon$  parameters [51, 52], which can be expressed as

$$\begin{aligned}
\epsilon_1 &= \Delta\rho \\
\epsilon_2 &= c_\theta^2 \Delta\rho + \frac{s_\theta^2}{c_{2\theta}} \Delta r_W - 2s_\theta^2 \Delta k \\
\epsilon_3 &= c_\theta^2 \Delta\rho + c_{2\theta} \Delta k
\end{aligned} \tag{25}$$

where

$$s_\theta^2 = 1 - c_\theta^2 = \frac{1}{2} \left[ 1 - \left( 1 - \frac{4\pi\alpha_{em}}{\sqrt{2}G_F M_Z^2} \right)^{1/2} \right] \tag{26}$$

with  $s_\theta \equiv \sin\theta$ ,  $c_\theta \equiv \cos\theta$  and  $\alpha_{em}$  the electromagnetic fine structure constant at zero momentum transfer.

Now  $\Delta r_W$  can be obtained by  $M_W/M_Z$  which is measured at Tevatron.  $\Delta k$  and  $\Delta\rho$  can be obtained by the LEPI, SLC measurements of asymmetries at the  $Z$  peak, and the  $Z$  widths.

For convenience we give also the relations among the  $\epsilon$  and the  $S$ ,  $T$ ,  $U$  parameters of [53]:

$$\begin{aligned}
\epsilon_1 &= \alpha_{em} T \\
\epsilon_2 &= -\frac{\alpha_{em}}{4s_\theta^2} U \\
\epsilon_3 &= \frac{\alpha_{em}}{4s_\theta^2} S
\end{aligned} \tag{27}$$

Using the chiral Lagrangian, the sum of eqs. (21)-(24), we get

$$\begin{aligned}
\epsilon_1 &= 2g^2 \beta_1 \\
\epsilon_2 &= g^2 \alpha_8 \\
\epsilon_3 &= -g^2 \alpha_1
\end{aligned} \tag{28}$$

Considering the experimental values [46]

$$\epsilon_1 = (4.1 \pm 1.2) \times 10^{-3} \quad \epsilon_2 = (-9.3 \pm 2.2) \times 10^{-3} \quad \epsilon_3 = (4.1 \pm 1.4) \times 10^{-3} \quad (29)$$

one can derive limits on  $\beta_1$ ,  $\alpha_1$  and  $\alpha_8$ . A recent evaluation of the  $S, T, U$  parameters, including loop effects can be found in [54].

The Lagrangian given by eq. (21) and eq. (24) contains also triple gauge vertices among  $W$ ,  $Z$  and  $\gamma$ . The study of  $W$  pair production at LEP II, LHC and LC can allow a determination of these parameters.

## 4 Scalar resonance models

The effect of new resonances can be introduced in the scattering amplitudes using Padé approximant [44] or  $N/D$  technique [3]. Here we choose to present models based on the effective lagrangian approach.

### 4.1 The chirally coupled model

The effective Lagrangian describing a scalar resonance can be built by considering in addition to the field  $U$ , a scalar field  $S$ , which is a singlet under  $SU(2)_L \otimes SU(2)_R$ . Then the effective Lagrangian at the lowest order is given by [55]

$$\begin{aligned} \mathcal{L} = & \frac{v^2}{4} \text{Tr} \partial_\mu U^\dagger \partial^\mu U \\ & + \frac{1}{2} \partial^\mu S \partial_\mu S - \frac{1}{2} M_S^2 S^2 \\ & + \frac{1}{2} k v S \text{Tr} \partial_\mu U^\dagger \partial^\mu U + \dots \end{aligned} \quad (30)$$

where  $M_S$  is the mass of the scalar resonance and

$$\Gamma_S = \frac{3k^2 M_S^3}{32\pi v^2} \quad (31)$$

is the width. For  $k = 1$  one has the usual Higgs-Goldstone couplings. Scattering amplitudes contain now the contribution of the isoscalar resonance

$$A(s, t, u) = \frac{s}{v^2} - \left( \frac{k^2 s^2}{v^2} \right) \frac{1}{s - M_S^2 + i M_S \Gamma_S} \quad (32)$$

In the phenomenological analysis [56, 57]  $M_S = 1 \text{ TeV}$  and  $\Gamma_S = 0.35 \text{ TeV}$  have been chosen.

## 4.2 $O(N)$ model

One starts with the linear Lagrangian of the symmetry breaking sector of the SM which is known to have the  $SU(2) \otimes SU(2)$  symmetry. Since  $SU(2) \otimes SU(2) \sim O(4)$  one can study an effective scalar Lagrangian based on the symmetry group  $O(N)$  in the limit of large  $N$  and then consider  $N = 4$  [24, 25]. The model has the property to be solved for all the values of the four-linear coupling  $\lambda = M_H^2/(2v^2)$ , to leading order in  $1/N$ . Proceeding in this way one can take into account the possibility of having, in addition to the Higgs, a bound state from the strong interacting system. An effective action for its interactions with Goldstone bosons and Higgs can be derived [25]. Scalar propagation is described by a two by two matrix which is degenerate. One has only a pole given by

$$M_\sigma^2[1 + \Delta(M_\sigma^2)] - M_H^2 = 0 \quad (33)$$

where

$$\Delta(s) = \frac{1}{8\pi^2} \frac{M_H^2}{v^2} [1 - \log(-\frac{s}{\mu^2})] \quad (34)$$

with  $\mu$  a renormalization scale of the effective Lagrangian. The location of the pole in the complex plane  $M_\sigma$  evolves from

$$M_\sigma^2 = M_H^2 [1 - i \frac{M_H^2}{8\pi v^2}] + \mathcal{O}(\frac{M_H^4}{v^4}) \quad (35)$$

for small  $M_H/v$  to

$$M_\sigma^2 = \frac{16\pi v^2}{3} [-i + \frac{16\pi}{3} \frac{v^2}{M_H^2} (1 - i \frac{2}{3\pi}) + \mathcal{O}(\frac{v^4}{M_H^4})] \quad (36)$$

for large  $M_H/v$ . One of the effects of the strong coupling is to increase the width of the Higgs with respect to the width of the Higgs as calculated at the lowest order in the SM. The scattering amplitude derived from this Lagrangian is

$$A(s, t, u) = -\sqrt{2} G_F M_H^2 s [s(1 + \Delta(s)) - M_H^2]^{-1} \quad (37)$$

In the limit of large  $M_H$  one obtains

$$A(s, t, u) = \frac{8\pi^2 s}{8\pi^2 v^2 - s[1 - \log(-s/\mu^2)]} \quad (38)$$

This amplitude is consistent with unitarity up to energies of the order  $\mu$ .

## 5 A vector resonance model

In this Section we review a model based on a general procedure to introduce vector resonances in chiral Lagrangians. The model contains a new triplet of vector bosons and

allows to derive their mixings to ordinary gauge bosons  $W$  and  $Z$  and their couplings to fermions. The model can describe as a special case a techni- $\rho$  resonance.

As we have already seen an effective description of the symmetry breaking mechanism in electroweak theories can be done in terms of a non linear  $\sigma$ -model formulated on the quotient space of the breaking of  $SU(2)_L \otimes SU(2)_R \rightarrow SU(2)_{L+R}$ . This is the case when considering the limit of a strong interacting Higgs sector ( $M_H \rightarrow \infty$ ). Vector resonances can be introduced in chiral Lagrangians following Weinberg [29] or, in equivalent way, by means of the hidden local symmetry approach [27] (see also [28]). The model so obtained, when this technique is applied to the electroweak symmetry breaking sector, is called BESS (Breaking the Electroweak Symmetry Strongly) [26].

It is known that any nonlinear  $\sigma$ -model corresponding to the coset space  $G/H$  is gauge equivalent to a linear model based on the symmetry  $G_{global} \otimes H_{local}$ . For the construction of the BESS model Lagrangian  $G_{global} = G = SU(2)_L \otimes SU(2)_R$  and  $H_{local} = H = SU(2)_V$ . One introduces the group variables  $g \in G$  with  $G = SU(2)_L \otimes SU(2)_R$

$$g = (L, R) \quad (39)$$

with  $L \in SU(2)_L$  and  $R \in SU(2)_R$ , which transform under the  $G \otimes H$  group, as follows:  $L \rightarrow g_L L h$ ,  $R \rightarrow g_R R h$ , with  $g_{L,R} \in SU(2)_{L,R}$  and  $h \in SU(2)_V$ .

One further introduces the Maurer-Cartan field

$$\omega_\mu = g^\dagger \partial_\mu g = (L^\dagger \partial_\mu L, R^\dagger \partial_\mu R) \quad (40)$$

which can be decomposed into  $\omega_\mu^\parallel$  lying in the Lie algebra of  $H$ , and into the orthogonal complement  $\omega_\mu^\perp$

$$\begin{aligned} \omega_\mu^\parallel &= \frac{1}{2}(L^\dagger \partial_\mu L + R^\dagger \partial_\mu R) \\ \omega_\mu^\perp &= \frac{1}{2}(L^\dagger \partial_\mu L - R^\dagger \partial_\mu R) \end{aligned} \quad (41)$$

Both  $\omega_\mu^\parallel$  and  $\omega_\mu^\perp$  are singlets of  $G$  and transform under  $H$  as

$$\begin{aligned} \omega_\mu^\parallel &\rightarrow h^\dagger \omega_\mu^\parallel h + h^\dagger \partial_\mu h \\ \omega_\mu^\perp &\rightarrow h^\dagger \omega_\mu^\perp h \end{aligned} \quad (42)$$

The non linear  $\sigma$ -model Lagrangian (5) describing the electroweak symmetry breaking sector can be easily reconstructed in terms of  $\omega_\mu^\perp$

$$\mathcal{L} = -v^2 \text{tr}(\omega_\mu^\perp \omega^{\perp\mu}) = \frac{v^2}{4} \text{tr}(\partial_\mu U^\dagger \partial^\mu U) \quad (43)$$

where  $U = LR^\dagger$  is a singlet under  $H$ .

Introducing a triplet of gauge bosons  $\mathbf{V}_\mu$  transforming as

$$\mathbf{V}_\mu \rightarrow h^\dagger \mathbf{V}_\mu h + h^\dagger \partial_\mu h \quad (44)$$

under the local group  $SU(2)_V$ , one can show that the most general Lagrangian, symmetric under  $G \otimes H$  and under the parity transformation  $L \leftrightarrow R$ , containing at most two derivatives, can be constructed as an arbitrary combination of two invariant terms. Furthermore, assuming that the gauge bosons of the hidden symmetry become dynamical [58, 59], we get

$$\begin{aligned}\mathcal{L} = & -v^2 [\text{tr}(\omega_\mu^\perp)^2 + \alpha \text{tr}(\omega_\mu^\parallel - \mathbf{V}_\mu)^2] \\ & + \frac{2}{g''^2} \text{tr}[F^{\mu\nu}(\mathbf{V})F_{\mu\nu}(\mathbf{V})]\end{aligned}\quad (45)$$

with  $\alpha$  an arbitrary parameter,

$$F_{\mu\nu}(\mathbf{V}) = \partial_\mu \mathbf{V}_\nu - \partial_\nu \mathbf{V}_\mu + [\mathbf{V}_\mu, \mathbf{V}_\nu] \quad (46)$$

and  $\mathbf{V}_\mu = \frac{i}{2} \frac{g''}{2} V_\mu^a \tau^a$ , with  $g''$  the new gauge coupling constant.

The Lagrangian can also be written as

$$\begin{aligned}\mathcal{L} = & -\frac{v^2}{4} [Tr(L^\dagger D_\mu L - R^\dagger D_\mu R)^2 + \alpha Tr(L^\dagger D_\mu L + R^\dagger D_\mu R)^2] \\ & + \frac{2}{g''^2} \text{tr}[F^{\mu\nu}(\mathbf{V})F_{\mu\nu}(\mathbf{V})]\end{aligned}\quad (47)$$

where we use the covariant derivatives  $D_\mu L = \partial_\mu L - L \mathbf{V}_\mu$ ,  $D_\mu R = \partial_\mu R - R \mathbf{V}_\mu$ .

Going to the unitary gauge

$$L = R^\dagger = \exp\left(\frac{i}{2v} \pi^a \tau^a\right) \quad (48)$$

one can derive an effective Lagrangian describing Goldstones and a new triplet of gauge vector bosons whose mass is given by

$$M_V^2 = \alpha \frac{v^2}{4} g''^2 \quad (49)$$

The scattering amplitudes of eq. (6) and eq. (8), using the Equivalence Theorem, can be expressed in terms of

$$A(s, t, u) = \frac{s}{4v^2} (4 - 3\alpha) + \frac{\alpha M_V^2}{4v^2} \left[ \frac{u - s}{t - M_V^2 + iM_V \Gamma_V} + \frac{t - s}{u - M_V^2 + iM_V \Gamma_V} \right] \quad (50)$$

where  $\Gamma_V$  is the width of  $V$  [60]

$$\Gamma(V \rightarrow \pi\pi) = \frac{\sqrt{2} G_F}{192\pi} \frac{M_V^5}{M_W^2} \left( \frac{g}{g''} \right)^2 \quad (51)$$

The unitarity limit of this model, from the  $J = 0$  partial wave, turns out to be

$$E \leq \frac{1.7 \text{ TeV}}{|1 - \frac{3}{4}\alpha|^{1/2}} \quad (52)$$

A more stringent bound can be obtained from the  $J = 0$ , isospin 2 partial wave [61].

Notice that the parameter  $\alpha$  can be also rewritten in terms of the width as

$$\alpha = \frac{192\pi v^2 \Gamma_V}{M_V^3} \quad (53)$$

One can also fully develop the model by including the  $W$ ,  $Z$  and  $\gamma$  gauge bosons. This is simply obtained, by the gauging of the standard  $SU(2)_L \otimes U(1)_Y$  group, substituting in (47) the ordinary derivatives with covariant left and right derivatives acting on the left and right group elements respectively

$$\begin{aligned} \partial_\mu L &\rightarrow (\partial_\mu + \tilde{\mathbf{W}}_\mu)L \\ \partial_\mu R &\rightarrow (\partial_\mu + \tilde{\mathbf{Y}}_\mu)R \end{aligned} \quad (54)$$

where  $\tilde{\mathbf{W}}_\mu = \frac{i}{2}g\tilde{W}_\mu^a\tau^a$  and  $\tilde{\mathbf{Y}}_\mu = \frac{i}{2}g'\tilde{Y}_\mu\tau^3$ , and by adding the standard kinetic terms for  $\tilde{\mathbf{W}}$  and  $\tilde{\mathbf{Y}}$

$$\mathcal{L}^{kin}(\tilde{\mathbf{W}}, \tilde{\mathbf{Y}}) = \frac{1}{2g^2}\text{tr}[F^{\mu\nu}(\tilde{\mathbf{W}})F_{\mu\nu}(\tilde{\mathbf{W}})] + \frac{1}{2g'^2}\text{tr}[F^{\mu\nu}(\tilde{\mathbf{Y}})F_{\mu\nu}(\tilde{\mathbf{Y}})] \quad (55)$$

with

$$\begin{aligned} F_{\mu\nu}(\tilde{\mathbf{W}}) &= \partial_\mu \tilde{\mathbf{W}}_\nu - \partial_\nu \tilde{\mathbf{W}}_\mu + [\tilde{\mathbf{W}}_\mu, \tilde{\mathbf{W}}_\nu] \\ F_{\mu\nu}(\tilde{\mathbf{Y}}) &= \partial_\mu \tilde{\mathbf{Y}}_\nu - \partial_\nu \tilde{\mathbf{Y}}_\mu \end{aligned} \quad (56)$$

Due to the gauge invariance of  $\mathcal{L}$  we can choose the gauge with  $L = R = I$  [26] and we get

$$\mathcal{L} = -\frac{v^2}{4}\left[\text{tr}(\tilde{\mathbf{W}}_\mu - \tilde{\mathbf{Y}}_\mu)^2 + \alpha\text{tr}(\tilde{\mathbf{W}}_\mu + \tilde{\mathbf{Y}}_\mu - 2\mathbf{V}_\mu)^2\right] + \mathcal{L}^{kin}(\tilde{\mathbf{W}}, \tilde{\mathbf{Y}}, \mathbf{V}) \quad (57)$$

We have used tilded quantities to recall that, due to the effects of the  $\mathbf{V}$  particles, they are not the physical fields.

From eq. (57) one can easily derive the mass eigenstates and the mixing angles among the standard gauge bosons and the new resonances [26]. Furthermore, since in the limit  $g'' \rightarrow \infty$ , the Lagrangian  $\mathcal{L}$  reproduces the SM gauge boson mass terms, corrections to the SM relations come in powers of  $1/g''$ .

Finally let us consider the fermions of the SM and denote them by  $\psi_L$  and  $\psi_R$  with

$$\psi = \begin{pmatrix} \psi_u \\ \psi_d \end{pmatrix}, \dots \quad (58)$$



They couple to  $\mathbf{V}$  via the mixing with the standard  $\tilde{\mathbf{W}}$  and  $\tilde{\mathbf{Y}}$ . In addition, direct couplings to the new vector bosons are allowed by the symmetries of  $\mathcal{L}$  [26]. In fact, we can define Fermi fields transforming as doublets under the local group  $SU(2)_V$  and singlets under the global one:  $\chi_L = L^\dagger \psi_L$ ; an invariant term acting on  $\chi_L$  by the covariant derivative with respect to  $SU(2)_V$  can be written. In the  $L = R = I$  gauge we get

$$\begin{aligned}\mathcal{L}_{fermion} &= \bar{\tilde{\psi}}_L i\gamma^\mu \left( \partial_\mu + \tilde{\mathbf{W}}_\mu + \frac{i}{2} g' (B - L) \tilde{Y}_\mu \right) \tilde{\psi}_L \\ &+ \bar{\tilde{\psi}}_R i\gamma^\mu \left( \partial_\mu + \tilde{\mathbf{Y}}_\mu + \frac{i}{2} g' (B - L) \tilde{Y}_\mu \right) \tilde{\psi}_R \\ &+ b \bar{\tilde{\psi}}_L i\gamma^\mu \left( \partial_\mu + \mathbf{V}_\mu + \frac{i}{2} g' (B - L) \tilde{Y}_\mu \right) \tilde{\psi}_L\end{aligned}\quad (59)$$

where  $B(L)$  is the baryon (lepton) number and  $b$  is a new parameter. Notice that due to the introduction of the direct coupling of the  $\mathbf{V}$  to the fermions, we have to rescale  $\tilde{\psi}_L = (1 + b)^{-1/2} \psi_L$  in order to get a canonical kinetic term for the fermions [26].

## 5.1 Masses and fermion couplings of the gauge bosons

In the charged sector the mass eigenvalues for the gauge bosons are, in the limit of large  $g''$ ,

$$M_W^2 = \frac{v^2}{4} g^2 \left( 1 - \frac{g^2}{g''^2} \right) \quad M_{V^\pm}^2 = \alpha \frac{v^2}{4} g''^2 \quad (60)$$

In the neutral sector we have

$$M_Z^2 = \frac{v^2}{4} (g^2 + g'^2) \left( 1 - \frac{(g^2 - g'^2)^2}{(g^2 + g'^2) g''^2} \right) \quad M_V^2 = \alpha \frac{v^2}{4} g''^2 \quad (61)$$

We also recall the couplings to the fermions which arise from (59). The charged couplings are given by

$$- 2e(a_W W_\mu^- + a_V V_\mu^-) J_L^{\mu(+)} + h.c. \quad (62)$$

with

$$\begin{aligned}a_W &= \frac{1}{2\sqrt{2}s_\theta} \frac{1}{1+b} \left( \frac{\cos \phi}{\cos \psi} - \frac{b \sin \phi}{2 \cos \psi} \frac{g''}{g} \right) \\ a_V &= \frac{1}{2\sqrt{2}s_\theta} \frac{1}{1+b} \left( \frac{\sin \phi}{\cos \psi} + \frac{b \cos \phi}{2 \cos \psi} \frac{g''}{g} \right)\end{aligned}\quad (63)$$

with  $s_\theta = g'/\sqrt{g^2 + g'^2}$ . The mixing angles in the  $M_V \gg M_W$  and large  $g''$  limit are

$$\phi = -\frac{g}{g''} \quad (64)$$

$$\psi = 2s_\theta \frac{g}{g''} \quad (65)$$

In the neutral sector the couplings of the fermions to the gauge bosons  $Z$  and  $V$  are

$$e \left( v_Z^f + \gamma_5 a_Z^f \right) \gamma_\mu Z^\mu + e \left( v_V^f + \gamma_5 a_V^f \right) \gamma_\mu V^\mu \quad (66)$$

where  $v_{Z,V}^f$  and  $a_{Z,V}^f$  are the vector and axial-vector couplings given by

$$\begin{aligned} v_Z^f &= \frac{1}{s_{2\theta}} \left( AT_3^L + 2BQ_{em} \right) \\ a_Z^f &= \frac{1}{s_{2\theta}} AT_3^L \\ v_V^f &= \frac{1}{s_{2\theta}} \left( CT_3^L + 2DQ_{em} \right) \\ a_V^f &= \frac{1}{s_{2\theta}} CT_3^L \end{aligned} \quad (67)$$

where

$$\begin{aligned} A &= \frac{\cos \xi}{\cos \psi} (1+b)^{-1} \left[ 1 + bs_\theta^2 \left( 1 - \frac{\tan \xi}{\tan \theta \sin \psi} \right) \right] \\ B &= -s_\theta^2 \frac{\cos \xi}{\cos \psi} \left( 1 - \frac{\tan \xi \sin \psi}{\tan \theta} \right) \\ C &= \frac{\sin \xi}{\cos \psi} (1+b)^{-1} \left[ 1 + bs_\theta^2 \left( 1 + \frac{\cot \xi}{\tan \theta \sin \psi} \right) \right] \\ D &= -s_\theta^2 \frac{\sin \xi}{\cos \psi} \left( 1 + \frac{\cot \xi \sin \psi}{\tan \theta} \right) \end{aligned} \quad (68)$$

with  $e = gs_\theta \cos \psi$ ,  $T_3^L = \pm 1/2$  and

$$\xi = -\frac{c_{2\theta}}{c_\theta} \frac{g}{g''} \quad (69)$$

Let us now evaluate the partial widths of the  $V$  bosons from decays into fermion-antifermion and  $WW$ . The lepton width of the charged boson is given by

$$\Gamma(V^- \rightarrow l\nu) = \frac{2}{3} \alpha M_V (a_V^l)^2 = \Gamma_V^0 \quad (70)$$

while the hadron width is

$$\Gamma(V^- \rightarrow q'\bar{q}) = 3|V_{qq'}|^2 \Gamma_V^0 \quad (71)$$

where  $|V_{qq'}|$  are the relevant Kobayashi-Maskawa matrix elements.

The  $WZ$  width is

$$\begin{aligned} \Gamma(V^- \rightarrow W^- Z) &= \frac{M_V}{48} \alpha_{em} g_{VWZ}^2 \left[ \left( 1 - \frac{M_Z^2 - M_W^2}{M_V^2} \right)^2 - 4 \frac{M_W^2}{M_V^2} \right]^{3/2} \left( \frac{M_V^4}{M_W^2 M_Z^2} \right) \\ &\times \left[ 1 + 10 \left( \frac{M_W^2 + M_Z^2}{M_V^2} \right) + \frac{M_W^4 + M_Z^4 + 10 M_W^2 M_Z^2}{M_V^4} \right] \end{aligned} \quad (72)$$

where, for large  $g''$ ,

$$g_{VWZ} = -\frac{1}{2s_\theta c_\theta} \frac{g}{g''} \quad (73)$$

The total neutral width is given by

$$\Gamma_V^h + 3(\Gamma_V^l + \Gamma_V^\nu) + \Gamma_V^W \quad (74)$$

where  $\Gamma_V^h$  is the sum of all quark-antiquark widths, with

$$\Gamma_V^f = \frac{M_V \alpha_{em}}{3} \left( v_V^f{}^2 + a_V^f{}^2 \right) \quad (75)$$

$$\begin{aligned} \Gamma_V^W &= \frac{M_V}{48} \alpha_{em} g_{VWW}^2 \left( 1 - 4 \frac{M_W^2}{M_V^2} \right)^{3/2} \left( \frac{M_V}{M_W} \right)^4 \\ &\times \left[ 1 + 20 \left( \frac{M_W}{M_V} \right)^2 + 12 \left( \frac{M_W}{M_V} \right)^4 \right] \end{aligned} \quad (76)$$

with, for large  $g''$ ,

$$g_{VWW} = -\frac{1}{2s_\theta} \frac{g}{g''} \quad (77)$$

For large  $M_V$  and  $g''$  from eqs. (72) and (76), one recovers (51).

For future calculations we also give the  $g_{ZWW}$  coupling

$$g_{ZWW} = \frac{1}{\tan \theta} \left[ 1 - 3 \left( 1 - \frac{1}{2c_\theta^2} \right) \left( \frac{g}{g''} \right)^2 \right] \quad (78)$$

Limits on the parameter space of the model can be obtained by computing the  $\epsilon$  parameters [51, 52].

In the limit of large  $M_V$  we get [62, 63]

$$\begin{aligned} \epsilon_1 &= 0 \\ \epsilon_2 &= 0 \\ \epsilon_3 &= -\frac{b}{2} + \left( \frac{g}{g''} \right)^2 \end{aligned} \quad (79)$$

In conclusion the model has no decoupling in the limit  $M_V \rightarrow \infty$ . To get decoupling, the limits of  $g'' \rightarrow \infty$  and  $b \rightarrow 0$  have to be taken.

We can derive restrictions on the BESS parameters by using the experimental data on  $\epsilon_3$ . The most recent value for  $\epsilon_3$  obtained by combining the LEP, CDF/UA2 and SLC data [46] is

$$\epsilon_3 = (4.1 \pm 1.4) \times 10^{-3} \quad (80)$$

In order to get these bounds one has to make some assumptions on the radiative corrections to the  $\epsilon$  parameters. By neglecting loop effects of new gauge vectors, and assuming for the BESS model the same one-loop radiative corrections as for the SM in which the Higgs mass is used as a cut-off  $\Lambda$ , adding to  $\epsilon_3$  given in eq. (79) the contribution coming from the radiative corrections  $(\epsilon_3)_{rad.corr.} = 6.4 \times 10^{-3}$  [46], (for  $M_H = \Lambda = 1 \text{ TeV}$  and  $m_{top} = 175 \text{ GeV}$ ), one gets the allowed region at 90% C.L. in the plane  $(b, g/g'')$  shown in Fig. 1. Therefore the model is strongly constrained.

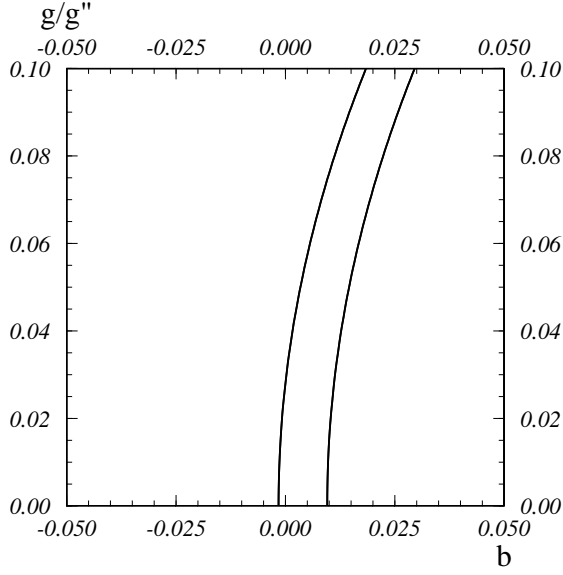


Figure 1: 90% C.L. contour in the plane  $(b, g/g'')$  for large  $M_V$  in the BESS model from LEP/Tevatron/SLC data for  $m_t = 175 \text{ GeV}$ . The allowed region is the internal one.

## 6 Vector axial-vector resonance models

A model with vector and axial-vector resonances can be built by considering in addition to the global symmetry  $G = SU(2)_L \otimes SU(2)_R$ , a local symmetry  $H' = SU(2)_L \otimes SU(2)_R$  and unbroken  $H_D = SU(2)$ , the diagonal subgroup of  $G' = G \otimes H'$  [30]. The nine Goldstone bosons, resulting from the spontaneous breaking of  $G'$  to  $H_D$ , can be described by three independent  $2 \times 2$  unitary matrices  $L$ ,  $R$  and  $M$ , with the following transformations with respect to  $G$  and  $H'$

$$L' = g_L L h_L, \quad R' = g_R R h_R, \quad M' = h_R^\dagger M h_L \quad (81)$$

with  $g_{L,R} \in SU(2)_{L,R} \subset G$  and  $h_{L,R} \in SU(2)_{L,R} \subset H'$ . We shall require the invariance under the discrete left-right transformation, denoted by  $P$

$$P : \quad L \leftrightarrow R, \quad M \leftrightarrow M^\dagger \quad (82)$$

which allows for a low-energy theory parity conserving.

The most general  $G' \otimes P$  invariant Lagrangian, up to second order derivatives, is given by [30]

$$\mathcal{L}_G = -\frac{v^2}{4} f(\mathbf{L}_\mu, \mathbf{R}_\mu) \quad (83)$$

where

$$f(\mathbf{L}_\mu, \mathbf{R}_\mu) = a_1 I_1 + a_2 I_2 + a_3 I_3 + a_4 I_4 \quad (84)$$

and by the kinetic terms  $\mathcal{L}_{kin}$  for the fields. The terms  $I_i$  ( $i = 1, \dots, 4$ ) are given by:

$$\begin{aligned} I_1 &= tr[(V_0 - V_1 - V_2)^2] \\ I_2 &= tr[(V_0 + V_2)^2] \\ I_3 &= tr[(V_0 - V_2)^2] \\ I_4 &= tr[V_1^2] \end{aligned} \quad (85)$$

and

$$V_0^\mu = L^\dagger D^\mu L, \quad V_1^\mu = M^\dagger D^\mu M, \quad V_2^\mu = M^\dagger (R^\dagger D^\mu R) M \quad (86)$$

with the following covariant derivatives

$$\begin{aligned} D_\mu L &= \partial_\mu L - L \mathbf{L}_\mu \\ D_\mu R &= \partial_\mu R - R \mathbf{R}_\mu \\ D_\mu M &= \partial_\mu M - M \mathbf{L}_\mu + \mathbf{R}_\mu M \end{aligned} \quad (87)$$

The kinetic term is

$$\mathcal{L}_{kin} = \frac{1}{g'^2} tr[F_{\mu\nu}(\mathbf{L})]^2 + \frac{1}{g'^2} tr[F_{\mu\nu}(\mathbf{R})]^2 \quad (88)$$

where  $g''$  is the gauge coupling constant for the gauge fields  $\mathbf{L}_\mu$  and  $\mathbf{R}_\mu$ ,

$$F_{\mu\nu}(\mathbf{L}) = \partial_\mu \mathbf{L}_\nu - \partial_\nu \mathbf{L}_\mu + [\mathbf{L}_\mu, \mathbf{L}_\nu] \quad (89)$$

and the same definition holds for  $F_{\mu\nu}(\mathbf{R})$ .

The quantities  $V_i^\mu$  ( $i = 0, 1, 2$ ) are invariant under the global symmetry  $G$  and covariant under the gauge group  $H'$

$$(V_i^\mu)' = h_L^\dagger V_i^\mu h_L \quad (90)$$

Using the  $V_i^\mu$  one can build six independent quadratic invariants, which reduce to the four  $I_i$  listed above, when parity conservation is required. In conclusion the Lagrangian is given by

$$\mathcal{L} = \mathcal{L}_G + \mathcal{L}_{kin} \quad (91)$$

The Lagrangian (83) can be studied in the unitary gauge

$$L = R^\dagger = \exp\left(\frac{i}{2v}(1-z)\pi^a \tau^a\right) \quad M = \exp\left(-\frac{i}{v}z\pi^a \tau^a\right) \quad (92)$$

where

$$z = \frac{a_3}{a_3 + a_4} \quad (93)$$

At the lowest order in power series of the Goldstone bosons, one gets the mass terms for the vector mesons:

$$\mathcal{L}_G = -\frac{v^2}{4} [a_2 tr(\mathbf{L}_\mu + \mathbf{R}_\mu)^2 + (a_3 + a_4) tr(\mathbf{L}_\mu - \mathbf{R}_\mu)^2] + \dots \quad (94)$$

where the dots stand for terms at least linear in the Goldstone modes. Using the combinations

$$\mathbf{V}_\mu = (\mathbf{L}_\mu + \mathbf{R}_\mu)/2 \quad \mathbf{A}_\mu = (\mathbf{R}_\mu - \mathbf{L}_\mu)/2 \quad (95)$$

we can rewrite

$$\mathcal{L}_G = -v^2 [a_2 \text{tr}(\mathbf{V}_\mu)^2 + (a_3 + a_4) \text{tr}(\mathbf{A}_\mu)^2] + \dots \quad (96)$$

Therefore, if  $\mathbf{V}_\mu = \frac{i}{2} \frac{g''}{2} V_\mu^a \tau^a$ ,  $\mathbf{A}_\mu = \frac{i}{2} \frac{g''}{2} A_\mu^a \tau^a$ , we get

$$M_V^2 = a_2 \frac{v^2}{4} g''^2 \quad M_A^2 = (a_3 + a_4) \frac{v^2}{4} g''^2 \quad (97)$$

Again one can compute the scattering amplitudes of eq. (6) and eq. (8) in terms of

$$A(s, t, u) = \frac{s}{4v^2} (4 - 3\beta) + \frac{\beta M_V^2}{4v^2} \left[ \frac{u - s}{t - M_V^2 + iM_V \Gamma_V} + \frac{t - s}{u - M_V^2 + iM_V \Gamma_V} \right] \quad (98)$$

with

$$\beta = 4 \frac{M_V^2}{g''^2 v^2} (1 - z^2)^2 = \frac{192\pi v^2 \Gamma_V}{M_V^3} \quad (99)$$

For generic values of the parameters  $a_1$ ,  $a_2$ ,  $a_3$ ,  $a_4$ , the Lagrangian  $\mathcal{L}$  is invariant under  $G' \otimes P = G \otimes H' \otimes P$ . There are however special choices which enlarge the symmetry group [64]. One of these choices corresponds to a generalization of Georgi vector symmetry [65].

The case of interest for the electroweak sector is provided by the choice:  $a_4 = 0$ ,  $a_2 = a_3$ . In order to discuss the symmetry properties it is useful to observe that the invariant  $I_1$  could be re-written as follows

$$I_1 = -\text{tr}(\partial_\mu U^\dagger \partial^\mu U) \quad (100)$$

with

$$U = LM^\dagger R^\dagger \quad (101)$$

Therefore the Lagrangian can be rewritten as

$$\mathcal{L}_G = \frac{v^2}{4} \{ a_1 \text{tr}(\partial_\mu U^\dagger \partial^\mu U) + 2 a_2 [\text{tr}(D_\mu L^\dagger D^\mu L) + \text{tr}(D_\mu R^\dagger D^\mu R)] \} \quad (102)$$

Each of the three terms in the above expressions is invariant under an independent  $SU(2) \otimes SU(2)$  group

$$U' = \omega_L U \omega_R^\dagger, \quad L' = g_L L h_L, \quad R' = g_R R h_R \quad (103)$$

The overall symmetry is  $G_{max} = [SU(2) \otimes SU(2)]^3$ , with a subgroup  $H'$  realized as a gauge symmetry.

With the particular choice  $a_4 = 0$ ,  $a_3 = a_2$ , as we see from eq. (94), the mixing between  $\mathbf{L}_\mu$  and  $\mathbf{R}_\mu$  is vanishing, and the new states are degenerate in mass. Moreover, as it follows from eq. (102), the longitudinal modes of the  $\mathbf{L}_\mu$  and  $\mathbf{R}_\mu$  (or  $\mathbf{V}_\mu$ ,  $\mathbf{A}_\mu$ ) fields are entirely provided by the would-be Goldstone bosons in  $L$  and  $R$ . This means that the

pseudoscalar particles remaining as physical states in the low-energy spectrum are those associated to  $U$ . They in turn can provide the longitudinal components to the  $W$  and  $Z$  particles, in an effective description of the electroweak breaking sector.

Since with this choice, from eq. (93),  $z = 1$ , this model has  $\beta = 0$  (eq. (99)) and therefore reproduces at the lowest order the low energy amplitudes of the chiral Lagrangian (5), as it can be seen from eq. (98).

We now consider the coupling of the model to the electroweak  $SU(2)_L \otimes U(1)_Y$  gauge fields via the minimal substitution

$$\begin{aligned} D_\mu L &\rightarrow D_\mu L + \tilde{\mathbf{W}}_\mu L \\ D_\mu R &\rightarrow D_\mu R + \tilde{\mathbf{Y}}_\mu R \\ D_\mu M &\rightarrow D_\mu M \end{aligned} \quad (104)$$

where

$$\tilde{\mathbf{W}}_\mu = i\tilde{W}_\mu^a \frac{\tau^a}{2}, \quad \tilde{\mathbf{Y}}_\mu = i\tilde{Y}_\mu \frac{\tau^3}{2} \quad (105)$$

$$\mathbf{L}_\mu = iL_\mu^a \frac{\tau^a}{2}, \quad \mathbf{R}_\mu = iR_\mu^a \frac{\tau^a}{2} \quad (106)$$

By introducing the canonical kinetic terms for  $W_\mu^a$  and  $Y_\mu$  we get the model [64] called Degenerate BESS, since in the large  $g''$  limit the new triplets  $\mathbf{L}_\mu$  and  $\mathbf{R}_\mu$  are degenerate in mass.

In the unitary gauge the Lagrangian is

$$\mathcal{L} = -\frac{v^2}{4} \left[ a_1 \text{tr}(\tilde{\mathbf{W}}_\mu - \tilde{\mathbf{Y}}_\mu)^2 + 2a_2 \text{tr}(\tilde{\mathbf{W}}_\mu - \mathbf{L}_\mu)^2 + 2a_2 \text{tr}(\tilde{\mathbf{Y}}_\mu - \mathbf{R}_\mu)^2 \right] + \mathcal{L}^{kin}(\tilde{\mathbf{W}}, \tilde{\mathbf{Y}}, \mathbf{L}, \mathbf{R}) \quad (107)$$

$$\begin{aligned} \mathcal{L}^{kin}(\tilde{\mathbf{W}}, \tilde{\mathbf{Y}}, \mathbf{L}, \mathbf{R}) &= \frac{1}{2\tilde{g}^2} \text{tr}[F^{\mu\nu}(\tilde{\mathbf{W}})F_{\mu\nu}(\tilde{\mathbf{W}})] + \frac{1}{2\tilde{g}'^2} \text{tr}[F^{\mu\nu}(\tilde{\mathbf{Y}})F_{\mu\nu}(\tilde{\mathbf{Y}})] \\ &+ \frac{1}{g''^2} \text{tr}[F^{\mu\nu}(\mathbf{L})F_{\mu\nu}(\mathbf{L})] + \frac{1}{g''^2} \text{tr}[F^{\mu\nu}(\mathbf{R})F_{\mu\nu}(\mathbf{R})] \end{aligned} \quad (108)$$

Tilded quantities are used to remind that, due to the effects of the  $\mathbf{L}$  and  $\mathbf{R}$  particles, they are not the physical parameters and fields. Notice that here we have also used tilded parameters for a reason of convenience to be clear in the following.

The SM relations are obtained in the limit  $g'' \gg \tilde{g}, \tilde{g}'$ . Actually, for a very large  $g''$ , the kinetic terms for the fields  $\mathbf{L}_\mu$  and  $\mathbf{R}_\mu$  drop out, and  $\mathcal{L}$  reduces to the first term in eq. (107). This term reproduces precisely, apart the  $\tilde{\mathbf{W}}$  and  $\tilde{\mathbf{Y}}$  kinetic terms, the mass term for the ordinary gauge vector bosons, provided  $a_1 = 1$ . The fermions couple to  $\mathbf{L}$  and  $\mathbf{R}$  via the mixing with the standard  $\tilde{\mathbf{W}}$  and  $\tilde{\mathbf{Y}}$ . For simplicity direct couplings to the new vector bosons will not be considered here.

Finally in order to have canonical kinetic terms for the gauge fields we perform the rescaling  $\tilde{W} \rightarrow \tilde{g}\tilde{W}$ ,  $\tilde{Y} \rightarrow \tilde{g}'\tilde{Y}$ ,  $\tilde{L} \rightarrow g''\tilde{L}/\sqrt{2}$ ,  $\tilde{R} \rightarrow g''\tilde{R}/\sqrt{2}$ .

## 6.1 Masses and couplings of the new resonances

Notice that the degenerate BESS model in the limit of infinite mass of the new resonances  $\mathbf{L}_\mu$  and  $\mathbf{R}_\mu$  just reproduces the Higgsless SM, provided one redefines

$$\frac{1}{2g^2} = \frac{1}{2\tilde{g}^2} + \frac{1}{g''^2} \quad \frac{1}{2g'^2} = \frac{1}{2\tilde{g}'^2} + \frac{1}{g''^2} \quad (109)$$

Therefore it turns out convenient to reexpress all the physical quantities in terms of  $g$  and  $g'$ .

The new triplets of vector bosons are denoted by  $(L^\pm, L_3)$  and  $(R^\pm, R_3)$ .

In the charged sector the fields  $R^\pm$  remain unmixed for any value of  $g''$ . Their mass is given by:

$$M_{R^\pm}^2 = \frac{v^2}{4} a_2 g''^2 \equiv M^2 \quad (110)$$

In the following we give approximate formulas in the limit  $M \rightarrow \infty$  and  $g'' \rightarrow \infty$ . The exact formulas can be found in [64]. The charged fields  $W^\pm$  and  $L^\pm$  have the following masses:

$$\begin{aligned} M_{W^\pm}^2 &= \frac{v^2}{4} g^2, \\ M_{L^\pm}^2 &= M^2(1 + 2x^2) \end{aligned} \quad (111)$$

where  $x = g/g''$  and  $g$  is the  $SU(2)$  gauge coupling constant defined in eq. (109).

In the neutral sector we have:

$$\begin{aligned} M_Z^2 &= \frac{M_W^2}{c_\theta^2} \\ M_{L_3}^2 &= M^2(1 + 2x^2) \\ M_{R_3}^2 &= M^2(1 + 2x^2 \tan^2 \theta) \end{aligned} \quad (112)$$

where  $\tan \theta = s_\theta/c_\theta = g'/g$  and  $g'$  is the  $U(1)_Y$  gauge coupling constant defined in eq. (109). As already observed for small  $x$  all the new vector resonances are degenerate in mass.

The charged part of the fermionic Lagrangian is

$$\mathcal{L}_{charged} = - (a_W W_\mu^- + a_L L_\mu^-) J_L^{(+)\mu} + h.c. \quad (113)$$

where

$$\begin{aligned} a_W &= \frac{g}{\sqrt{2}} \\ a_L &= -gx \end{aligned} \quad (114)$$

apart from higher order terms in  $x$ , and  $J_L^{(+)\mu} = \bar{\psi}_L \gamma^\mu \tau^+ \psi_L$  with  $\tau^+ = (\tau_1 + i\tau_2)/2$ . Let us notice that the  $R^\pm$  fields are not coupled to the fermions.



In the neutral sector the couplings of the fermions to the gauge bosons are

$$-\frac{1}{2}\bar{\psi}[(v_Z^f + \gamma_5 a_Z^f)\gamma_\mu Z^\mu + (v_{L_3}^f + \gamma_5 a_{L_3}^f)\gamma_\mu L_3^\mu + (v_{R_3}^f + \gamma_5 a_{R_3}^f)\gamma_\mu R_3^\mu]\psi \quad (115)$$

where  $v^f$  and  $a^f$  are the vector and axial-vector couplings given by

$$\begin{aligned} v_Z^f &= AT_3^L + 2BQ_{em} \\ a_Z^f &= AT_3^L \\ v_{L_3}^f &= CT_3^L + 2DQ_{em} \\ a_{L_3}^f &= CT_3^L \\ v_{R_3}^f &= ET_3^L + 2FQ_{em} \\ a_{R_3}^f &= ET_3^L \end{aligned} \quad (116)$$

Notice the different normalization with respect to eq. (63) and eq. (67). In the limit  $M \rightarrow \infty$ ,  $x \rightarrow 0$ ,

$$\begin{aligned} A &= \frac{g}{c_\theta} & B &= -\frac{gs_\theta^2}{c_\theta} \\ C &= -\sqrt{2}gx & D &= 0 \\ E &= \sqrt{2}g\frac{x}{c_\theta}\tan^2\theta & F &= -E \end{aligned} \quad (117)$$

In general, the total width of a vector boson  $V$  corresponding to the decay into fermion - antifermion is

$$\Gamma_V^{fermion} = \Gamma_V^h + 3(\Gamma_V^l + \Gamma_V^\nu) \quad (118)$$

where  $\Gamma_V^h$  includes the contribution of all the allowed quark-antiquark decays. The partial widths are given by

$$\Gamma_V^f = \frac{M_V}{48\pi} F(m_f^2/M_V^2) \quad (119)$$

with

$$F(r_f) = (1 - r_f)^{1/2}((v_V^f)^2(1 + 2r_f) + (a_V^f)^2(1 - 4r_f)) \quad (120)$$

and  $m_f$  the mass of the fermion.

Concerning the new charged resonances, only  $L^\pm$  decay into fermions. The leptonic width is, neglecting fermion masses,

$$\Gamma(L^- \rightarrow l\bar{\nu}_l) = \frac{1}{24\pi} a_L^2 M_L \equiv \Gamma_L^0 \quad (121)$$

The decay widths into quark pairs is

$$\Gamma(L^- \rightarrow q'\bar{q}) = 3|V_{qq'}|^2 \Gamma_L^0 \quad (122)$$

In the case of the  $\bar{t}b$  decay, we have, neglecting the bottom mass:

$$\Gamma(L^- \rightarrow b\bar{t}) = 3|V_{tb}|^2(1 - \frac{3}{2}r_t + \frac{1}{2}r_t^3)\Gamma_L^0 \quad (123)$$

where  $r_t = m_t^2/M_L^2$ .

For the neutral resonances, in the usual limit, at the order  $(g/g'')^2$ , and neglecting the fermion mass corrections we get

$$\begin{aligned} \Gamma_{L_3}^{fermion} &= \frac{2\sqrt{2}G_F M_W^2}{\pi} M_{L_3} \left(\frac{g}{g''}\right)^2 \\ \Gamma_{R_3}^{fermion} &= \frac{10\sqrt{2}G_F M_W^2}{3\pi} \frac{s_\theta^4}{c_\theta^4} M_{R_3} \left(\frac{g}{g''}\right)^2 \\ \Gamma_{L^\pm}^{fermion} &= \frac{2\sqrt{2}G_F M_W^2}{\pi} M_{L^\pm} \left(\frac{g}{g''}\right)^2 \end{aligned} \quad (124)$$

The other possible decay channel for a neutral vector boson  $V$  is the one corresponding to the a  $WW$  pair. The partial width is

$$\begin{aligned} \Gamma_V^W &= \frac{M_V}{192\pi} g_{VW^+W^-}^2 \left(1 - 4\frac{M_W^2}{M_V^2}\right)^{3/2} \left(\frac{M_V}{M_W}\right)^4 \\ &\times \left[1 + 20\left(\frac{M_W}{M_V}\right)^2 + 12\left(\frac{M_W}{M_V}\right)^4\right] \end{aligned} \quad (125)$$

The other possible decay channel for  $L^\pm$  is the one corresponding to a  $WZ$  pair. The partial width is

$$\begin{aligned} \Gamma_L^{WZ} &= \frac{M_L}{192\pi} g_{ZW^+L^-}^2 \left[\left(1 - \frac{M_Z^2 - M_W^2}{M_L^2}\right)^2 - 4\frac{M_W^2}{M_L^2}\right]^{3/2} \left(\frac{M_L^4}{M_W^2 M_Z^2}\right) \\ &\times \left[1 + 10\left(\frac{M_W^2 + M_Z^2}{M_L^2}\right) + \frac{M_W^4 + M_Z^4 + 10M_W^2 M_Z^2}{M_L^4}\right] \end{aligned} \quad (126)$$

The relevant trilinear couplings are, always in the limit of large  $g''$ ,

$$\begin{aligned} g_{L_3 W^+ W^-} &= \sqrt{2}g \frac{g}{g''} \frac{M_W^2}{M^2} \\ g_{R_3 W^+ W^-} &= \sqrt{2}g \frac{s_\theta^2}{c_\theta^2} \frac{g}{g''} \frac{M_W^2}{M^2} \\ g_{ZW^+ L^-} &= \sqrt{2} \frac{g}{c_\theta} \frac{g}{g''} \frac{M_W^2}{M^2} \end{aligned} \quad (127)$$

Using these trilinear gauge couplings we get the following widths:

$$\Gamma_{L_3}^{WW} = \frac{\sqrt{2}G_F M_W^2}{24\pi} M_{L_3} \left(\frac{g}{g''}\right)^2$$

$$\begin{aligned}
\Gamma_{R_3}^{WW} &= \frac{\sqrt{2}G_F M_W^2}{24\pi} \frac{s_\theta^4}{c_\theta^4} M_{R_3} \left( \frac{g}{g''} \right)^2 \\
\Gamma_{L^\pm}^{WZ} &= \frac{\sqrt{2}G_F M_W^2}{24\pi} M_{L^\pm} \left( \frac{g}{g''} \right)^2
\end{aligned} \tag{128}$$

By comparing the widths of the new gauge bosons into vector boson pairs with those into fermions:

$$\begin{aligned}
\Gamma_{L_3}^{fermion} &= 48 \Gamma_{L_3}^{WW} \\
\Gamma_{R_3}^{fermion} &= 80 \Gamma_{R_3}^{WW} \\
\Gamma_{L^\pm}^{fermion} &= 48 \Gamma_{L^\pm}^{WZ}
\end{aligned} \tag{129}$$

we see that the fermionic channel is dominant due to the multiplicity.

As already observed, the absence of couplings among  $U$  and the states  $\mathbf{L}_\mu$  and  $\mathbf{R}_\mu$  results in a suppression of the decay rate of these states into  $W$  and  $Z$ . Consider, for instance, the decay of the new neutral gauge bosons into  $W$  pairs. In a model with only vector resonances this decay channel is largely the dominant one. The corresponding width is indeed given by [60]

$$\Gamma(V \rightarrow WW) = \frac{\sqrt{2}G_F}{192\pi} \frac{M^5}{M_W^2} \left( \frac{g}{g''} \right)^2 \tag{130}$$

and it is enhanced with respect to the partial width into a fermion pair, by a factor  $(M/M_W)^4$

$$\Gamma(V \rightarrow \bar{f}f) \approx G_F M_W^2 \left( \frac{g}{g''} \right)^2 M \tag{131}$$

This fact is closely related to the existence of a coupling of order  $g''$  among  $V$  and the unphysical scalars absorbed by the  $W$  boson. Indeed the fictitious width of  $V$  into these scalars provides, via the Equivalence Theorem [19], a good approximation to the width of  $V$  into a pair of longitudinal  $W$  and it is precisely given by eq. (130).

On the contrary, if there is no direct coupling among the new gauge bosons and the would-be Goldstone bosons which provide the longitudinal degrees of freedom to the  $W$ , then their partial width into longitudinal  $W$ 's will be suppressed compared to the leading behaviour in eq. (130), and the width into a  $W$  pair could be similar to the fermionic width. The same argument also holds for the charged case.

In usual strong interacting models an enhancement of  $W_L W_L$  scattering is expected. Due to the previous considerations, this case is quite different. If we study  $W_L W_L$  scattering the lowest order result violates unitarity at energies above 1.7 TeV, as in the SM in the formal limit  $M_H \rightarrow \infty$ . So we expect this model to be valid up to energies of this order.

## 6.2 Low energy limits

Again one can get limits on the parameter space of the vector axial-vector model by considering the  $\epsilon$  parameters. For the general model of Section 6, at the leading order in the limit of large  $\mathbf{V}$  and  $\mathbf{A}$  masses, one gets [62]

$$\epsilon_1 = \epsilon_2 = 0, \quad \epsilon_3 = (1 - z^2)(g/g'')^2 \quad (132)$$

The axial-vector resonances contribute with opposite sign with respect to the vector particles. This is easily understood by noticing that  $\epsilon_3$  can be expressed in terms of the combination  $(\Pi_{VV} - \Pi_{AA})$  of the correlators of the vector and of the axial-vector currents [53].

The parameter  $z$  is free. Notice that in the degenerate limit  $z = 1$  all the  $\epsilon$  vanish (at the leading order). One can compute the next to leading order in the expansion  $p^2/M^2$  and the result is [64]

$$\begin{aligned} \epsilon_1 &= -\frac{c_\theta^4 + s_\theta^4}{c_\theta^2} X \\ \epsilon_2 &= -c_\theta^2 X \\ \epsilon_3 &= -X \end{aligned} \quad (133)$$

where

$$X = 2 \left( \frac{g}{g''} \right)^2 \frac{M_Z^2}{M^2} \quad (134)$$

All these deviations are of order  $X$  and therefore contain a double suppression factor  $M_Z^2/M^2$  and  $(g/g'')^2$ . The fact that in Degenerate BESS in the limit  $M \rightarrow \infty$  all the  $\epsilon$  vanish follows from the  $(SU(2) \otimes SU(2))^3$  symmetry. Again, assuming the same radiative corrections to the  $\epsilon$  parameters as in the SM with  $M_H = 1 \text{ TeV}$ , that is [46]

$$\epsilon_1 = 3.65 \times 10^{-3} \quad \epsilon_2 = -7.10 \times 10^{-3} \quad \epsilon_3 = 6.38 \times 10^{-3} \quad (135)$$

and considering their experimental values [46], one can derive a 90% C.L. limit in the plane  $(M, g/g'')$ , given in Fig. 2.

For low value of  $M$  we have also considered the bounds from Tevatron. In Fig. 3 we show 95% C.L. upper bounds on  $g/g''$  vs.  $M$  from LEP/Tevatron/SLC data (solid line) and CDF with  $L = 19.7 \text{ pb}^{-1}$  (dashed line). The dotted line corresponds to the extrapolation of the CDF bounds to  $L = 100 \text{ pb}^{-1}$ .

## 6.3 Comparison with technicolor theories

The model of Section 5 (BESS) describes in a rather general way vector resonances; therefore it can be specialized to describe the vector resonances of a theory like technicolor. The idea of hidden gauge symmetries [27], in terms of which BESS can be formulated [26], was successfully used to describe the ordinary strong interacting vector resonances, like  $\rho$  etc. [27].

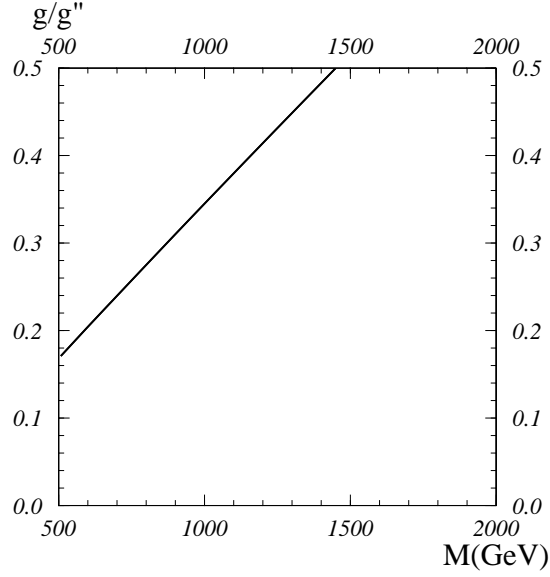


Figure 2: 90% C.L. upper bounds on  $g/g''$  vs.  $M$  in the Degenerate BESS model from the  $\epsilon$  parameters of eq. (133) and LEP/Tevatron/SLC data.

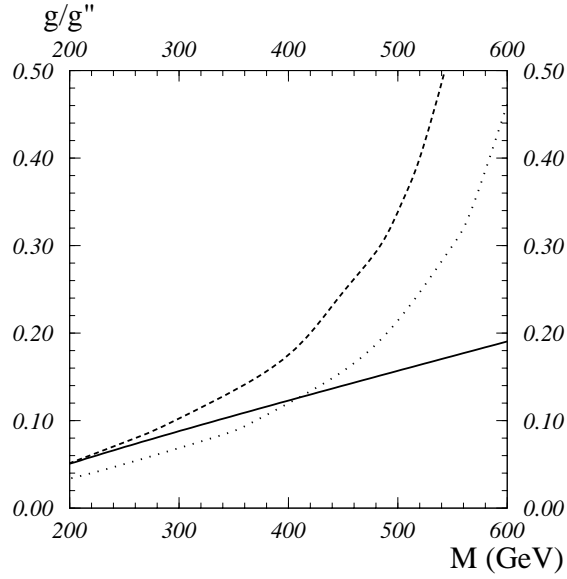


Figure 3: 95% C.L. upper bounds on  $g/g''$  vs.  $M$  in the Degenerate BESS model from LEP/Tevatron/SLC data (solid line) and CDF with  $L = 19.7 \text{ pb}^{-1}$  (dashed line). The dotted line shows the extrapolation of the CDF bounds to  $L = 100 \text{ pb}^{-1}$ .

Technicolor was one of the earliest suggestions [5, 6] to provide for an alternative to the spontaneous symmetry breaking mechanism of the SM, based on elementary scalars, which is considered as theoretically unsatisfactory. The one-doublet model has a single techniquark doublet, of charge  $+1/2$  and  $-1/2$  for anomaly cancellation. The one-family model has four doublets (3 colors + 1 lepton), anomaly cancellation going as in quark-lepton families, with flavor symmetry  $SU(8) \otimes SU(8)$  and  $SU(N_{TC})$  of technicolor. Technifermion condensates break flavor into diagonal  $SU(8)$ , giving 63 Goldstone bosons, three of which provide the  $W, Z$  longitudinal degrees of freedom. Generation of masses for ordinary fermions has led to extended technicolor and is generally associated with difficulties because of the limitations on flavor-changing neutral-currents. To solve these problems, subsequent proposals have been advanced like walking technicolor [16], topcolor assisted technicolor [17] and non commuting extended technicolor [18]. Pseudo-Goldstones are in general a very sensitive and potentially dangerous feature, especially in the original technicolor models. They are absent in the one-doublet model. However in the one-family model some of the 63 pseudo-Goldstones would be low in mass and are expected to be produced as charged scalar pairs from  $e^+e^-$ . Also, virtual pseudo-Goldstones would contribute to radiative corrections. The overall technicolor contribution to electroweak radiative corrections will however result from a number of effects, among which one of the most ambiguous comes from technipions. Therefore, if one realistically believes in the full  $SU(8) \otimes SU(8)$  one-family model, or in a more complicated model, one will have to qualify all the quantitative statements for technicolor because of the ambiguities related at least to technipion masses and calculation of their virtual contributions. A detailed analysis under various assumptions can be found in [66].

The dynamics in technicolor theories is usually believed to be roughly readable from QCD by simply scaling the fundamental scale  $\Lambda_{QCD}$  to  $\Lambda_{TC}$ . In QCD, vector dominance has revealed itself to be a useful concept leading to results comparing very well to the experimental data. Therefore it is natural to assume that vector dominance works as well in technicolor theories as in QCD. In this spirit one can specialize the BESS model to technicolor, as taken in a vector dominance approximation. Strictly speaking, BESS would correspond to a technicolor model involving a single technidoublet. However we will take here the simplest assumption of neglecting dynamical contributions from technipions. By doing so one can specialize BESS also to technicolor models involving more than one technidoublet. To translate BESS parameters into such technicolor specialization [67], we recall that for  $SU(N_{TC})$  of technicolor one scales directly from QCD the techni- $\rho$  mass

$$M_{\rho_{TC}} = M_0 \left( \frac{3}{N_{TC}} \right)^{1/2} \left( \frac{4}{N_d} \right)^{1/2} \quad (136)$$

where  $N_d$  is the number of technidoublets and  $M_0$  is a scale parameter roughly of order  $1 \text{ TeV}$ . As repeatedly said, technicolor dynamics is obtained by scaling QCD, so the Kawarabayashi, Suzuki, Fayazzuddin, Ryazzuddin (KSFR) relations are supposed to be valid also in technicolor. The first KSFR relation for technicolor would read

$$g_{\gamma\rho_{TC}} = 2N_d f_{TC}^2 g_{\rho_{TC}\pi_{TC}\pi_{TC}} \quad (137)$$

relating the  $\gamma - \rho_{TC}$  coupling to the technipion decay-coupling constant and to the  $\rho_{TC} - \pi_{TC} - \pi_{TC}$  trilinear coupling. This relation is automatically satisfied in BESS, where

$$g_{\gamma V} = -\frac{1}{2}\alpha g'' v^2 \quad (138)$$

$$g_{V\pi\pi} = -\frac{1}{4}\alpha g'' \quad (139)$$

with  $v = \sqrt{N_d} f_{TC}$ , the decay coupling constant of the Goldstone  $\pi$ . So this relation does not impose any condition on the BESS parameters  $\alpha$  and  $g''$ . On the other hand the second KSRF relation,

$$M_{\rho_{TC}}^2 = 2N_d f_{TC}^2 g_{\rho_{TC}\pi_{TC}\pi_{TC}}^2 \quad (140)$$

requires  $\alpha = 2$  in the BESS model by using eqs. (49) and (137)-(139). No restrictions are imposed on  $g''$  and by comparing the techni- $\rho$  mass expression (136) to the BESS expression for  $M_V$ , one can establish the following relation between  $g''$  and the product  $N_{TC}N_d$

$$g'' = \frac{M_0}{v} \sqrt{\frac{24}{N_{TC}N_d}} \quad (141)$$

To compare the experimental bounds on BESS with those for technicolor the following relation is useful

$$\frac{g}{g''} = \frac{M_W}{M_0} \sqrt{\frac{N_{TC}N_d}{6}} = \sqrt{2} \frac{M_W}{M_{\rho_{TC}}} \quad (142)$$

Therefore the upper bound for  $g/g''$  can be translated into a lower bound for  $M_{\rho_{TC}}$ .

In technicolor theories one also expects axial-vector resonances. To translate this part in BESS we recall that in the hidden gauge symmetry approach to QCD including axial-vector resonances, one should take the parameter  $z$  equal to  $1/2$ . This follows from vector dominance and Weinberg sum rules. Furthermore one has the Weinberg mass relation  $M_A^2 = 2M_V^2$ . In this case the contribution to the  $\epsilon_3$  parameter comes out  $\epsilon_3 = 3/4(g/g'')^2$ . Therefore using eqs. (29) and (135) we get that QCD rescaled technicolor is strongly excluded.

To complete the technicolor translator for this specialized BESS we consider the role of the  $b$  parameter of BESS, characterizing a direct coupling of  $V$  to the fermions as described in eq. (59). The four-fermion interaction of extended technicolor, of the form

$$\frac{1}{\Lambda_{ETC}^2} \left( \bar{\psi}_{TC}^L \gamma_\mu \frac{\vec{\tau}}{2} \psi_{TC}^L \right) \left( \bar{\psi}_f^L \gamma_\mu \frac{\vec{\tau}}{2} \psi_f^L \right) \quad (143)$$

would induce a similar direct coupling of  $\rho_{TC}$  to fermions, through technifermion loops, given by an effective interaction

$$\frac{1}{\Lambda_{ETC}^2} \frac{M_{\rho_{TC}}^2}{g_{\rho_{TC}\pi_{TC}\pi_{TC}}} \vec{\rho}_{TC} \cdot \vec{J}_L \quad (144)$$

Using eqs. (49) and (139) for the BESS model ( $\alpha = 2$ ), we find (for small  $b$ )

$$b \approx -2 \left( \frac{v}{\Lambda_{ETC}} \right)^2 \quad (145)$$

When translating the specialized BESS to technicolor, one sees that  $b$  can be interpreted as a parameter of extended technicolor, its magnitude being expected to be inversely related to the square of the extended technicolor scale.

## 7 Generalizations

A model describing vector, axial-vector and a scalar resonance has been recently proposed [68]. This is obtained by adding to the Lagrangian  $\mathcal{L}$  of eq. (83) the term

$$\mathcal{L}_S = \frac{1}{2} \partial^\mu S \partial_\mu S - \frac{1}{2} M_S^2 S^2 - \frac{vk}{2} S f(\mathbf{L}_\mu, \mathbf{R}_\mu) \quad (146)$$

where  $S$  is a scalar field singlet under the symmetry group  $G \otimes H' \otimes P$ ,  $k$  is a dimensionless parameter and  $f$  is given in eq. (84).

The scattering amplitude (98) receives an additional contribution

$$A(s, t, u) = \frac{s}{4v^2} (4 - 3\beta) + \frac{\beta M_V^2}{4v^2} \left[ \frac{u - s}{t - M_V^2 + iM_V \Gamma_V} + \frac{t - s}{u - M_V^2 + iM_V \Gamma_V} \right] - \frac{k^2 s^2}{v^2} \frac{1}{s - M_S^2 + i\Gamma_S M_S} \quad (147)$$

It has been shown [68] that in the limit of low energy with respect to the masses of the new resonances the Lagrangian becomes equivalent to the chiral Lagrangian (12) with the following identification

$$\alpha_4 = \frac{(1 - z^2)^2}{4g'^2}, \quad \alpha_4 + \alpha_5 = \frac{kv^2}{8M_S^2} \quad (148)$$

Notice that  $\alpha_4$  can be related to the vector resonance width by

$$\alpha_4 = \frac{12\pi v^4 \Gamma_V}{M_V^5} \quad (149)$$

A model based on Adler-Weisberger sum-rules was recently proposed [69]. It is known from strong interactions that all Adler-Weisberger sum-rules can be satisfied by the four meson states  $\pi$ ,  $\rho$ ,  $\sigma$  and  $a_1$  [70, 71]. Weinberg has also shown [72] that this is a result of the algebraic structure of the broken symmetry and that the zero helicity states of  $\pi$ ,  $\rho$ ,  $\sigma$  and  $a_1$  should form a complete representation of the  $SU(2) \otimes SU(2)$  symmetry. Such a behavior for the electroweak sector inspired the model [69]. Eight Adler-Weisberger sum-rules are satisfied by a scalar resonance  $S$ , a triplet of vectors  $V$ , a triplet of axial-vectors  $A$  and an isoscalar vector  $\omega$ . The sum-rules are satisfied by the following relations

$$M_V^2 = M_\omega^2 = M_S^2 \tan^2 \psi + M_Z^2 (1 - \tan^2 \psi) \quad (150)$$



$$M_A^2 = \frac{M_V^2}{\sin^2 \psi} - M_Z^2 \cot^2 \psi \quad (151)$$

$$g_{SWW}^2 = \frac{4}{v^2} \sin^2 \psi \quad g_{\omega VW}^2 = \frac{4}{v^2} \quad g_{VWW}^2 = \frac{M_V^2}{v^2} \cos^2 \psi \quad (152)$$

$$g_{ASW}^2 = \frac{M_A^2}{v^2} \cos^2 \psi \quad g_{AVW}^2 = \frac{16}{v^2} \frac{M_A^2 M_V^2}{(M_A^2 - M_V^2)^2} \sin^2 \psi \quad (153)$$

where  $\psi$  is a mixing angle. An effective Lagrangian was built in terms of these fields; however many but not all of the relations coming from the sum-rules can be satisfied.

## 8 $e^+e^- \rightarrow f^+f^-$ channel

Before entering into the details of the analysis we briefly review in Table 1 the parameters of the proposed  $e^+e^-$  LC's [73, 74, 75, 76].

Two distinct approaches have been followed; in the first (JLC and NLC) one has developed a design, based on improving the efficiency in using standard copper accelerating cavities, in the second (TESLA) one uses superconducting cavities. CLIC project is based on beam acceleration by traveling wave structures powered by a superconducting drive linac.

In the discussion of the physics at high energy LC's, we start considering the fermion annihilation channels. We would like to analyze the effect of new neutral vector bosons from a strong interacting sector in cross-sections and asymmetries for the channels  $e^+e^- \rightarrow l^+l^-$  and  $e^+e^- \rightarrow q\bar{q}$ .

In principle the neutral resonances could be produced as real resonances if their mass is known to be below the collider energy by just tuning the beam energies. In this case the machine could operate like a  $Z'$  factory and the properties of these new resonances can be studied with precision by measuring the line shape.

If instead the masses are higher than the maximum c.m. energy, they would give rise to indirect effects in the  $e^+e^- \rightarrow f^+f^-$  that we discuss below.

	TESLA	JLC	NLC	CLIC	TESLA	NLC	CLIC
$E_{CM}(GeV)$	500	500	500	500	800	1000	1000
$\mathcal{L}(10^{33})$	6	5.2	7.1	4.8	5.7	14.5	10
$grad(MV/m)$	25	73	50	80	40	85	80
$LClength(km)$	33	10.4	15.6	11.2	33	18.7	20.0

**Table 1:** Parameters of proposed linear colliders and of their upgrading.  $\mathcal{L}$  is the final luminosity.

The clean environment of  $e^+e^-$  colliders allows to study these virtual effects. One could take into account radiative corrections and in particular initial state QED corrections. However one can remove the effect of these corrections by a suitable cut on the photon energy  $E_\gamma/E_{beam} < 1 - M_Z^2/s$  [77]. We perform first a general study of the observables, giving the analytical formulas for cross sections and asymmetries in the case of the BESS model or for a new triplet of vector bosons. The case of two triplets can be easily derived from these equations and can be found in [64].

An analysis of the effect of new vector particles from a strong electroweak symmetry breaking sector on the lepton and hadron channels was also done in [78]. The authors use a formalism where the corresponding oblique corrections to cross-sections and asymmetries are expressed as once subtracted dispersion integrals. The subtraction constants are provided by using LEP results.

## 8.1 Observables

In models with additional gauge vector bosons one usually performs the analysis using the following observables:

$$\begin{aligned} &\sigma^\mu, \quad R = \sigma^h/\sigma^\mu \\ &A_{FB}^{e^+e^- \rightarrow \mu^+\mu^-}, \quad A_{FB}^{e^+e^- \rightarrow \bar{b}b} \\ &A_{LR}^{e^+e^- \rightarrow \mu^+\mu^-}, \quad A_{LR}^{e^+e^- \rightarrow \bar{b}b}, \quad A_{LR}^{e^+e^- \rightarrow had} \end{aligned} \quad (154)$$

with  $\sigma^{h(\mu)}$  the total hadronic ( $\mu^+\mu^-$ ) cross section.  $A_{FB}$  is the forward-backward asymmetry given by

$$A_{FB} = \frac{\sigma_F - \sigma_B}{\sigma_F + \sigma_B} \quad (155)$$

where  $\sigma_{F,B}$  are respectively the cross sections in the forward and backward hemispheres of the detector, and  $A_{LR}$  the left-right asymmetry

$$A_{LR} = \frac{\sigma_L - \sigma_R}{\sigma_L + \sigma_R} \quad (156)$$

where  $\sigma_{L,R}$  are the cross sections for left and right longitudinal polarization states of the incoming electron.

The total cross section for the process  $e^+e^- \rightarrow f^+f^-$  is given by (at tree level)

$$\sigma = \frac{\pi\alpha_{em}^2 s}{3} \sum_{h_f, h_e} |F(h_f, h_e)|^2 \quad (157)$$

with  $\alpha_{em} = e^2/(4\pi)$  and

$$F(h_f, h_e) = -\frac{1}{s}e_f + \frac{(v_Z^f + h_f a_Z^f)(v_Z + h_e a_Z)}{s - M_Z^2 + iM_Z\Gamma_Z} + \frac{(v_V^f + h_f a_V^f)(v_V + h_e a_V)}{s - M_V^2 + iM_V\Gamma_V} \quad (158)$$

where  $h_f, h_e = \pm 1$  are the helicities of  $f$  and  $e$  respectively,  $e_f$  is the electric charge of  $f$  (in units of  $e_{\text{proton}} = 1$ ),  $v_{Z,V} = v_{Z,V}^e$  and  $a_{Z,V} = a_{Z,V}^e$ , and  $\Gamma_{Z,V}$  are the widths of the neutral gauge bosons. For instance for the BESS model the couplings are given in eq. (67).

The forward-backward asymmetry in the present case is given by

$$A_{FB}^{e^+e^- \rightarrow f^+f^-} = \frac{x}{1 + \frac{1}{3}x^2} \frac{(1-P) \sum_{h_f, h_e} h_f h_e |F(h_f, h_e)|^2 + 2P \sum_{h_f} h_f |F(h_f, 1)|^2}{(1-P) \sum_{h_f, h_e} |F(h_f, h_e)|^2 + 2P \sum_{h_f} |F(h_f, 1)|^2} \quad (159)$$

where  $x$  is the detector acceptance ( $x \leq 1$ ), and  $P$  is the degree of longitudinal polarization of the electron beam. In the analysis presented in Section 10 and Section 11  $x = 1$  is assumed.

The left-right asymmetry is given by

$$A_{LR}^{e^+e^- \rightarrow f^+f^-} = P \frac{\sum_{h_f, h_e} h_e |F(h_f, h_e)|^2}{\sum_{h_f, h_e} |F(h_f, h_e)|^2} \quad (160)$$

The notations are the same as for the forward-backward asymmetry.

## 9 $e^+e^- \rightarrow WW$ channel

In this Section we will consider the  $WW$  channel, which is expected to be more sensitive, at high energy, than the  $f\bar{f}$  channel to effects coming from a strongly interacting electroweak symmetry breaking sector. In the case of a vector resonance this is simply due to the strong coupling between the resonance and the longitudinal  $W$  bosons. Furthermore this interaction, in general, destroys the fine cancellation between the  $\gamma - Z$  exchange and the neutrino contribution occurring in the SM. This effect gives rise, for instance in the case of the BESS model, to a differential cross-section increasing linearly with  $s$ . However this is no more true in the Degenerate BESS model due to the cancellation between the vector and axial-vector resonances.

Usually one considers the  $WW$  channel, with one  $W$  decaying leptonically and the other hadronically. The main reason for choosing this decay channel is to get a clear signal to reconstruct the polarization of the  $W$ 's (see for example [79]).

In fact by reconstructing the decay of  $W$  pairs one can get information on their helicities, as shown by the decay angular distributions

$$d\Gamma/d\cos\theta \sim \begin{cases} (1 + \cos\theta)^2 & h_W = -1 \\ 2\sin^2\theta & h_W = 0 \\ (1 - \cos\theta)^2 & h_W = +1 \end{cases} \quad (161)$$

where we have denoted by  $\theta$  the polar  $W^-$  decay angle and by  $h_W$  its helicity. Simulation studies and reconstruction of decay angles of  $W$  can be found in [80].

Furthermore longitudinally polarized beams will be considered; in fact by selecting initial polarized beams one can enhance the final polarization. For instance an initial  $e_R^-$  beam produces mostly longitudinal  $W$  pairs.

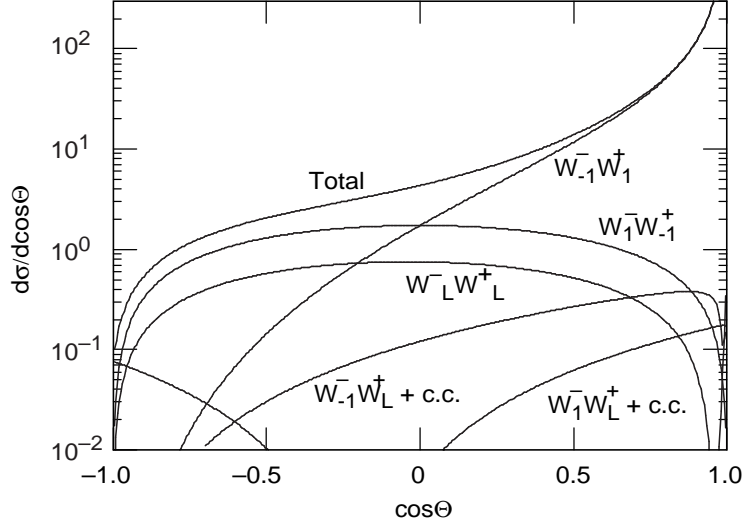


Figure 4: Angular distributions for  $W$  bosons of various helicity in  $e_L^- e_R^+ \rightarrow W^+ W^-$ . The differential cross sections are given in units of  $R = 86.8 \text{ fb/s}(TeV^2)$  at  $\sqrt{s} = 1 \text{ TeV}$ , from [81].

The reaction  $e_L^- e_R^+ \rightarrow W^+ W^-$  is shown in Fig. 4. The subscripts 1, -1,  $L$ , denote the transverse and longitudinal helicity polarization states of a massive vector boson. For initial  $e_R$  the cross section is dominantly  $W_L W_L$  with a rate 1/5 with respect to the  $W_L W_L$  cross section shown in Fig. 4 [81].

## 9.1 Observables

Let us consider first the following observables: the differential cross section and the left right asymmetry

$$\begin{aligned} \frac{d\sigma}{d\cos\Theta}(e^+e^- \rightarrow W^+W^-) \\ A_{LR}^{e^+e^- \rightarrow W^+W^-} = \left( \frac{d\sigma}{d\cos\Theta}(P_e = +P) - \frac{d\sigma}{d\cos\Theta}(P_e = -P) \right) / \frac{d\sigma}{d\cos\Theta} \end{aligned} \quad (162)$$

where  $\Theta$  is the  $e^+e^-$  center of mass scattering angle. In the  $e^+e^-$  center of mass frame the angular distribution  $d\sigma/d\cos\Theta$  and the left-right asymmetry read [82]

$$\begin{aligned} \frac{d\sigma}{d\cos\Theta} = & \frac{2\pi\alpha_{em}^2 p}{\sqrt{s}} \left\{ 2a_W^4 \left[ \frac{4}{M_W^2} + p^2 \sin^2\Theta \left( \frac{1}{M_W^4} + \frac{4}{t^2} \right) \right] \right. \\ & + G_1 p^2 \left[ \frac{4s}{M_W^2} + \left( 3 + \frac{sp^2}{M_W^4} \right) \sin^2\Theta \right] \\ & \left. + G'_1 \left[ 8 \left( 1 + \frac{M_W^2}{t} \right) + 16 \frac{p^2}{M_W^2} + \frac{p^2}{s} \sin^2\Theta \left( \frac{s^2}{M_W^4} - 2 \frac{s}{M_W^2} - 4 \frac{s}{t} \right) \right] \right\} \end{aligned} \quad (163)$$

and

$$\begin{aligned}
A_{LR}(\cos \Theta) = & -P \frac{2\pi\alpha_{em}^2 p}{\sqrt{s}} \left\{ 2a_W^4 \left[ \frac{4}{M_W^2} + p^2 \sin^2 \Theta \left( \frac{1}{M_W^4} + \frac{4}{t^2} \right) \right] \right. \\
& + G_2 p^2 \left[ \frac{4s}{M_W^2} + \left( 3 + \frac{sp^2}{M_W^4} \right) \sin^2 \Theta \right] \\
& + G'_1 \left[ 8 \left( 1 + \frac{M_W^2}{t} \right) + 16 \frac{p^2}{M_W^2} \right. \\
& \left. \left. + \frac{p^2}{s} \sin^2 \Theta \left( \frac{s^2}{M_W^4} - 2 \frac{s}{M_W^2} - 4 \frac{s}{t} \right) \right] \right\} / \frac{d\sigma}{d \cos \Theta}
\end{aligned} \tag{164}$$

where

$$\begin{aligned}
p = & \frac{1}{2} \sqrt{s} (1 - 4M_W^2/s)^{1/2} \\
t = & M_W^2 - \frac{1}{2} s [1 - \cos \Theta (1 - 4M_W^2/s)^{1/2}]
\end{aligned} \tag{165}$$

The quantity  $a_W$  is the  $\nu e W$  coupling and is given in eq. (63) for the BESS model. Furthermore

$$\begin{aligned}
G_1 = & \left( \frac{e_e}{s} \right)^2 + (v_Z^2 + a_Z^2) g_{ZWW}^2 \frac{1}{(s - M_Z^2)^2 + M_Z^2 \Gamma_Z^2} \\
& + 2 \frac{e_e}{s} v_Z g_{ZWW} \frac{s - M_Z^2}{(s - M_Z^2)^2 + M_Z^2 \Gamma_Z^2} \\
& + (v_V^2 + a_V^2) g_{VWW}^2 \frac{1}{(s - M_V^2)^2 + M_V^2 \Gamma_V^2} \\
& + 2 \frac{e_e}{s} v_V g_{VWW} \frac{s - M_V^2}{(s - M_V^2)^2 + M_V^2 \Gamma_V^2} \\
& + 2(v_Z v_V + a_Z a_V) g_{ZWW} g_{VWW} \\
& \times \frac{(s - M_Z^2)(s - M_V^2) + M_Z \Gamma_Z M_V \Gamma_V}{[(s - M_Z^2)^2 + M_Z^2 \Gamma_Z^2][(s - M_V^2)^2 + M_V^2 \Gamma_V^2]}
\end{aligned} \tag{166}$$

$$\begin{aligned}
G'_1 = & a_W^2 \left[ \frac{e_e}{s} \right. \\
& + g_{ZWW} (v_Z + a_Z) \frac{s - M_Z^2}{(s - M_Z^2)^2 + M_Z^2 \Gamma_Z^2} \\
& \left. + g_{VWW} (v_V + a_V) \frac{s - M_V^2}{(s - M_V^2)^2 + M_V^2 \Gamma_V^2} \right]
\end{aligned} \tag{167}$$

$$G_2 = 2 \left( \frac{e_e}{s} a_Z g_{ZWW} \frac{s - M_Z^2}{(s - M_Z^2)^2 + M_Z^2 \Gamma_Z^2} + \frac{e_e}{s} a_V g_{VWW} \frac{s - M_V^2}{(s - M_V^2)^2 + M_V^2 \Gamma_V^2} \right)$$

$$\begin{aligned}
& +a_Z v_Z g_{ZWW}^2 \frac{1}{(s - M_Z^2)^2 + M_Z^2 \Gamma_Z^2} + a_V v_V g_{VWW}^2 \frac{1}{(s - M_V^2)^2 + M_V^2 \Gamma_V^2} \\
& + (a_Z v_V + v_Z a_V) g_{ZWW} g_{VWW} \\
& \times \frac{(s - M_Z^2)(s - M_V^2) + M_Z \Gamma_Z M_V \Gamma_V}{[(s - M_Z^2)^2 + M_Z^2 \Gamma_Z^2][(s - M_V^2)^2 + M_V^2 \Gamma_V^2]}
\end{aligned} \tag{168}$$

where  $g_{VWW}$  and  $g_{ZWW}$ , for the BESS model, are given in eq. (77) and eq. (78).

Assuming that the final  $W$  polarization can be reconstructed, using the  $W$  decay distributions, it is convenient to examine the cross sections for  $W_L W_L$ ,  $W_T W_L$ , and  $W_T W_T$ . One has [83]

$$\begin{aligned}
\frac{d\sigma_{LL}}{d\cos\Theta} = & \frac{2\pi\alpha_{em}^2 p}{\sqrt{s}} \left\{ \frac{a_W^4}{8} \frac{1}{M_W^4} \frac{1}{t^2} [s^3(1 + \cos^2\Theta) - 4M_W^4(3s + 4M_W^2) \right. \\
& - 4(s + 2M_W^2)p\sqrt{s}\cos\Theta] \sin^2\Theta \\
& + \frac{1}{16} G_1 \frac{1}{M_W^4} \sin^2\Theta (s^3 - 12sM_W^4 - 16M_W^6) \\
& + G_1' \sin^2\Theta \frac{1}{2t} [ps\sqrt{s}\cos\Theta \frac{1}{2M_W^4} (s + 2M_W^2) \\
& \left. - \frac{1}{4M_W^4} (s^3 - 12sM_W^4 - 16M_W^6)] \right\}
\end{aligned} \tag{169}$$

$$\begin{aligned}
\frac{d\sigma_{TL}}{d\cos\Theta} = & \frac{2\pi\alpha_{em}^2 p}{\sqrt{s}} \left\{ a_W^4 \frac{1}{t^2 M_W^2} [s^2(1 + \cos^4\Theta) + 4M_W^4(1 + \cos^2\Theta) \right. \\
& - 4(4p^2 + s\cos^2\Theta)p\sqrt{s}\cos\Theta + 2s(s - 6M_W^2)\cos^2\Theta - 4sM_W^2] \\
& + 2G_1 s \frac{p^2}{M_W^2} (1 + \cos^2\Theta) \\
& \left. + 2G_1' \frac{p\sqrt{s}}{t M_W^2} [\cos\Theta(4p^2 + s\cos^2\Theta) - 2p\sqrt{s}(1 + \cos^2\Theta)] \right\}
\end{aligned} \tag{170}$$

$$\begin{aligned}
\frac{d\sigma_{TT}}{d\cos\Theta} = & \frac{2\pi\alpha_{em}^2 p}{\sqrt{s}} \left\{ 2a_W^4 \frac{1}{t^2} [s(1 + \cos^2\Theta) - 2M_W^2 - 2p\sqrt{s}\cos\Theta] \sin^2\Theta \right. \\
& \left. + 2G_1 p^2 \sin^2\Theta + G_1' \frac{\sin^2\Theta}{2t} [4p\sqrt{s}\cos\Theta - 8p^2] \right\}
\end{aligned} \tag{171}$$

The left-right asymmetries for longitudinal and/or transverse polarized  $W$  can be easily obtained as in eq. (164).

At LEP II we can add to the previous observables the  $W$  mass measurement, coming from the  $e^+e^- \rightarrow WW$  channel.

## 10 Results for the BESS model

Let us first discuss the fermion channel.

The results we will present are obtained by performing a  $\chi^2$  comparison between the BESS predictions and the SM ones for the observables  $\mathcal{O}_i$  discussed in Section 8.1:

$$\chi^2 = \sum_{i=1}^n \left[ \frac{\mathcal{O}_i - \mathcal{O}_i^{SM}}{\delta \mathcal{O}_i} \right]^2 \quad (172)$$

Following the existing studies of 500 GeV  $e^+e^-$  linear colliders [84, 85], we present the results assuming a relative systematic error in luminosity of  $\delta\mathcal{L}/\mathcal{L} = 1\%$ ,  $\delta\epsilon_{\text{hadr}}/\epsilon_{\text{hadr}} = 1\%$ , and  $\delta\epsilon_{\mu}/\epsilon_{\mu} = 0.5\%$ , where  $\epsilon_{\text{hadr},\mu}$  denote the selection efficiencies. The same systematic errors for the 1 and 2 TeV machines are also assumed.

Finally integrated luminosities  $L = 20 \text{ fb}^{-1}$  for  $\sqrt{s} = 500 \text{ GeV}$ ,  $L = 80 \text{ fb}^{-1}$  for  $\sqrt{s} = 1 \text{ TeV}$ , and  $L = 20 \text{ fb}^{-1}$  for  $\sqrt{s} = 2 \text{ TeV}$  have been considered.

Unfortunately the most sensitive observables are the left-right asymmetries, which means that, if the beams are not polarized, one does practically get no advantage over LEP from this channel.

The contours shown in Fig. 5 correspond to the regions which are allowed at 90% C.L. in the plane  $(b, g/g'')$ , assuming that the BESS deviations for the observables of eq. (154) from the SM predictions are within the experimental errors. The results are obtained assuming a longitudinal polarization of the electron  $P = 0.5$  (solid line) and  $P = 0$  (dashed line). In Fig. 5 the energy of the collider is  $\sqrt{s} = 500 \text{ GeV}$  and the mass of the vector resonance  $M_V = 600 \text{ GeV}$ . It is clear that there is no big improvement with respect to the already existing bounds from LEP. Increasing the energy of the machine does not drastically change the results.

All these conclusions become much more negative if one assumes a higher systematic error for the hadron selection efficiency. Therefore in conclusions the fermion channel is not much efficient in this case.

Let us then consider the  $W$  channel.

Fig. 6 shows the deviations of the BESS model with respect to the SM for  $b = 0.01$  and  $g/g'' = 0.04$ ,  $M_V = 600 \text{ GeV}$ , for the longitudinally polarized  $W$  differential cross-section at  $\sqrt{s} = 500 \text{ GeV}$ . The branching ratio for decay of one  $W$  leptonically and the other hadronically is included. The continuous line represents the BESS prediction and the dashed line the SM one.

The following systematics have been assumed:  $\delta B/B = 0.005$  [87], where  $B$  denotes the product of the branching ratio for  $W \rightarrow \text{hadrons}$  and that for  $W \rightarrow \text{leptons}$ , 1% for the reconstruction efficiency, 1% for luminosity relative errors. An angular cut has been imposed on the  $W$  scattering angle ( $|\cos \Theta| \leq 0.95$ ) and 18 angular bins have been considered.

An overall detection efficiency of 10% including the branching ratio  $B = 0.29$  and the loss of luminosity from beamstrahlung [79] has been assumed.

As already noticed [86], the bigger deviations are away from the forward region. In the longitudinal channel the deviations are much bigger and concentrated in the central region.

For a collider at  $\sqrt{s} = 500 \text{ GeV}$  the results are illustrated in Fig. 7. This figure illustrates the 90% C.L. allowed regions for  $M_V = 600 \text{ GeV}$  obtained by considering the

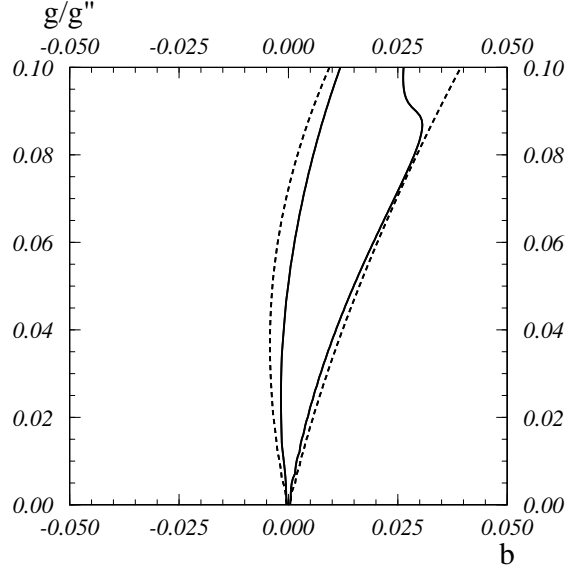


Figure 5: BESS 90% C.L. contours in the plane  $(b, g/g'')$  for  $\sqrt{s} = 500 \text{ GeV}$  and  $M_V = 600 \text{ GeV}$  from the fermion channel. The solid line corresponds to polarization  $P = 0.5$  while the dashed line is for unpolarized electron beams. The allowed regions are the internal ones.

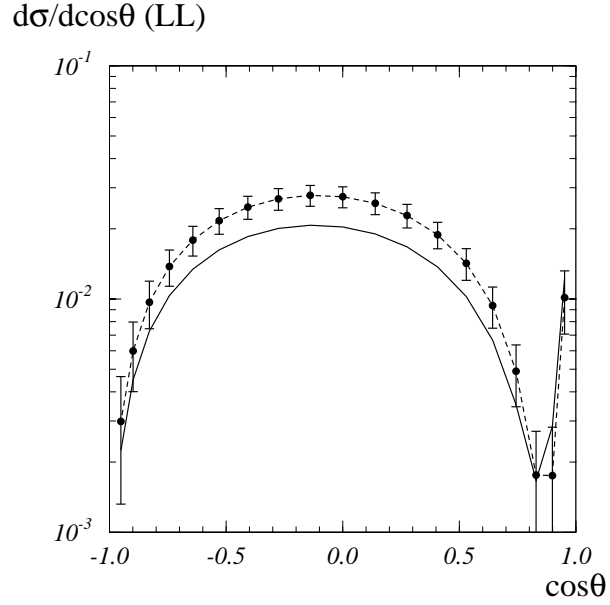


Figure 6: Differential cross section  $d\sigma/d\cos\Theta(W_L W_L)$  for the BESS model for  $b = 0.01$ ,  $g/g'' = 0.04$  and  $M_V = 600 \text{ GeV}$  (continuous line) and for the SM (dashed line). The error bars are also shown.



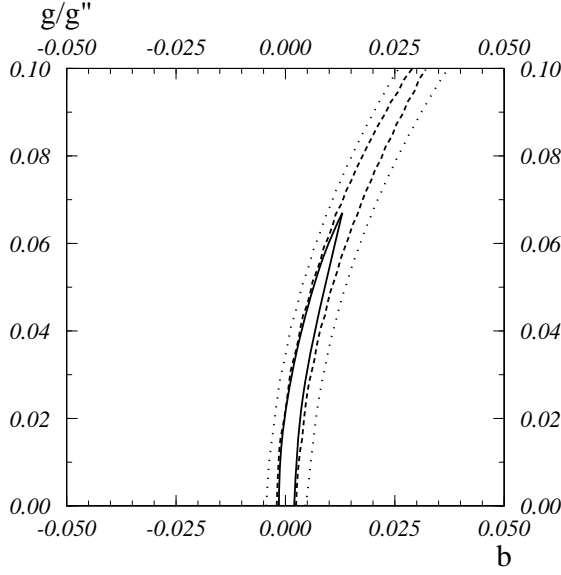


Figure 7: BESS 90% C.L. contours in the plane  $(b, g/g'')$  for  $\sqrt{s} = 500 \text{ GeV}$  and  $M_V = 600 \text{ GeV}$ . The dotted line corresponds to the bound from the  $WW$  differential cross section, the dashed line to the bound from  $W_L W_L$  differential cross section, and the continuous line to the bound combining the differential  $W_{L,T} W_{L,T}$  cross sections and  $WW$  left-right asymmetries.

unpolarized  $WW$  differential cross-section (dotted line), the  $W_L W_L$  cross section (dashed line), and the combination of the left-right asymmetry with all the differential cross-sections for the different final  $W$  polarizations (solid line). We see that measurements of cross-sections for polarized  $W$  allow to get important restrictions with respect to LEP.

For colliders with  $\sqrt{s} = 1, 2 \text{ TeV}$  and for  $M_V = 1.2$  and  $2.5 \text{ TeV}$  respectively, the allowed region, combining all the observables, reduces in practice to a line and the analysis is better discussed in the plane  $(M_V, g/g'')$ , as we shall see later on. Therefore, even the unpolarized  $WW$  differential cross section measurements can improve the bounds.

In Fig. 8 we show the restrictions in the plane  $(M_V, g/g'')$  for three different choices of the collider energy, assuming the same integrated luminosity of  $20 \text{ fb}^{-1}$ . It is a 90% C.L. contour for  $\sqrt{s} = 0.3, 0.5, 1 \text{ TeV}$  and  $b = 0$ . The solid line represents the upper bound on  $g/g''$  from the unpolarized  $WW$  differential cross-section, the dashed line from the combination of the left-right asymmetry with all the differential cross-sections for the different final  $W$  polarizations.

In Fig. 9 the 90% C.L. upper bound on  $g/g''$  are shown for  $M_V = 1.5 \text{ TeV}$  and  $b = 0$  as a function of the center of mass of the LC for  $20 \text{ fb}^{-1}$ . The lines correspond to unpolarized  $WW$  differential cross-section (solid),  $W_L W_L$  differential cross-section (dashed), the combination of the left-right asymmetry with all the differential cross-sections for the different final  $W$  polarizations (dotted line), all the  $W$  and fermion observables (dash-dotted). The black dots correspond to  $80 \text{ fb}^{-1}$  of integrated luminosity.

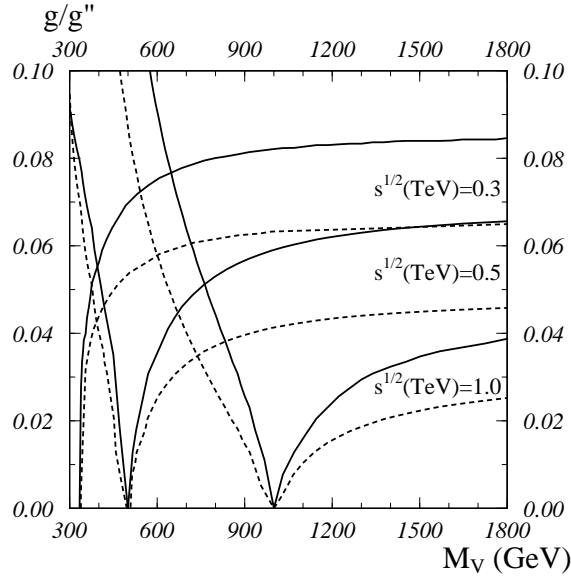


Figure 8: BESS 90% C.L. contours in the plane  $(M_V, g/g'')$  for  $\sqrt{s} = 0.3, 0.5, 1 \text{ TeV}$ ,  $L = 20 \text{ fb}^{-1}$  and  $b = 0$ . The solid line corresponds to the bound from the unpolarized  $WW$  differential cross section, the dashed line to the bound from all the polarized differential cross sections  $W_L W_L$ ,  $W_T W_L$ ,  $W_T W_T$  combined with the  $WW$  left-right asymmetries. The lines give the upper bounds on  $g/g''$ .

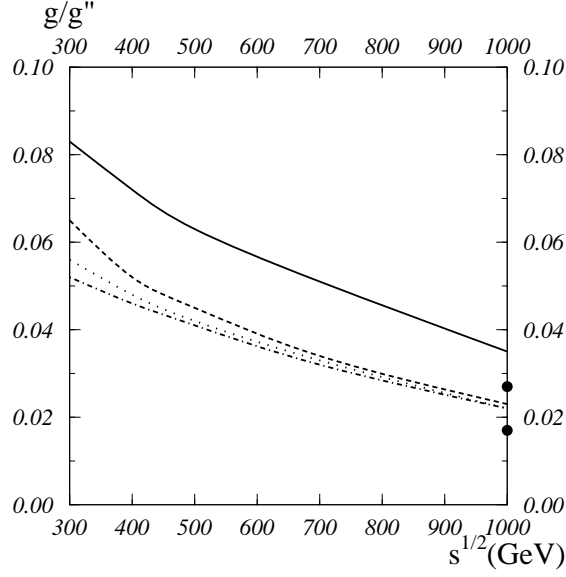


Figure 9: BESS 90% C.L. contours in the plane  $(\sqrt{s}, g/g'')$  for  $M_V = 1.5 \text{ TeV}$ ,  $b = 0$  and  $L = 20 \text{ fb}^{-1}$  from the unpolarized  $WW$  differential cross section (solid line), from the  $W_L W_L$  differential cross section (dashed line), from all the differential cross sections for  $W_L W_L$ ,  $W_T W_L$ ,  $W_T W_T$  combined with the  $WW$  left-right asymmetries (dotted line) and from all the  $WW$  and fermion observables with  $P = 0.5$  (dash-dotted line). The black dots are the bounds for the unpolarized  $WW$  differential cross section and from all the  $WW$  and fermion observables by considering  $\sqrt{s} = 1 \text{ TeV}$  and  $L = 80 \text{ fb}^{-1}$ . The lines give the upper bounds on  $g/g''$ .

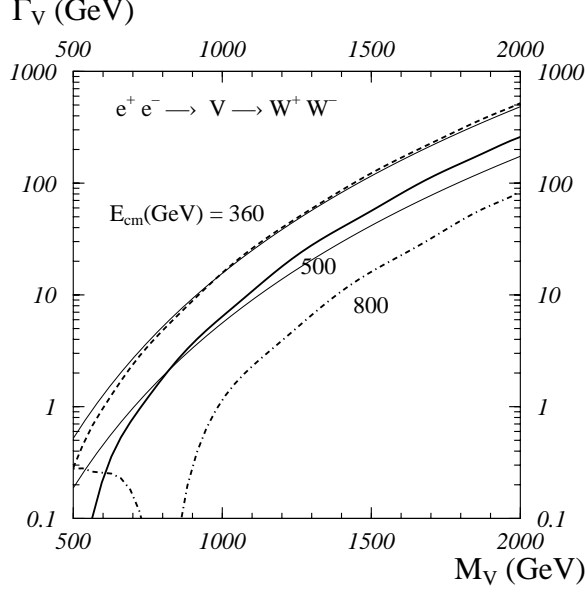


Figure 10: 90% C.L. contour in the  $(M_V, \Gamma_V)$  plane from measurements of differential cross sections and left-right asymmetries;  $W$  polarizations are reconstructed from the decay in lepton and quark jets. Energy and luminosity are the following:  $\sqrt{s} = 360 \text{ GeV}$ ,  $L = 10 \text{ fb}^{-1}$  (dashed)  $\sqrt{s} = 500 \text{ GeV}$ ,  $L = 20 \text{ fb}^{-1}$  (solid) and  $\sqrt{s} = 800 \text{ GeV}$ ,  $L = 80 \text{ fb}^{-1}$  (dash-dotted). The lower narrow solid line is the limit from LEP measurements. The upper narrow solid line is obtained by considering the deviation with respect to the SM prediction and assuming the LEP errors for the corresponding observables.

In Fig. 10 the regions in the parameter space  $(M_V, \Gamma_V)$  which can be probed at  $\sqrt{s} = 360 \text{ GeV}$ ,  $L = 10 \text{ fb}^{-1}$  (dashed),  $\sqrt{s} = 500 \text{ GeV}$ ,  $L = 20 \text{ fb}^{-1}$  (continuous) and  $\sqrt{s} = 800 \text{ GeV}$ ,  $L = 50 \text{ fb}^{-1}$  (dot-dashed) by measuring  $W_{L,T}W_{L,T}$  differential cross sections and left-right asymmetries are shown. The lower narrow solid line is the limit from LEP measurements. The upper narrow solid line is obtained by considering the deviation with respect to the SM prediction and assuming the LEP errors for the corresponding observables.

For instance for  $\sqrt{s} = 500 \text{ GeV}$ , one is sensitive for  $M_V = 2 \text{ TeV}$  to  $\Gamma_V \geq 250 \text{ GeV}$ , for  $M_V = 1.5 \text{ TeV}$  to  $\Gamma_V \geq 60 \text{ GeV}$ , in agreement with Barklow results [88].

In conclusion measurements of cross sections with different final  $W$  polarizations at a LC with  $\sqrt{s} = 500 \text{ GeV}$  improve LEP bounds up to  $M_V \sim 800 \text{ GeV}$ . At  $\sqrt{s} = 800 \text{ GeV}$  the sensitivity exceeds the LEP bound for all values of  $M_V$ .

This is a more conservative result with respect to [88] and [89] mainly because the BESS model takes into account the mixing of the new vector bosons to the usual  $\gamma$ ,  $W$  and  $Z$  gauge bosons and as a consequence LEP bounds have to be considered.

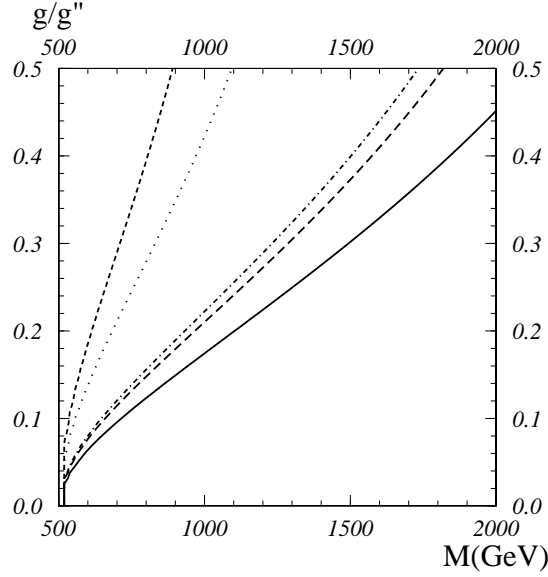


Figure 11: Degenerate BESS 90% C.L. contours on the plane  $(M, g/g'')$  from  $e^+e^-$  at  $\sqrt{s} = 500 \text{ GeV}$  with an integrated luminosity of  $20 \text{ fb}^{-1}$  for various observables. The dash-dotted line represents the limit from  $\sigma^h$  with an assumed error of 2%; the dashed line near the latter is  $\sigma^\mu$  (error 1.3%); the dotted line is  $A_{FB}^\mu$  (error 0.5%); the uppermost dashed line is  $A_{FB}^b$  (error 0.9%). The continuous line represents the combined limits.

## 11 Results for the Degenerate BESS

In this Section we present an analysis done for the model with two new resonances, vector and axial-vector degenerate in mass (Degenerate BESS model). As already observed the model evades the LEP bounds and therefore low masses are still allowed for these new resonances.

With respect to the previous analysis where the  $WW$  channel is the dominant one, here the fermion channel is much more relevant.

The comparison with LEPI bounds shows that LEPII do not improve considerably the existing limits [90].

To further test the model the following options for a high energy  $e^+e^-$  collider have been studied:  $\sqrt{s} = 360 \text{ GeV}$  with an integrated luminosity of  $L = 10 \text{ fb}^{-1}$ ,  $\sqrt{s} = 500 \text{ GeV}$   $L = 20 \text{ fb}^{-1}$ ,  $\sqrt{s} = 800 \text{ GeV}$   $L = 50 \text{ fb}^{-1}$  and  $\sqrt{s} = 1 \text{ TeV}$   $L = 80 \text{ fb}^{-1}$ .

In Fig. 11 the 90% C.L. contour on the plane  $(M, g/g'')$  from  $e^+e^-$  at  $\sqrt{s} = 500 \text{ GeV}$  with an integrated luminosity of  $20 \text{ fb}^{-1}$  for various observables are compared. The dash-dotted line represents the limit from  $\sigma^h$ ; the dashed line near the latter is  $\sigma^\mu$ , the dotted line is  $A_{FB}^\mu$  and the uppermost dashed line is  $A_{FB}^b$ . It is evident that more stringent bounds come from the cross section measurements. Asymmetries give less restrictive bounds because of a compensation between  $L_3$  and  $R_3$  exchange. By combining all the deviations in the previously considered observables we get the limit shown in Fig. 11 by

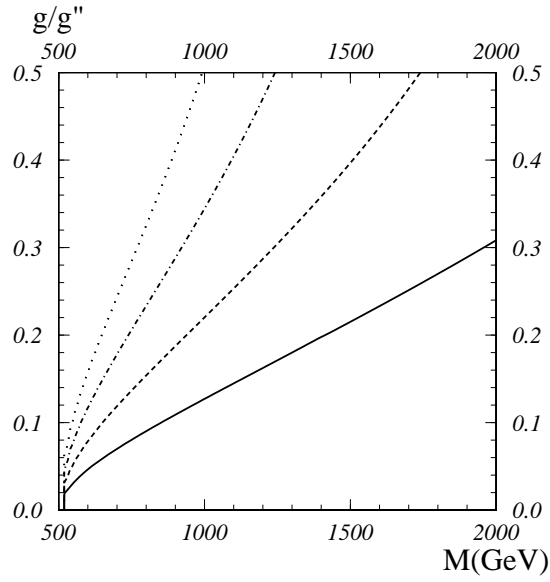


Figure 12: Degenerate BESS 90% C.L. contour on the plane  $(M, g/g'')$  from  $e^+e^-$  at  $\sqrt{s} = 500 \text{ GeV}$  with an integrated luminosity of  $20 \text{ fb}^{-1}$  and a polarization  $P = 0.5$  for various observables. The dash-dotted line represents the limit from  $A_{LR}^\mu$  with an assumed error of 0.6%; the dashed line is  $A_{LR}^h$  (error 0.4%); the dotted line is  $A_{LR}^b$  (error 1.1%). The continuous line is obtained by combining the polarized and the unpolarized observables:  $\sigma^h$ ,  $\sigma^\mu$ ,  $A_{FB}^\mu$ ,  $A_{FB}^b$ ,  $A_{LR}^\mu$ ,  $A_{LR}^h$ ,  $A_{LR}^b$ .

the continuous line.

Polarized electron beams allow to get further limit on the parameter space as shown in Fig. 12. The error on the measurement of the polarization has been neglected and the polarization  $P = 0.5$ . The dash-dotted line represents the limit from  $A_{LR}^\mu$ , the dashed line from  $A_{LR}^h$ , the dotted line from  $A_{LR}^b$ . The bound shown in Fig. 12 by the continuous line is obtained by combining all the polarized and unpolarized beam observables. In conclusion even without polarized beams a substantial improvement with respect to the LEP bound is obtained.

As expected, increasing the energy of the collider and rescaling the integrated luminosity result in stronger bounds on the parameter space (the comparison of different LC's results is made in Section 17).

Let us finally consider the  $WW$  final state.

An angular cut has been imposed on the  $W$  scattering angle ( $|\cos \Theta| \leq 0.95$ ) and 18 angular bins have been considered. An overall detection efficiency of 10%, including the branching ratio  $B = 0.29$  and the loss of luminosity by beamstrahlung have been assumed.

All the new bounds coming from the  $WW$  channel do not alter the strong limits obtained from the fermion final state. This is because, as already noticed, the degenerate model has no strong enhancement of the  $W_L W_L$  channel, present in the usual strong electroweak models.

## 12 Final state rescattering

A different approach [91, 86] has also been presented. It consists in considering the effects of a strong interacting electroweak sector through final state rescattering. The final state  $W$  rescattering is described making use of the Omnés function  $F_T$ :

$$M(e^+e^- \rightarrow W_L^+ W_L^-) = M_0(e^+e^- \rightarrow W_L^+ W_L^-) F_T \quad (173)$$

where

$$F_T = \exp\left[\frac{1}{\pi} \int_0^\infty ds' \delta(s') \left\{ \frac{1}{s' - s - i\epsilon} - \frac{1}{s'} \right\}\right] \quad (174)$$

with  $\delta$  the phase shift depending on the dynamics. For instance Barklow [88] has considered

$$\delta(s) = \frac{1}{96\pi} \frac{s}{v^2} + \frac{3\pi}{8} \left[ \tanh\left(\frac{s - M_V^2}{M_V \Gamma_V}\right) + 1 \right] \quad (175)$$

where  $M_V$  and  $\Gamma_V$  are mass and width of the vector resonance.

Note that for infinite  $M_V$  one recovers the Low Energy Theorem (LET) results.

A full final state helicity analysis on  $e^+e^- \rightarrow W^+W^-$  was done [88] by considering one  $W$  decaying hadronically and the second one leptonically. The following multidifferential cross section has been considered

$$\frac{d\sigma(\cos \Theta, \cos \theta, \phi, \cos \bar{\theta}, \bar{\phi})}{d \cos \Theta d \cos \theta d \phi d \cos \bar{\theta} d \bar{\phi}} \quad (176)$$

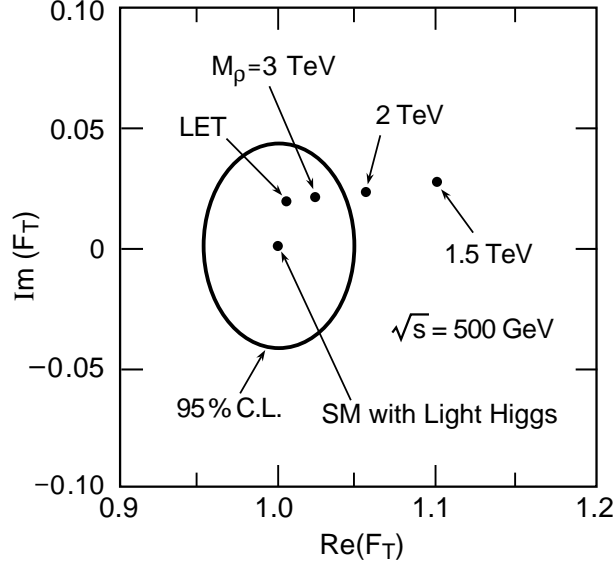


Figure 13: 95% C.L. contour for  $ReF_T$  and  $ImF_T$  for  $\sqrt{s} = 500 \text{ GeV}$  and predictions for various techni- $\rho$  masses, from [88].

where the angle  $\Theta$  is defined to be the angle between the initial state  $e^-$  and the  $W^-$  in the  $e^+e^-$  rest frame,  $\theta$  and  $\phi$  the polar and azimuthal angles of the fermion  $f_1$  in the  $W^-$  rest frame ( $W^- \rightarrow f_1 \bar{f}_2$ ),  $\bar{\theta}$  and  $\bar{\phi}$  the polar and azimuthal angles of the antifermion  $\bar{f}_4$  in the  $W^+$  rest frame ( $W^+ \rightarrow f_3 \bar{f}_4$ ). These five angles are reconstructed by measuring energies and angles of decay leptons and quarks. The masses of the two  $W$  are reconstructed by a kinematic fit of the momentum of the lepton  $\vec{P}_l$  and the four momentum of the hadronically decaying  $W$ ,  $(E_H, \vec{P}_H)$ , with

$$E_H + E_l + \sqrt{\vec{P}_\nu^2} = \sqrt{s} \quad (177)$$

and

$$\vec{P}_\nu = -(\vec{P}_l + \vec{P}_H) \quad (178)$$

where  $E_l$  is the lepton energy.

Two cuts are imposed:  $|\cos \Theta| < 0.9$  in order to ensure the event to be within the detector, and the  $W^+W^-$  invariant mass is required to be within few  $\text{GeV}$  of the  $e^+e^-$  center of mass energy.

A maximum log likelihood analysis is performed and the contour for the real and imaginary parts of  $F_T$  are shown in Figs. 13, 14. Beamstrahlung, bremsstrahlung and finite  $W$  width effects are included.

Figure 13 shows the 95% C.L. contour for the real and imaginary parts of  $F_T$  at  $\sqrt{s} = 500 \text{ GeV}$ . Also indicated are values of  $F_T$  for various techni- $\rho$  masses. We see that the LC at  $\sqrt{s} = 500 \text{ GeV}$  can exclude techni- $\rho$  masses up to about  $2.5 \text{ TeV}$  and can discover techni- $\rho$  resonances with masses of more than  $1.5 \text{ TeV}$ . The significance of



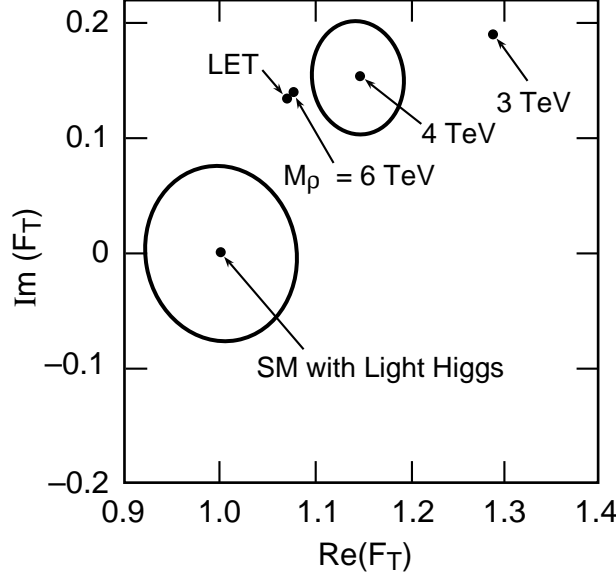


Figure 14: 95% C.L. contour for  $ReF_T$  and  $ImF_T$  for  $\sqrt{s} = 1.5 \text{ TeV}$  and predictions for various techni- $\rho$  masses, from [88].

the  $1.5 \text{ TeV}$  techni- $\rho$  signal would be  $6.7\sigma$ . A  $1.0 \text{ TeV}$  techni- $\rho$  would produce a  $17.7\sigma$  signal. Notice that these values for the masses of the resonances are already excluded by the LEP results if one assumes a QCD rescaled technicolor.

In Fig. 14 the chosen parameters are  $\sqrt{s} = 1.5 \text{ TeV}$  with  $190 \text{ fb}^{-1}$ . The contour about the light Higgs value is a 95% C.L. contour; the contour about the point, corresponding to the technicolor with  $M_\rho = 4 \text{ TeV}$ , is a 68% C.L. contour.

The non-resonant LET point is well outside the light Higgs 95% C.L. region and corresponds to a  $4.5\sigma$  signal.

The results are obtained assuming  $\Gamma_V/M_V = 0.22$ . However they are not much dependent on this assumption. In this model, when the vector resonance mass is taken to infinity, its effect on the form factor decreases and what is left behind is the residual scattering predicted by the LET. The values for high-mass techni- $\rho$  indicate this decoupling. A  $2 \text{ TeV}$  techni- $\rho$  would produce a  $37\sigma$  signal.

A similar analysis was done also in [89]. These authors consider again a phase shift corresponding to a vector resonance and investigate the cross section with suitable cuts to enhance the ratio  $W_L W_L$  to  $W_T W_T$ . Using the cut  $\cos \Theta \leq 0.95$  they study the ratio

$$R = \frac{N(-0.95 \leq \cos \Theta \leq \cos \Theta_0)}{N(-0.95 \leq \cos \Theta \leq 0.95)} \quad (179)$$

choosing  $\Theta_0 = 0.6\pi$ . This last cut enhances the  $W_L W_L$  signal as it is clear from the differential distribution of Fig. 4. Therefore with an integrated luminosity of  $10 \text{ fb}^{-1}$  they find that a vector resonance of  $M_V = 1 \text{ TeV}$  and  $\Gamma_V = 54 \text{ GeV}$  gives a  $6\sigma$  effect already at  $\sqrt{s} = 500 \text{ GeV}$  and that even without the final state helicity analysis it can be discovered.

A similar analysis was done in [92] using  $\sqrt{s} = 500 \text{ GeV}$  and  $L = 50 \text{ fb}^{-1}$ ; with this choice the sensitivity to  $M_V$  exceeds  $2 \text{ TeV}$ .

## 13 Anomalous trilinear gauge boson couplings

Another interesting sector of gauge boson interaction is given by the triple gauge boson vertices. Observing deviations of these vertices with respect to their SM values can give some hints of new physics.

We review in this section the effective parametrization for anomalous gauge boson couplings and their measurements at future LC's.

The most general CP invariant effective Lagrangian describing such terms can be written as [93, 50]

$$\begin{aligned} \frac{1}{g_{WWV}} \mathcal{L}_{WWV} &= i g_1^V (W_{\mu\nu}^+ W^{-\mu} V^\nu - W_{\mu\nu}^- W^{+\mu} V^\nu) + i k_V W_\mu^+ W_\nu^- V^{\mu\nu} \\ &+ i \frac{\lambda_V}{\Lambda^2} W_{\mu\nu}^+ W^{-\nu} V^{\rho\mu} + g_5^V \epsilon^{\mu\nu\rho\sigma} [W_\mu^+ (\partial_\rho W_\nu^-) - (\partial_\rho W_\mu^+) W_\nu^-] V_\sigma \end{aligned} \quad (180)$$

where  $V \equiv \gamma$  or  $Z$ ,  $W_{\mu\nu}^\pm = \partial_\mu W_\nu^\pm - \partial_\nu W_\mu^\pm$ ,  $V_{\mu\nu}^\pm = \partial_\mu V_\nu^\pm - \partial_\nu V_\mu^\pm$ .  $\Lambda$  denotes the scale of the new physics responsible for the symmetry breaking.

The couplings  $g_{WW\gamma}$  and  $g_{WWZ}$  are given by

$$g_{WW\gamma} = -e \quad g_{WWZ} = -e \frac{c_\theta}{s_\theta} \quad (181)$$

with  $s_\theta$  defined in eq. (26). It should be noted that in general these new couplings, that we assume as constants, are momentum dependent form-factors. In the SM one has  $g_1^V = k_V = 1$  and  $g_5^V = \lambda_V = 0$ .

The magnetic dipole moment  $\mu_W$  and the quadrupole moment  $Q_W$  of the  $W$  are given by

$$\mu_W = \frac{e}{2M_W} (1 + k_\gamma + \lambda_\gamma), \quad Q_W = -\frac{e}{M_W^2} (k_\gamma - \lambda_\gamma) \quad (182)$$

Using eqs. (21) and (24) one finds

$$\begin{aligned} g_1^Z - 1 &= \frac{g^2}{c_{2\theta}} \beta_1 + \frac{g^2 s_\theta^2}{c_\theta^2 c_{2\theta}} \alpha_1 + \frac{g^2}{c_\theta^2} \alpha_3 \\ g_1^\gamma - 1 &= 0 \\ k_Z - 1 &= \frac{g^2}{c_{2\theta}} \beta_1 + \frac{g^2 s_\theta^2}{c_\theta^2 c_{2\theta}} \alpha_1 + g^2 \frac{s_\theta^2}{c_\theta^2} (\alpha_1 - \alpha_2) + g^2 (\alpha_3 - \alpha_8 + \alpha_9) \\ k_\gamma - 1 &= g^2 (-\alpha_1 + \alpha_2 + \alpha_3 - \alpha_8 + \alpha_9) \\ g_5^Z &= \frac{g^2}{c_\theta^2} \alpha_{11} \\ g_5^\gamma &= \lambda_Z = \lambda_\gamma = 0 \end{aligned} \quad (183)$$

In the previous expressions there are also contributions coming from gauge boson two point functions.

In the literature there is also a second parametrization [94]. Assuming CP invariance and for the electromagnetic interaction also C invariance, one has [94]

$$\begin{aligned}
\mathcal{L} = & -ie\{[(W_{\mu\nu}^- W^{+\nu} - W_{\mu\nu}^+ W^{-\nu})A^\mu + (1+x_\gamma)F^{\mu\nu}W_\mu^+ W_\nu^-] \\
& + (\frac{c_\theta}{s_\theta} + \delta_Z)[(W_{\mu\nu}^- W^{+\nu} - W_{\mu\nu}^+ W^{-\nu})Z^\mu + (1 + \frac{x_Z}{\frac{c_\theta}{s_\theta} + \delta_Z})Z^{\mu\nu}W_\mu^+ W_\nu^-] \\
& + \frac{1}{M_W^2}(y_\gamma F^{\nu\lambda} + y_Z Z^{\nu\lambda})W_{\lambda\mu}^+ W^{-\mu}_\nu\} \\
& + \frac{e z_Z}{M_W^2} \partial_\alpha \tilde{Z}_{\rho\sigma} (\partial^\rho W^{-\sigma} W^{+\alpha} - \partial^\rho W^{-\alpha} W^{+\sigma} + (\alpha \leftrightarrow \sigma))
\end{aligned} \tag{184}$$

where

$$\tilde{Z}_{\rho\sigma} = \frac{1}{2} \epsilon_{\rho\sigma\alpha\beta} Z^{\alpha\beta} \tag{185}$$

The conversion is given by (assuming in eq. (180)  $\Lambda \equiv M_W^2$ )

$$x_\gamma = \Delta k_\gamma \quad \delta_Z = \frac{c_\theta}{s_\theta} \Delta g_Z^1 \quad x_Z = \frac{c_\theta}{s_\theta} (\Delta k_Z - \Delta g_Z^1) \quad y_\gamma = \lambda_\gamma \quad y_Z = \frac{c_\theta}{s_\theta} \lambda_Z \tag{186}$$

with

$$\Delta k_\gamma = k_\gamma - 1 \quad \Delta k_Z = k_Z - 1 \quad \Delta g_1^Z = g_1^Z - 1 \tag{187}$$

For what concerns the last term of eq. (180) and eq. (184) the comparison is less simple, because the two operators are of dimension four and six respectively and therefore a  $q^2$  dependence appears [95].

The best present limits on anomalous couplings come from hadron collider experiments. Preliminary CDF and D0 results using  $W\gamma$ ,  $WW$  and  $WZ$  production give 95% C.L. bounds on the parameters which are of order unity [96, 97]. LEP II can improve these bounds to  $O(10^{-1})$  [98] by considering the process  $e^+e^- \rightarrow W^+W^-$  with three main topologies: those in which both  $W$  decay hadronically, in which one decays hadronically, the other leptonically, and in which both decay leptonically. Anomalous couplings can be measured from the multidifferential cross section (176) by using a maximum likelihood method. This analysis has been also repeated for future LC's, by considering events with  $|\cos \Theta| < 0.8$  and the topology in which one  $W$  decays hadronically, the other leptonically [94, 95, 99, 100, 101, 102]. The common result is that one can reach precisions of  $O(10^{-3})$ , at a LC of  $\sqrt{s} = 500 \text{ GeV}$  especially if beam polarization is available.

In a recent work the analysis of the anomalous trilinear gauge couplings [103] has been performed by considering at the same time also fermion anomalous couplings, because in general there are strong correlations. The corrections to the fermion couplings, assuming universality, are parametrized in terms of the  $\epsilon_3$  parameter (in many models the  $SU(2)$  symmetry guarantees  $\epsilon_1 = \epsilon_2 = 0$ ) and therefore existing bounds on  $\epsilon_3$  give also limits on anomalous fermion couplings.

A recent review on anomalous gauge couplings is given in [104].

## 14 Fusion subprocesses and vector resonances

Another mechanism to produce  $W^+W^-$  pairs is the fusion of a pair of ordinary gauge bosons, each being initially emitted from an electron or a positron. This process allows to study  $WW$  scattering and therefore possible strong interacting electroweak breaking. This was first investigated in [105, 106, 107, 108].

In the so called effective  $W$  approximation the initial  $W, Z, \gamma$  are assumed to be real and the cross section for producing a  $W^+W^-$  pair is obtained by a convolution of the fusion subprocess with the luminosities of the initial  $W, Z, \gamma$  inside the electrons and positrons. There are two fusion subprocesses which contribute to produce  $W^+W^-$  pairs. The first one is

$$e^+e^- \rightarrow W_{L,T}^+ W_{L,T}^- e^+e^- \quad (188)$$

It is mediated by  $W^\pm$  and  $V^\pm$  exchanges in the  $t$  and  $u$  channels. The second fusion subprocess is

$$e^+e^- \rightarrow W_{L,T}^+ W_{L,T}^- \bar{\nu}\nu \quad (189)$$

It is mediated by  $\gamma, Z$  and  $V^0$  exchanges in the  $s$  and  $t$  channels. Both processes get a contribution from the gauge boson fourlinear couplings.

In principle, the fusion processes are interesting because they allow to study a wide range of mass spectrum for the  $V$  resonance for one given  $e^+e^-$  c.m. energy.

In the  $e^+e^-$  center-of-mass frame the invariant mass distribution  $d\sigma/dM_{WW}$  reads

$$\begin{aligned} \frac{d\sigma}{dM_{WW}} = & \frac{1}{4\pi s} \frac{1}{M_{WW}^2} \sum_{i,j} \sum_{l_1,l_2} \int_{(p_T^2)_{min}}^{M_{WW}^2/4} dp_T^2 \int_{\log \sqrt{\tau}}^{-\log \sqrt{\tau}} dy f_i^{l_1}(\sqrt{\tau}e^y) f_j^{l_2}(\sqrt{\tau}e^{-y}) \\ & \cdot \frac{p'}{p} \frac{1}{\sqrt{M_{WW}^2 - 4p_T^2}} |M(V_i^{l_1} V_j^{l_2} \rightarrow W_{l_3}^+ W_{l_4}^-)|^2 \end{aligned} \quad (190)$$

where  $p_T$  is the transverse momentum of the outgoing  $W$ ,  $\tau = M_{WW}^2/s$ ,  $p$  and  $p'$  are the absolute values of the three momenta for incoming and outgoing pairs of vector bosons:  $p = (E_1^2 - M_1^2)^{1/2} = (E_2^2 - M_2^2)^{1/2}$  and  $p' = (\sqrt{M_{WW}^2}/2)(1 - 4M_W^2/M_{WW})^{1/2}$  with  $E_i$  the energy of the vector boson  $V_i$  with mass  $M_i$  and helicity  $l_i$ . The structure functions  $f$  appearing in the previous formula are

$$\begin{aligned} f^+(x) &= \frac{\alpha_{em}}{4\pi} \frac{[(v+a)^2 + (1-x)^2(v-a)^2]}{x} \log \frac{s}{M^2} \\ f^-(x) &= \frac{\alpha_{em}}{4\pi} \frac{[(v-a)^2 + (1-x)^2(v+a)^2]}{x} \log \frac{s}{M^2} \\ f^0(x) &= \frac{\alpha_{em}}{\pi} (v^2 + a^2) \frac{1-x}{x} \end{aligned} \quad (191)$$

and represent the probability of having inside the electron a vector boson of mass  $M$  with fraction  $x$  of the electron energy. In eq. (191)  $v$  and  $a$  are the vector and axial-vector couplings of the gauge bosons to fermions. We present here the results for the BESS

model. For the photon,  $v = -1$  and  $a = 0$ ; for  $Z$ ,  $v = v_Z^f$  and  $a = a_Z^f$  as given in eq. (67); and, for  $W$ ,  $v = a = a_W$  as given in eq. (63). The quadrilinear couplings are

$$\begin{aligned}
g_{WWWW} &= \frac{e^2}{\sin^2 \theta} \frac{\cos^4 \phi}{\cos^2 \psi} + \frac{g''^2}{4} \sin^4 \phi \\
g_{WWZZ} &= \frac{e^2}{\cos^2 \phi} g_{ZWW}^2 + \frac{g''^2}{4} \sin^2 \phi \sin^2 \xi \cos^2 \psi \\
g_{WW\gamma\gamma} &= e^2 \cos^2 \phi + \frac{g''^2}{4} \sin^2 \phi \sin^2 \psi = e^2 \\
g_{WWZ\gamma} &= e^2 g_{ZWW} - \frac{g''^2}{4} \sin^2 \phi \sin \xi \sin \psi \cos \psi
\end{aligned} \tag{192}$$

with  $g_{ZWW}$  as given in eq. (78) and the mixing angles  $\xi$ ,  $\psi$  and  $\phi$  in eqs. (69), (65) and (64).

The amplitudes of the vector bosons scattering processes within the BESS model are:

$$\begin{aligned}
M(W_1^+ W_2^- \rightarrow W_3^+ W_4^-) &= -ie^2 \frac{f_s}{s} - ie^2 g_{ZWW}^2 \frac{f_s}{s - M_Z^2} \\
&\quad - ie^2 g_{VWW}^2 \frac{f_s}{s - M_V^2 + i\Gamma_V M_V} + (s \rightarrow t) \\
&\quad + ig_{WWWW} [2(\epsilon_1 \cdot \epsilon_4^*)(\epsilon_2 \cdot \epsilon_3^*) - (\epsilon_1 \cdot \epsilon_2)(\epsilon_3^* \cdot \epsilon_4^*) \\
&\quad - (\epsilon_1 \cdot \epsilon_3^*)(\epsilon_2 \cdot \epsilon_4^*)]
\end{aligned} \tag{193}$$

$$\begin{aligned}
M(\gamma_1 \gamma_2 \rightarrow W_3^+ W_4^-) &= -ie^2 \frac{h_t}{t - M_W^2} + (t \rightarrow u) \\
&\quad - ig_{WW\gamma\gamma} [2(\epsilon_1 \cdot \epsilon_2)(\epsilon_3^* \cdot \epsilon_4^*) - (\epsilon_1 \cdot \epsilon_3^*)(\epsilon_2 \cdot \epsilon_4^*) \\
&\quad - (\epsilon_1 \cdot \epsilon_4^*)(\epsilon_2 \cdot \epsilon_3^*)]
\end{aligned} \tag{194}$$

$$\begin{aligned}
M(\gamma_1 Z_2 \rightarrow W_3^+ W_4^-) &= -ie^2 g_{ZWW} \frac{h_t}{t - M_W^2} + (t \rightarrow u) \\
&\quad - ig_{WWZ\gamma} [2(\epsilon_1 \cdot \epsilon_2)(\epsilon_3^* \cdot \epsilon_4^*) - (\epsilon_1 \cdot \epsilon_3^*)(\epsilon_2 \cdot \epsilon_4^*) \\
&\quad - (\epsilon_1 \cdot \epsilon_4^*)(\epsilon_2 \cdot \epsilon_3^*)]
\end{aligned} \tag{195}$$

$$\begin{aligned}
M(Z_1 Z_2 \rightarrow W_3^+ W_4^-) &= -ie^2 g_{ZWW}^2 \frac{h_t}{t - M_W^2} \\
&\quad - ie^2 g_{VWW}^2 \frac{h_t}{t - M_V^2 + i\Gamma_V M_V} + (t \rightarrow u) \\
&\quad - ig_{WWZZ} [2(\epsilon_1 \cdot \epsilon_2)(\epsilon_3^* \cdot \epsilon_4^*) - (\epsilon_1 \cdot \epsilon_3^*)(\epsilon_2 \cdot \epsilon_4^*) \\
&\quad - (\epsilon_1 \cdot \epsilon_4^*)(\epsilon_2 \cdot \epsilon_3^*)]
\end{aligned} \tag{196}$$

where

$$f_s = [(\epsilon_1 \cdot \epsilon_2)(p_2 - p_1)_\lambda - 2(\epsilon_1 \cdot p_2)\epsilon_{2\lambda} + 2(\epsilon_2 \cdot p_1)\epsilon_{1\lambda}] \cdot [(\epsilon_3^* \cdot \epsilon_4^*)(p_3 - p_4)^\lambda - 2(\epsilon_4^* \cdot p_3)\epsilon_3^{*\lambda} + 2(\epsilon_3^* \cdot p_4)\epsilon_4^{*\lambda}] \quad (197)$$

and  $f_t$  can be deduced from  $f_s$  with the substitution  $p_2 \leftrightarrow -p_3$  and  $\epsilon_2 \leftrightarrow \epsilon_3^*$ , while

$$h_t = [2(\epsilon_1 \cdot p_3)\epsilon_{3\lambda}^* - (\epsilon_1 - \epsilon_3^*)(p_3 + p_1)_\lambda + 2(p_1 \cdot \epsilon_3^*)\epsilon_{1\lambda}] \cdot [2(\epsilon_2 \cdot p_4)\epsilon_4^{*\lambda} - (\epsilon_2 \cdot \epsilon_4^*)(p_4 + p_2)^\lambda + 2(p_2 \cdot \epsilon_4^*)\epsilon_2^\lambda] + (\epsilon_1 \cdot \epsilon_3^*)(p_1^2 - p_3^2)(\epsilon_2 \cdot \epsilon_4^*)(p_2^2 - p_4^2)/M_W^2 \quad (198)$$

and  $h_u$  can be deduced from  $h_t$  with the substitution  $p_3 \leftrightarrow p_4$  and  $\epsilon_3^* \leftrightarrow \epsilon_4^*$ .

In eqs. (193-196)  $g_{ZWW}$  and  $g_{VWW}$  are given in eq. (78) and (77) respectively and  $\Gamma_V$  is the width of the  $V$  resonance.

For comparison, the amplitudes within the SM can be obtained from eqs. (193-196) by taking all the trilinear and quadrilinear vector boson couplings in the limit  $g'' \rightarrow \infty$  and  $b \rightarrow 0$  and adding the contribution due to the Higgs boson exchange. All the non-annihilation graphs contributing to the processes  $e^+e^- \rightarrow W^+W^-e^+e^-$  and  $e^+e^- \rightarrow W^+W^-\nu\bar{\nu}$  (at the order  $\alpha_{em}^2$ ) in which the final  $W$ 's are emitted from the electron (positron) legs are not considered. This is because their contribution is expected mostly in a kinematical region different from the one in which  $p_T \sim M_W$ . This is the typical momentum of a longitudinal  $W$  radiated by an initial electron or positron.

The result of the analysis for the BESS model is that there are not significative differences with respect to the SM differential cross section in the case of the process  $e^+e^- \rightarrow W^+W^-e^+e^-$ . This is due, first of all, to the absence of the  $s$  channel exchange of the  $V$  resonance, secondly, to the dominance of the  $\gamma\gamma$  fusion contribution, and to the fact that in the BESS model the couplings of the photon to the fermions and to  $W^+W^-$  are the same as in the SM.

Concerning the process  $e^+e^- \rightarrow W^+W^-\nu\bar{\nu}$ , the differential cross sections  $d\sigma/dM_{WW}$  both for the SM with  $M_H = 100 \text{ GeV}$  and for the BESS model have been evaluated [108, 109]. The only channel which turns out to be useful is the one corresponding to longitudinally polarized final  $W$ 's. The results of the analysis are illustrated in [108, 109] for two different choices of the BESS parameters.

In both cases cuts are not applied except for  $(p_T)_{min} = 10 \text{ GeV}$ .

Although theoretically there is a clear difference between the curves of the two models, the experimental situation is quite different.

Let us first consider the case of  $\sqrt{s} = 1.5 \text{ TeV}$ . By integrating the differential cross section for  $500 < M_{WW}(\text{GeV}) < 1500$  and considering an integrated luminosity of  $80 \text{ fb}^{-1}$  one obtains 127  $W_L$  pairs for the SM and 158 for the BESS model (with  $M_V = 1 \text{ TeV}$ ,  $g'' = 13$  and  $b = 0.01$ ) corresponding to a statistical significance  $S/\sqrt{B}$  of 2.7. By considering, for comparison with other calculations, the higher luminosity of  $200 \text{ fb}^{-1}$  this ratio becomes 4.4. In this analysis the branching ratio  $BR(W \rightarrow jj)$  in final dijets is not taken into account.

The case of a resonance with  $M_V = 1.5 \text{ TeV}$ ,  $g'' = 13$  and  $b = 0.01$  has been considered for an energy of  $2 \text{ TeV}$  and by considering an integrated luminosity of  $20 \text{ fb}^{-1}$ . By integrating the differential cross section for  $1000 < M_{WW}(\text{GeV}) < 2000$  one gets 7  $W_L$  pairs for the SM and 13 for the BESS model corresponding to a statistical significance of 2.3 (which increases to 7.2 by considering  $200 \text{ fb}^{-1}$ ).

The channel corresponding to transverse-longitudinal final  $W$ 's leads to a very small bump in the region of the resonance above the SM backgrounds which is not observable.

In conclusion this analysis shows that it is possible to discover new vector resonances from the fusion process at high energy LC's, but a high luminosity of the order  $200 \text{ fb}^{-1}$  is required, in agreement with the results of [56].

## 15 Fusion: comparison of models

A more detailed analysis, taking into account not only the  $W^+W^- \rightarrow W^+W^-$  but also  $W^+W^- \rightarrow ZZ$ , and considering a more accurate choice of cuts and also the dijet mass resolution in  $W, Z \rightarrow jj$  was done in [56]. The authors study not only the vector model, but also the chirally coupled scalar (CCS) model of Section 4.1, the LET model, given by the simplest chiral Lagrangian and using  $K$  matrix unitarization, and the SM Heavy Higgs model. The calculations for the last two models were done from the complete SM and defining the signal as the excess with respect to the case of  $M_H = 0$ . Calculations for the CCS and the vector models were done using the effective  $W$  approximation.

While in studies at LHC it is necessary for identification of  $W$  and  $Z$  to consider their leptonic decays which have small branching fractions, at LC's  $W$  and  $Z$  bosons are detected via the dijet mode and identified using the invariant masses  $M(W \rightarrow jj)$ ,  $M(Z \rightarrow jj)$  with an identification probability of the order of 75% for  $WW$  and 60% for  $ZZ$ .

Concerning the background coming from

$$e^+e^- \rightarrow ZW^+W^- \rightarrow \bar{\nu}\nu W^+W^- \quad (199)$$

it can be reduced using the so called recoil mass or the invariant mass of all the final particles excluding  $WW$ . The recoil mass spectrum has a peak at  $M_Z$ , and therefore a cut as  $M_{rec} > 200 \text{ GeV}$  suppresses this background.

To isolate  $WW$  scattering at high energy, the authors of [56] require also high invariant mass  $M_{WW}$ , high transverse momentum  $p_T(W)$ , and a large angle with respect to the beam axis:

$$M_{WW} > 500 \text{ GeV}, \quad p_T(W) > 150 \text{ GeV}, \quad |\cos \theta(W)| < 0.8 \quad (200)$$

The remaining major background comes from

$$e^+e^- \rightarrow e^+e^-W^+W^-, e^+e^-ZZ, e^\pm\nu W^\mp Z \quad (201)$$

where the final state electron disappears along the beam pipe.

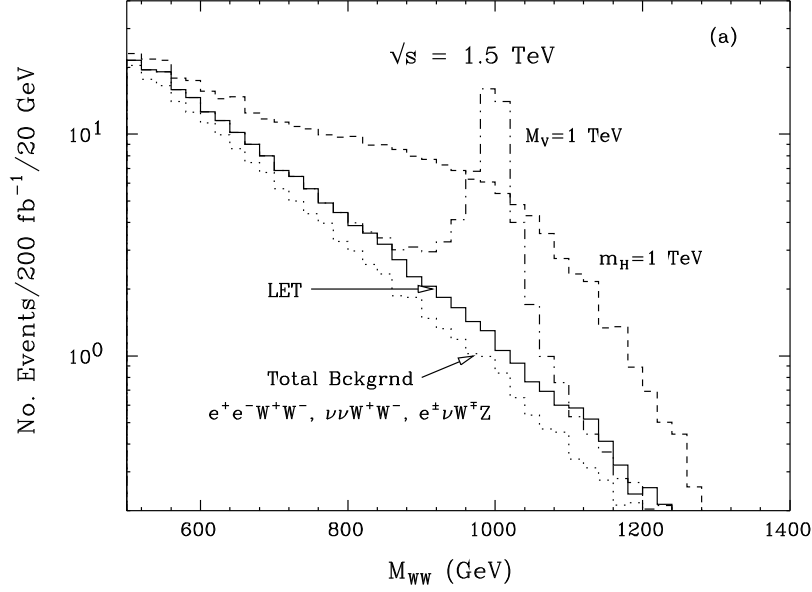


Figure 15: Signal and background events versus the diboson invariant mass in the channel  $e^+e^- \rightarrow \bar{\nu}\nu W^+W^-$  for  $200 \text{ fb}^{-1}$  and  $\sqrt{s} = 1.5 \text{ TeV}$ . The dashed curve denotes the SM with  $M_H = 1 \text{ TeV}$ , the solid one the SM with  $M_H \rightarrow \infty$  (LET); the dot-dashed curve denotes the vector model with  $M_V = 1 \text{ TeV}$  and  $\Gamma_V = 30 \text{ GeV}$ , the dotted curve the total background. The CCS model is close to the SM with  $M_H = 1 \text{ TeV}$ , from [56].

This is reduced through the following cuts (at  $\sqrt{s} = 1.5 \text{ TeV}$ )

$$50 \text{ GeV} < p_T(WW) < 300 \text{ GeV}, \quad 20 \text{ GeV} < p_T(ZZ) < 300 \text{ GeV} \quad (202)$$

and a veto on hard electrons

$$\text{no } e^\pm \text{ with } E > 50 \text{ GeV and } |\cos \theta_e| < \cos(0.15 \text{ rad}) \quad (203)$$

The results for the collisions at  $\sqrt{s} = 1.5 \text{ TeV}$  are presented in Fig. 15, 16. The branching fractions  $BR(W \rightarrow jj) = 67.8\%$  and  $BR(Z \rightarrow jj) = 69.9\%$  and the  $W, Z$  identification /miseidentifications factors are included. The results summarized in Table 2 show that in order to have a statistical significant signal one needs a high luminosity ( $200 \text{ fb}^{-1}$ ).

The authors find a  $5.7 \sigma$  signal for LET amplitudes in the  $ZZ$  final state, and  $22 \sigma$  in the  $WW$  channel for the vector model with  $M_V = 1 \text{ TeV}$  and  $\Gamma_V = 30 \text{ GeV}$  (This would correspond to a BESS parameter  $g/g'' = 0.08$ ).

At the LC it is interesting to consider also the effect of polarization. The results, assuming initial  $e_L^+$  and  $e_R^-$ , are listed in Table 3.

In conclusion  $W^+W^- \rightarrow W^+W^-$  and  $W^+W^- \rightarrow ZZ$  channels are sensitive to different dynamics of the electroweak breaking. Signals are enhanced at  $\sqrt{s} = 2 \text{ TeV}$  colliders and at  $\mu^+\mu^-$  colliders [57].



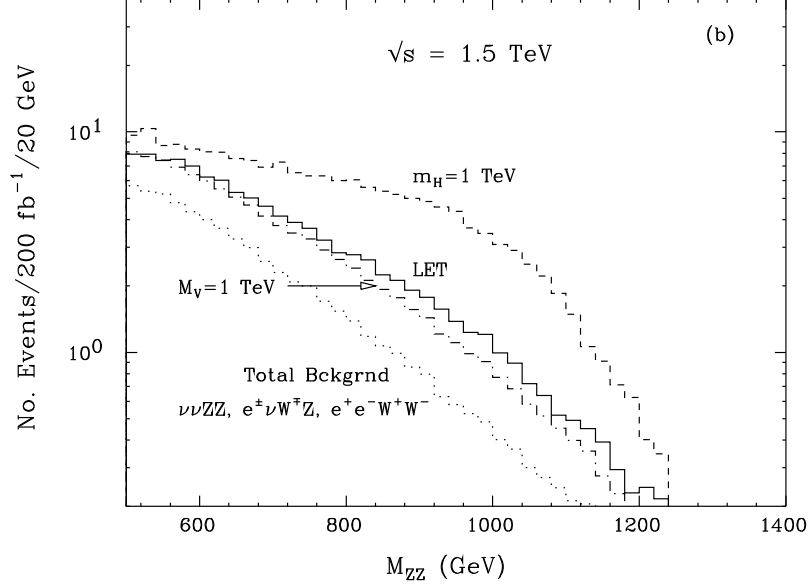


Figure 16: Signal and background events versus the diboson invariant mass in the channel  $e^+e^- \rightarrow \bar{\nu}\nu ZZ$  for  $200 \text{ fb}^{-1}$  and  $\sqrt{s} = 1.5 \text{ TeV}$ . The dashed curve denotes the SM with  $M_H = 1 \text{ TeV}$ , the solid one the SM with  $M_H \rightarrow \infty$  (LET); the dot-dashed curve denotes the vector model with  $M_V = 1 \text{ TeV}$  and  $\Gamma_V = 30 \text{ GeV}$ , the dotted curve the total background. The CCS model is close to the SM with  $M_H = 1 \text{ TeV}$ , from [56].

Channels	SM ( $M_H = 1 \text{ TeV}$ )	CCS ( $M_S = 1 \text{ TeV}$ )	V ( $M_V = 1 \text{ TeV}$ )	LET
$S(e^+e^- \rightarrow \bar{\nu}\nu WW)$	160	160	46	31
B	170	170	4.5	170
$S/\sqrt{B}$	12	12	22	2.4
$S(e^+e^- \rightarrow \bar{\nu}\nu ZZ)$	120	130	36	45
B	63	63	63	63
$S/\sqrt{B}$	15	17	4.5	5.7

**Table 2:** Total number of  $WW$ ,  $ZZ$  signal and background at  $\sqrt{s} = 1.5 \text{ TeV}$  and integrated luminosity  $200 \text{ fb}^{-1}$ . Events are summed over the mass range  $0.5 < M_{WW}(\text{TeV}) < 1.5$  except for the vector case  $V$  ( $0.9 < M_{WW}(\text{TeV}) < 1.1$ ).

Channels	SM ( $M_H = 1 \text{ TeV}$ )	CCS ( $M_S = 1 \text{ TeV}$ )	V ( $M_V = 1 \text{ TeV}$ )	LET
S( $e^+e^- \rightarrow \bar{\nu}\nu WW$ )	330	320	92	62
B	280	280	7.1	280
S/ $\sqrt{B}$	20	20	35	3.7
S( $e^+e^- \rightarrow \bar{\nu}\nu ZZ$ )	240	260	72	90
B	110	110	110	110
S/ $\sqrt{B}$	23	25	6.8	8.5

**Table 3:** Total number of  $WW$ ,  $ZZ$  signal and background at  $\sqrt{s} = 1.5 \text{ TeV}$  and integrated luminosity  $200 \text{ fb}^{-1}$  with 100% polarized beams. Events are summed over the mass range  $0.5 < M_{WW}(\text{TeV}) < 1.5$  except for the vector case  $V$  ( $0.9 < M_{WW}(\text{TeV}) < 1.1$ ).

## 16 Measuring chiral parameters

At energies below the new resonances, vector boson scattering amplitudes can generally be described, as we have already seen, by electroweak chiral Lagrangians.

For a LC with center of mass energy of  $\sqrt{s} = 1.6 \text{ TeV}$  and an integrated luminosity of  $200 \text{ fb}^{-1}$  the sensitivity on the chiral parameters  $\alpha_4$  and  $\alpha_5$ , defined in eq. (12), has been recently investigated [110]. The processes  $e^+e^- \rightarrow W^+W^-\bar{\nu}\nu$  and  $e^+e^- \rightarrow ZZ\bar{\nu}\nu$  have been considered, by performing a complete calculation which includes all relevant Feynman diagrams at tree level, without relying on the Equivalence Theorem or the effective  $W$  approximation. The following set of optimized cuts as in [56] have been applied to the  $WW$  channel

$$\begin{aligned}
& |\cos\theta(W)| < 0.8 \\
& 150 \text{ GeV} < p_T(W) \\
& 50 \text{ GeV} < p_T(WW) < 300 \text{ GeV} \\
& 200 \text{ GeV} < M_{inv}(\bar{\nu}\nu) \\
& 700 \text{ GeV} < M_{inv}(WW) < 1200 \text{ GeV}
\end{aligned}$$

The lower bound on  $p_T(WW)$  is necessary because of the large  $W^+W^-e^+e^-$  background which is concentrated at low  $p_T$  if both electrons disappear into the beampipe. The window  $700 \text{ GeV} < M_{inv}(WW) < 1200 \text{ GeV}$  is used to avoid regions of possible violation of unitarity. For the  $ZZ$  final state the same cuts have been applied except for  $p_T^{min}(ZZ) = 30 \text{ GeV}$ . Hadronic decays of the  $W^+W^-$  pairs and hadronic as well as  $e^+e^-$  and  $\mu^+\mu^-$  decays of the  $ZZ$  pairs have been used.

From this analysis in the case of a LC with center of mass energy  $\sqrt{s} = 1.6 \text{ TeV}$  and an integrated luminosity of  $200 \text{ fb}^{-1}$  with polarized beams (90% for electrons and 60% for positron) one gets  $\alpha_4 \leq 0.003$  and  $\alpha_5 \leq 0.002$  at 91.7% C.L.

## 17 Comparison LC - LHC

Complementarity of LC and LHC has been already advocated referring to different aspects of the electroweak symmetry breaking problem [111, 75, 112, 14]. We perform here a critical discussion of the results that can be obtained at future LC's and LHC on strong electroweak sector.

Let us first consider the case of models for strong electroweak sector with no resonance or with a new very heavy scalar resonance. Then one can measure the chiral lagrangian parameters given in eq. (12).

By rescaling the result [110] from the channels  $e^+e^- \rightarrow \nu\bar{\nu}ZZ$  and  $e^+e^- \rightarrow e^+e^-W^+W^-$  to  $100 \text{ fb}^{-1}$  and longitudinal polarization  $P = 0.8$  one gets [113]  $\alpha_5 \leq 1.8 \times 10^{-3}$  at 95% C.L. to be compared with  $\alpha_5 \leq 3.5 \times 10^{-3}$  at 95% C.L [114] from the reaction  $qq \rightarrow qqZZ$  at LHC, using the scheme of cuts of CMS [115].

This can be translated, using eq. (148), in a lower limit on the scalar resonance

$$M_S (\text{TeV}) \geq 1.8 @ LC(E = 1.6 \text{ TeV}, L = 100 \text{ fb}^{-1}) \quad M_S (\text{TeV}) \geq 1.6 @ LHC \quad (204)$$

Therefore to get a result which is comparable or better than LHC, one needs a high energy and luminosity LC.

In presence of new vector resonances the annihilation channels are much more efficient than the fusion ones because all the center of mass energy is used to produce the new particles.

The result for the BESS model has already been shown in Fig. 10 on the plane  $(M_V, \Gamma_V)$ . The comparison between LHC and LC is shown in Fig. 17 on the plane  $(b, g/g'')$  for a LC of  $\sqrt{s} = 500 \text{ GeV}$  and  $L = 20 \text{ fb}^{-1}$ , assuming  $M_V = 1 \text{ TeV}$  [116]. The dotted line corresponds to the 90% C.L. bound from the  $WW$  differential cross section, the dashed line to the bound from  $W_L W_L$  differential cross section, and the continuous line to the bound combining the differential  $W_{L,T} W_{L,T}$  cross sections and  $WW$  left-right asymmetries. The dot-dashed line represents the bound from LHC. The allowed regions are those between the lines. The bound from LHC is obtained by considering the total cross section  $pp \rightarrow W^\pm, V^\pm \rightarrow W^\pm Z \rightarrow \mu\nu\mu^+\mu^-$  and assuming that no deviation is observed with respect to the SM within the experimental errors: a systematic error of 5% and the statistical one have been considered.

The above channel is for LHC the more efficient one in the case of a vector resonance strongly coupled to longitudinal  $W$ . LHC can discover new vector resonances in a large region of the parameter space up to masses  $M_V = 1.5 - 2 \text{ TeV}$  in the channel  $pp \rightarrow W^\pm, V^\pm \rightarrow W^\pm Z$  [117, 115, 118, 55]. If such a  $2 \text{ TeV}$  resonance is not found at LHC then an upgrade of the LC to  $\sqrt{s} = 800 \text{ GeV}$  and  $L = 50 \text{ fb}^{-1}$  can be very effective in getting bounds on the parameter space of the model, as shown in Fig. 18, where 90% C.L. contours in the plane  $(b, g/g'')$  for  $M_V = 2 \text{ TeV}$  are presented [116]. The bounds come from the same observables as in Fig. 17 at a LC of  $\sqrt{s} = 800 \text{ GeV}$  and  $L = 50 \text{ fb}^{-1}$ . Again the dot-dashed line corresponds to the bound from the total cross section  $pp \rightarrow W^\pm, V^\pm \rightarrow W^\pm Z$  at LHC.

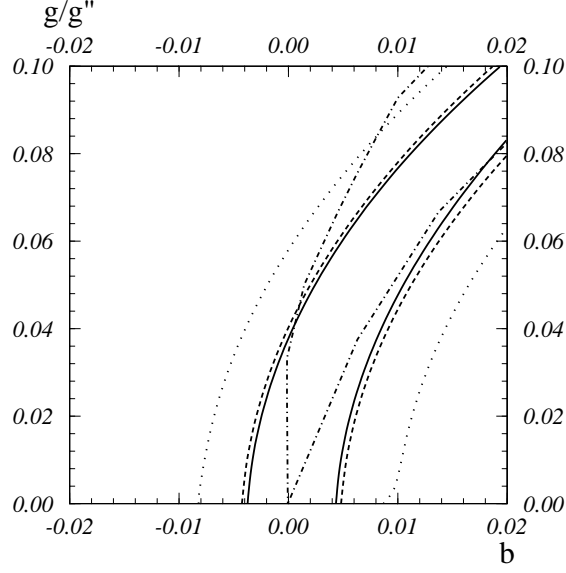


Figure 17: BESS 90% C.L. contours in the plane  $(b, g/g'')$  for  $M_V = 1 \text{ TeV}$ . The dotted line corresponds to the bound from the  $WW$  differential cross section, the dashed line from  $W_L W_L$  differential cross section and the continuous line from the differential  $W_{L,T} W_{L,T}$  cross sections and  $WW$  left-right asymmetries at a  $500 \text{ GeV}$  LC. The dot-dashed line corresponds to the bound from the total cross section  $pp \rightarrow W^\pm, V^\pm \rightarrow W^\pm Z$  at LHC. The allowed regions are the internal ones.

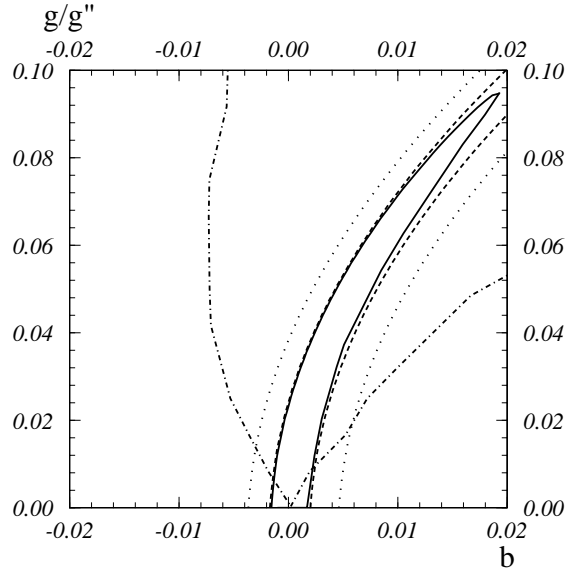


Figure 18: Same as in Fig. 17 for  $M_V = 2 \text{ TeV}$  and a  $800 \text{ GeV}$  LC with  $L = 80 \text{ fb}^{-1}$ .

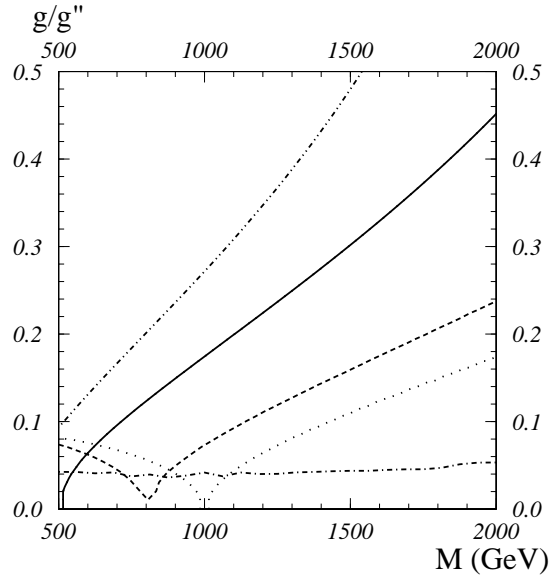


Figure 19: Degenerate BESS 90% C.L. contour on the plane  $(M, g/g'')$  from  $e^+e^-$  at different  $\sqrt{s}$  values: the dash-double dotted line represents the limit from the combined unpolarized observables at  $\sqrt{s} = 360 \text{ GeV}$  with an integrated luminosity of  $L = 10 \text{ fb}^{-1}$ , the continuous line at  $\sqrt{s} = 500 \text{ GeV}$  and  $L = 20 \text{ fb}^{-1}$ , the dashed line at  $\sqrt{s} = 800 \text{ GeV}$  and  $L = 50 \text{ fb}^{-1}$ , the dotted line at  $\sqrt{s} = 1000 \text{ GeV}$  and  $L = 80 \text{ fb}^{-1}$ . The dot-dashed line represents the limit from LHC.

The neutral channel at LHC  $pp \rightarrow \gamma, Z, V \rightarrow W^+W^-$  suffers of severe background from  $t\bar{t}$  production.

Nevertheless the new neutral vector bosons can be studied at LHC by considering their lepton decay up to masses of the order 1  $TeV$  [119].

Notice that while LHC is more sensitive to the charged new vector bosons, the LC is sensitive to the neutral ones (at least in the annihilation channels).

As a general conclusion it seems that for models of new vector resonances, if one is able to reconstruct the final  $W$  polarization, the measurement of polarized  $e^+e^- \rightarrow W_L W_L$  gives strong bounds on the parameter space of the model.

In the case of the model with vector and axial-vector resonances degenerate in mass (degenerate BESS), LHC is sensitive to the new particles in the channels  $pp \rightarrow W^\pm, L^\pm \rightarrow \mu\nu$  and  $pp \rightarrow \gamma, Z, L_3, R_3 \rightarrow \mu^+\mu^-$  up to masses of the order 2  $TeV$  as shown in Fig. 19. The bounds are obtained by assuming no deviations with respect to the SM in the total cross section  $pp \rightarrow W^\pm, L^\pm \rightarrow \mu\nu$  within the experimental errors: a systematic error of 5% and the statistical one have been considered. The limits are compared with those coming from LC's in Fig. 19 [116]. The double dot-dashed line represents the limit from the combined unpolarized observables at  $\sqrt{s} = 360 GeV$  with an integrated luminosity of  $L = 10 fb^{-1}$ ; the continuous line from  $\sqrt{s} = 500 GeV$  and  $L = 20 fb^{-1}$ ; the dashed line from  $\sqrt{s} = 800 GeV$  and  $L = 50 fb^{-1}$  and the dotted line from  $\sqrt{s} = 1000 GeV$   $L = 80 fb^{-1}$ . The dot-dashed line represents the limit from LHC. Therefore to be competitive with LHC one has to consider a LC of still higher energy than those considered.

The statistical significances of strong symmetry breaking signals at the LC and LHC are summarized in Table 4 from [112].

Collider	Process	$\sqrt{s}$ (TeV)	$\mathcal{L}$ (fb $^{-1}$ )	$M_V$ 1.5 TeV	$M_H$ 1 TeV	LET
LC	$e^+e^- \rightarrow W^+W^-$	.5	80	$7\sigma$	–	–
LC	$e^+e^- \rightarrow W^+W^-$	1.0	200	$35\sigma$	–	–
LC	$e^+e^- \rightarrow W^+W^-$	1.5	190	$366\sigma$	–	$5\sigma$
LC	$W^+W^- \rightarrow ZZ$	1.5	190	–	$22\sigma$	$8\sigma$
LC	$W^-W^- \rightarrow W^-W^-$	1.5	190	–	$4\sigma$	$6\sigma$
LHC	$W^+W^- \rightarrow W^+W^-$	14	100	–	$14\sigma$	–
LHC	$W^+W^+ \rightarrow W^+W^+$	14	100	–	$3\sigma$	$6\sigma$
LHC	$W^+Z \rightarrow W^+Z$	14	100	$7\sigma$	–	–

**Table 4:** Statistical significance of strong electroweak sector at LC and LHC, from [112].

The LHC results are taken from the ATLAS design report [118]. If an entry is blank it

means that the process is insensitive to the corresponding model or that the analysis has not been done. An electron beam with 90% left-handed polarization has been assumed. For both the LC and LHC results it was assumed that  $M_V = 1.5 \text{ TeV}$  and  $\Gamma_V = 0.33 \text{ TeV}$ .

For vector resonances a LC with  $\sqrt{s} = 500 \text{ GeV}$  and  $L = 80 \text{ fb}^{-1}$  has the same sensitivity as LHC.

At a LC with  $\sqrt{s} = 1500 \text{ GeV}$  the effects of a strong interacting sector becomes more relevant even if the  $WW$  channel is not resonant.

Notice however that systematic errors have largely been ignored both for the LHC and for the LC.

## 18 Conclusions

In this paper we have reviewed some theoretical aspects for a strong interacting electroweak sector and its phenomenological consequences. Different models of strong breaking, all based on the common assumption of a chiral symmetry breaking  $SU(2)_L \otimes SU(2)_R \rightarrow SU(2)_{L+R}$ , but with a different content of particles (Goldstones, spin one vector and axial-vector resonances, scalars) have been surveyed. These models are built using the effective lagrangian approach which makes use of the chiral symmetry and of an expansion in the energy. Bounds from already existing measurements have been taken into account by computing the effects beyond the SM on the corresponding observables. Since the Goldstone scattering amplitudes are at high energy equivalent to the corresponding scattering of longitudinal components of  $W$  and  $Z$  gauge bosons, the scattering of these gauge bosons at future colliders in principle can give access to the mechanism of electroweak symmetry breaking. In this review we have considered how future  $e^+e^-$  linear colliders can investigate this phenomenon. Different channels have been studied: the annihilation processes  $e^+e^- \rightarrow f^+f^-$  and  $e^+e^- \rightarrow W^+W^-$  are in particular relevant if a new vector resonance mixed with  $Z$  is present. These channels are already important at a LC of a center of mass energy of  $500 \text{ GeV}$  for a new resonance up to masses of the order of  $1 \text{ TeV}$ . In principle if LHC has already discovered such a new vector boson, one can tune the LC energy to study its properties and decays. Otherwise the LC can give bounds on its couplings and masses. The process  $e^+e^- \rightarrow W^+W^-$  is particularly relevant because, using the topology in which one  $W$  decays hadronically and the other leptonically, the angular distributions of the  $W$  can be measured and therefore the corresponding  $W$  polarization reconstructed. In this way one has access to  $W_L W_L$  scattering.

The fusion processes  $e^+e^- \rightarrow \bar{\nu}\nu W^+W^-$  and  $e^+e^- \rightarrow \bar{\nu}\nu ZZ$  can be used to study  $WW$  scattering also in absence of new resonances but, as we have seen, for this much higher energy (of the order  $1.5 \text{ TeV}$ ) and luminosity ( $200 \text{ fb}^{-1}$ ) would be required. One can reach a  $5.7 \sigma$  signal for LET amplitudes,  $12 \sigma$  for the CCS with  $M_S = 1 \text{ TeV}$  and  $\Gamma_S = 0.35 \text{ TeV}$ , and  $22 \sigma$  for the vector model with  $M_V = 1 \text{ TeV}$ ,  $\Gamma_V = 30 \text{ GeV}$ .

All these processes are suitable for neutral vector bosons. LHC is complementary because it is more efficient for the channel  $pp \rightarrow W^\pm, V^\pm \rightarrow W^\pm Z \rightarrow \mu\nu\mu^+\mu^-$  when the new vector resonance is strongly coupled to longitudinal  $W$ . LHC can discover new

charged vector resonances in a large region of the parameter space up to masses  $M_V = 1.5 - 2 \text{ TeV}$ . The neutral channel  $pp \rightarrow \gamma, Z, V \rightarrow W^+W^-$  suffers of background from  $t\bar{t}$  production, nevertheless the new neutral vector bosons can be studied at LHC by considering their lepton decay up to masses of the order  $1 \text{ TeV}$ .

In the case of the model with vector and axial-vector resonances degenerate in mass, LHC is sensitive to the new particles in the channels  $pp \rightarrow W^\pm, L^\pm \rightarrow \mu\nu$  and  $pp \rightarrow \gamma, Z, L_3, R_3 \rightarrow \mu^+\mu^-$  up to masses of the order  $2 \text{ TeV}$ . To be competitive with LHC one needs to consider a LC with a c.m. energy of the order  $1.5 \text{ TeV}$ .

Finally let us mention that the symmetry group can be larger than  $SU(2)_L \times SU(2)_R$  like in the one family technicolor model based on the chiral symmetry  $SU(8)_L \times SU(8)_R$  [6]. In this review we have not considered such models. These models have a rich particle spectrum with new pseudo-Goldstone bosons which in principle could be produced at future LC's. Their phenomenology has been for instance considered in [120, 121, 122, 123]. Furthermore we have not considered the  $\gamma\gamma$  and the  $e\gamma$  options of LC's (see for example [32, 33] for recent reviews).

## 19 Appendix

The most simple description of the symmetry breaking in the SM is obtained by considering a  $2 \times 2$  unitary matrix field  $U$ , satisfying  $U^\dagger U = 1$ . This field transforms as  $U \rightarrow g_L U g_R^\dagger$  under the group  $SU(2)_L \otimes SU(2)_R$  and describes the spontaneous breaking  $SU(2)_L \otimes SU(2)_R \rightarrow SU(2)_{L+R}$ . This corresponds to the infinite Higgs mass limit in the SM. In this non linear realization of the symmetry breaking no Higgs is left in the spectrum. Due to the condition  $U^\dagger U = 1$  the symmetry is non linearly realized.

We will therefore briefly review this technique of non linear group realization of a group  $G$  which breaks spontaneously to a subgroup  $H$  [40].

Let  $G$  be a compact, connected and semisimple Lie group of dimension  $n$  and  $H$  a subgroup. Let us denote by  $V_i$  ( $i = 1, \dots, n-d$ ) the generators of  $H$  and by  $A_l$  ( $l = 1, \dots, d$ ) the remaining generators. Every group element  $g \in G$  can be decomposed as

$$g = e^{\xi \cdot A} e^{u \cdot V} \quad (205)$$

where  $\xi \cdot A = \xi_l A_l$  and  $u \cdot V = u_i V_i$  and  $u$  and  $v$  are real parameters. For every element  $g_0 \in G$  one has

$$g_0 e^{\xi \cdot A} = e^{\xi' \cdot A} e^{u' \cdot V} \quad (206)$$

where  $\xi' = \xi'(\xi, g_0)$  and  $u' = u'(\xi, g_0)$ .

Let  $D$  denote a linear representation of the subgroup  $H$

$$h : \quad \psi \rightarrow D(h)\psi \quad (207)$$

then the transformation

$$g_0 : \quad \xi \rightarrow \xi', \quad \psi \rightarrow D(e^{u' \cdot V})\psi \quad (208)$$



gives a nonlinear realization of  $G$ . In fact if

$$g_1 e^{\xi' \cdot A} = e^{\xi'' \cdot A} e^{u'' \cdot V} \quad (209)$$

then

$$g_1 g_0 e^{\xi \cdot A} = e^{\xi'' \cdot A} e^{u''' \cdot V} \quad (210)$$

with

$$e^{u''' \cdot V} = e^{u'' \cdot V} e^{u' \cdot V} \quad (211)$$

Since  $D$  is a representation

$$D(e^{u''' \cdot V}) = D(e^{u'' \cdot V}) D(e^{u' \cdot V}) \quad (212)$$

If  $g_0 = h \in H$  then

$$e^{\xi \cdot A} \rightarrow h e^{\xi \cdot A} h^{-1}, \quad \psi \rightarrow D(h) \psi \quad (213)$$

and the symmetry is linearly realized.

There is a special case in which the transformation on  $\xi$  can be simplified. This is the case in which the group has a parity like transformation  $P : g \rightarrow P(g)$  such that

$$V \rightarrow V, \quad A \rightarrow -A \quad (214)$$

Applying this operation to eq. (206) one gets

$$P(g_0) e^{-\xi \cdot A} = e^{-\xi' \cdot A} e^{u' \cdot V} \quad (215)$$

and combining eqs. (206) and (215),

$$g_0 e^{2\xi \cdot A} P(g_0^{-1}) = e^{2\xi' \cdot A} \quad (216)$$

One can easily verify in this form that the transformation on  $\xi$  is a realization of the group which becomes linear when restricted to the subgroup.

In the case we are interested,  $G = SU(2)_L \otimes SU(2)_R$

$$g = \begin{pmatrix} L & 0 \\ 0 & R \end{pmatrix} \quad (217)$$

with  $L(R) \in SU(2)_{L(R)}$ . Furthermore

$$V^i = T_L^i + T_R^i = i \begin{pmatrix} \frac{\tau^i}{2} & 0 \\ 0 & \frac{\tau^i}{2} \end{pmatrix}, \quad A^i = T_L^i - T_R^i = i \begin{pmatrix} \frac{\tau^i}{2} & 0 \\ 0 & -\frac{\tau^i}{2} \end{pmatrix} \quad (218)$$

A parity transformation  $P$  exists,  $P : L \rightarrow R$ , and using eq. (216) one has the following transformation properties

$$\begin{pmatrix} \exp(i\xi^i \tau^i) & 0 \\ 0 & \exp(-i\xi^i \tau^i) \end{pmatrix} \rightarrow \begin{pmatrix} L & 0 \\ 0 & R \end{pmatrix} \begin{pmatrix} \exp(i\xi^i \tau^i) & 0 \\ 0 & \exp(-i\xi^i \tau^i) \end{pmatrix} \begin{pmatrix} R^\dagger & 0 \\ 0 & L^\dagger \end{pmatrix} \quad (219)$$

Therefore one can construct the Lagrangian using the field  $\exp(i\xi \cdot \tau)$  or introducing the usual normalization  $U(x) = \exp(i\pi^a(x)\tau^a/v)$ , transforming under  $G$  as  $(2, 2)$  or  $U \rightarrow g_L U g_R^\dagger$ ,  $g_{L(R)} \in SU(2)_{L(R)}$ .

## Acknowledgments

I would like to thank R.Casalbuoni, P.Chiappetta, A.Deandrea, S.De Curtis, F.Feruglio, R.Gatto and M.Grazzini for the fruitful and enjoyable collaboration on the topics covered here. I am grateful to R.Casalbuoni, S.De Curtis and R.Gatto for a critical reading of the manuscript.

This work is part of the EEC project “Test of electroweak symmetry breaking and future european colliders”, CHRXCT94/0579.

## References

- [1] Altarelli G., hep-ph/9710434, to be published on the *Proceedings of XVIII International Symposium on Lepton-Photon Interactions*, Hamburg, 1997.
- [2] Lüscher M. and Weisz P., *Nucl. Phys. B*, **318** (1989) 705;  
Kuti J., Lin L. and Shen Y., *Phys. Rev. Lett.*, **61** (1988) 678;  
Hasenfratz A., Jansen K., Lang C.B., Neuhaus T. and Yoneyama H., *Nucl. Phys. B*, **317** (1989) 81;  
Heller U.M., Neuberger H. and Vranas P., *Nucl. Phys. B*, **399** (1993) 271.
- [3] Lee B.W., Quigg C. and Thacker H.B., *Phys. Rev. D*, **16** (1977) 1519; *Phys. Rev. Lett.*, **16** (1977) 883;  
see also Dicus D. and Mathur V., *Phys. Rev. D*, **7** (1973) 3111.
- [4] Cabibbo N., Maiani L., Parisi G. and Petronzio R., *Nucl. Phys. B*, **158** (1979) 295;  
Sher M., *Phys. Rev.*, **179** (1989) 273;  
Maiani L., Parisi G. and Petronzio R., *Nucl. Phys. B*, **136** (1978) 115;  
Lindner M., *Z. Phys. C*, **31** (1986) 295;  
Lindner M., Sher M. and Zaglauer H., *Phys. Lett.*, **228** (1989) 139.
- [5] Weinberg S., *Phys. Rev. D*, **13** (1976) 974; **19** (1979) 1277;  
Susskind L., *Phys. Rev. D*, **20** (1979) 2619.
- [6] for a review see Farhi E. and Susskind L., *Phys. Rep.*, **74** (1981) 277.
- [7] Orava R., Eerola P., and Nordberg M., eds. *Physics and Experiments with Linear Colliders*, (World Scientific, Singapore, 1992).
- [8] Harris F.A., Olsen S.L., Pakvasa S. and Tata X., eds. *Physics and Experiments with Linear  $e^+e^-$  Colliders*, (World Scientific, Singapore, 1993).
- [9] Miyamoto A. and Fujii Y., eds. *Physics and Experiments with Linear Colliders*, (World Scientific, Singapore, 1996).
- [10] Zerwas P.M., ed.  *$e^+e^-$  Collisions at 500 GeV: The Physics Potential*, vols. A, B, DESY report DESY-92-123 (1992).
- [11] Zerwas P.M., ed.  *$e^+e^-$  Collisions at 500 GeV: The Physics Potential*, vol. C, DESY report DESY-93-123C (1993).
- [12] Zerwas P.M., ed.  *$e^+e^-$  Collisions at 500 GeV: The Physics Potential*, vol. D, DESY report DESY-96-123D (1996).
- [13] Barklow T.L., Haber H.E., Dawson S., and Siegrist J.L., eds. *Electroweak Symmetry Breaking and New Physics at the TeV Scale*, (World Scientific, Singapore, 1996).

- [14] Accomando E. et al., *ECFA/DESY LC Physics Working Group*. DESY-97-100, May 1997, hep-ph/9705442.
- [15] Dimopoulos S. and Susskind L., *Nucl. Phys. B*, **155** (1979) 237;  
Eichten E. and Lane K., *Phys. Lett. B*, **90** (1980) 125.
- [16] Holdom B., *Phys. Rev. D*, **24** (1981) 1441; *Phys. Lett. B*, **150** (1985) 301;  
Yamawaki K., Bando Y. and Matumoto K., *Phys. Rev. Lett.*, **56** (1986) 1335;  
Appelquist T., Karabali D. and Wijewardhana L.C.R., *Phys. Rev. Lett.*, **57** (1986) 957.
- [17] Hill C.T., *Phys. Lett. B*, **345** (1995) 483.
- [18] Chivukula R.S., Simmons E.H. and Terning J., *Phys. Lett. B*, **331** (1994) 383; *Phys. Rev. D*, **53** (1996) 5258.
- [19] Cornwall J.M., Levin D.N. and Tiktopoulos G., *Phys. Rev. D*, **10** (1974) 1145;  
Vayonakis C.G., *Lett. Nuovo Cimento*, **17** (1976) 17;  
Chanowitz M.S. and Gaillard M.K., *Nucl. Phys. B*, **261** (1985) 379;  
Gounaris G.J., K gerler R. and Neufeld H., *Phys. Rev. D*, **34** (1986) 3257;  
Yao Y. and Yuan C.-P., *Phys. Rev. D*, **38** (1988) 2237;  
Bagger J. and Schmidt C.R., *Phys. Rev. D*, **41** (1990) 264;  
Veltman H., *Phys. Rev. D*, **41** (1990) 2294;  
He H.J., Kuang Y.P. and Li X., *Phys. Rev. Lett.*, **69** (1992) 2619; *Phys. Lett. B*, **329** 278 (1994).
- [20] Veltman M., *Acta Phys. Pol. B*, **8** (1977) 475; *Phys. Lett. B*, **70** (1977) 253; *Phys. Lett. B*, **139** (1984) 307.
- [21] Appelquist T. and Bernard C., *Phys. Rev. D*, **22** 200 (1980);
- [22] Longhitano A.C., *Phys. Rev. D*, **22** 1166 (1980); *Nucl. Phys. B*, **188** 118 (1981).
- [23] Chadha S. and Peskin M.E., *Nucl. Phys. B*, **185** (1981) 61;  
Renken R. and Peskin M.E., *Nucl. Phys. B*, **211** (1983) 93.
- [24] Einhorn M.B., *Nucl. Phys. B*, **246** 75 (1984).
- [25] Casalbuoni R., Dominici D. and Gatto R., *Phys. Lett. B*, **147** 460 (1984).
- [26] Casalbuoni R., De Curtis S., Dominici D. and Gatto R., *Phys. Lett. B*, **155** (1985) 95; *Nucl. Phys. B*, **282** (1987) 235.
- [27] Bando M., Kugo T. and Yamawaki K., *Phys. Rep.*, 164 (1988) 217.
- [28] Balachandran A.P., Stern A. and Trahern G., *Phys. Rev. D*, **19** (1979) 2416.
- [29] Weinberg S., *Phys. Rev.*, **166** (1968) 1568.

- [30] Casalbuoni R., De Curtis S., Dominici D., Feruglio F. and Gatto R., *Int. Jour. Mod. Phys. A*, **4** (1989) 1065.
- [31] Chivukula R.S., Rosenfeld R., Simmons E.H. and Terning J., in [13].
- [32] Golden M., Han T. and Valencia G., in [13].
- [33] Jikia G., Talk given at *International Conference on the Structure and the Interactions of the Photon (Photon 97)* including the *11th International Workshop on Photon-Photon Collisions*, Egmond aan Zee, Netherlands, May 10-15, 1997; hep-ph/9706508, FREIBURG-THEP-97-11, May 1997.
- [34] Weinberg S., *Physica A*, **96** (1979) 327.
- [35] Georgi H., *Weak Interactions and Modern Particle Theory*, The Benjamin/Cummings Pub. Company, Inc., Menlo Park, CA, 1984;  
Manohar A. and Georgi H., *Nucl. Phys. B*, **234** (1984) 189.
- [36] Gasser J. and Leutwyler H., *Ann. Phys. (NY)*, **158** (1984) 142; *Nucl. Phys. B*, **250** (1985) 465.
- [37] Gomis J. and Weinberg S., *Nucl. Phys. B* **469** (1996) 475.
- [38] Dobado A. and Herrero M., *Phys. Lett. B*, **228** (1989) 228;  
Donoghue J. and Ramirez J., *Phys. Lett. B*, **234** (1990) 361;  
Dobado A., Herrero M.J. and Terron J., *Z. Phys. C*, **50**, (1991) 205; *ibidem*, (1991) 465;  
Golden M. and Randall L., *Nucl. Phys. B*, **361** (1991) 3;  
Holdom B. and Terning J., *Phys. Lett. B*, **247** (1990) 88;  
Bagger J., Dawson S. and Valencia G., *Nucl. Phys. B* **399**, (1993) 364.
- [39] Weinstein M., *Phys. Rev. D*, **8** (1973) 2511  
Sikivie P., Susskind L., Voloshin M. and Zakharov V., *Nucl. Phys. B*, **173** (1980) 189.
- [40] Coleman S., Wess J. and Zumino B., *Phys. Rev.*, **177** (1969) 2239;  
Callan C.G., Coleman S., Wess J. and Zumino B., *Phys. Rev.*, **177** (1969) 2247.
- [41] Gupta S.N., *Quantum Electrodynamics*, (Gordon and Breach, New York, 1981).
- [42] Cheyette O. and Gaillard M.K., *Phys. Lett. B*, **197** (1987) 205.
- [43] Basdevant J.L., *Fortsch. Phys.*, **20** (1972) 283.
- [44] Dobado A., Herrero M.J. and Truong T.N., *Phys. Lett. B*, **235** (1990) 129.
- [45] Hikasa K., in [7], p. 451;  
Hikasa K. and Igi K., *Phys. Rev. D*, **48** 3055 (1993).

- [46] Altarelli G., hep-ph/9611239, CERN-TH/96-265; for a recent update of the values of the  $\epsilon$  parameters see Altarelli G., in [1].
- [47] Chanowitz M., Golden M. and Georgi H., *Phys. Rev. Lett.*, **57** 2344 (1986); *Phys. Rev. D*, **36** 1490 (1987).
- [48] Feruglio F., *Int. J. Mod. Phys. A*, **8** (1993) 4937.
- [49] Wudka J., *Int. J. Mod. Phys. A*, **9** (1994) 2301.
- [50] Appelquist T. and Wu G.-H., *Phys. Rev. D*, **48** (1993) 3235.
- [51] Altarelli G. and Barbieri R., *Phys. Lett. B*, **253** (1991) 161;  
Altarelli G., Barbieri R. and Jadach S., *Nucl. Phys. B*, **369** (1992) 3;  
Altarelli G., Barbieri R. and Caravaglios F., *Nucl. Phys. B*, **405** (1993) 3.
- [52] Barbieri R., Caravaglios F. and Frigeni M., *Phys. Lett. B*, **279** (1992) 169.
- [53] Peskin M.E. and Takeuchi T., *Phys. Rev. Lett.*, **65** (1990) 964 and *Phys. Rev. D*, **46** (1991) 381.
- [54] Alam S., Dawson S. and Szalapski R., KEK-TH 519, KEL preprint 97-88, BNL-HET-SD-97-003, hep-ph/9706542.
- [55] Bagger J., Barger V., Cheung K., Gunion J., Han T., Ladinsky G.A., Rosenfeld R. and Yuan C.-P., *Phys. Rev. D*, **49** (1994) 1246;  
Barger V., Cheung K., Gunion J., Han T., Ladinsky G.A., Rosenfeld R. and Yuan C.-P., *Phys. Rev. D*, **52** (1995) 3878.
- [56] Barger V., Cheung K., Han T. and Phillips R.J.N., *Phys. Rev. D*, **52** (1995) 3815.
- [57] Barger V., Berger M.S., Gunion J. and Han T., *Phys. Rev. D*, **55** (1997) 142.
- [58] D’Adda A., Di Vecchia P. and Lüscher M., *Nucl. Phys. B*, **146** (1978) 63; *Nucl. Phys. B*, **152** (1979) 125;  
Aref’eva I.Ya. and Azakov S.I., *Nucl. Phys. B*, **162** (1980) 298.
- [59] Bando M., Taniguchi Y. and Tanimura S., *Progr. Theor. Phys.*, **97** (1997) 665.
- [60] Casalbuoni R., Chiappetta P., Deandrea A., De Curtis S., Dominici D., and Gatto R., *Z.Physik C*, **60** (1993) 315.
- [61] Bagger J., Han T. and Rosenfeld R., in *1990 DPF Summer Study on High Energy Physics: Research Directions for the Decade*, p.208, ed. Berger E.L. (World Scientific, Singapore, 1992); see also Casalbuoni R., De Curtis S., Deandrea A., Dominici D., Gatto R. and Gunion J.F., hep-ph/9801243.
- [62] Casalbuoni R., De Curtis S., Dominici D., Feruglio F. and Gatto R., *Phys. Lett. B*, **258** (1991) 161.

- [63] Anichini L., Casalbuoni R. and De Curtis S., *Phys. Lett. B*, **348** (1995) 521.
- [64] Casalbuoni R., Deandrea A., De Curtis S., Dominici D., Feruglio F., Gatto R. and Grazzini M., *Phys. Lett. B*, **349** (1995) 533;  
Casalbuoni R., Deandrea A., De Curtis S., Dominici D., Gatto R. and Grazzini M., *Phys. Rev. D*, **53**, 5201 (1996).
- [65] Georgi H., *Nucl. Phys. B*, **331** (1990) 311.
- [66] Casalbuoni R., Deandrea A., De Curtis S., Di Bartolomeo N., Dominici D., Feruglio F. and Gatto R., *Nucl. Phys. B*, **409** (1993) 257.
- [67] Casalbuoni R., De Curtis S., Dominici D., Feruglio F. and Gatto R., *Phys. Lett. B*, **269** (1991) 361.
- [68] Casalbuoni R., De Curtis S. and Dominici D., *Phys. Lett. B*, **403** (1997) 86.
- [69] Han T., Huang Z. and Hung P.Q., *Mod. Phys. Lett. A*, **11** (1996) 1131.
- [70] Gilman F. and Harari H., *Phys. Rev.*, **165** (1968) 1803.
- [71] Weinberg S., *Phys. Rev.*, **177** (1969) 2604.
- [72] Weinberg S., *Phys. Rev. Lett.*, **65** (1990) 1177.
- [73] *Conceptual Design of a 500 GeV  $e^+e^-$  Linear Collider with Integrated X-ray Laser Facility*, eds. Brinkmann R., Materlik G., Rossbach J. and Wagner A., DESY 1997-048 ECFA 1997-182.
- [74] Loew G. et al, *International Linear Collider Technical Review Committee Report 1995*, SLAC-303 (1996).
- [75] Murayama H. and Peskin M.E., *Ann. Rev. Nucl. Part. Sci.*, **46** (1996) 533.
- [76] *The Compact Linear Collider Study*,  
<http://www.cern.ch/CERN/Divisions/PS/CLIC/Welcome.html>.
- [77] Djouadi A., Leike A., Riemann T., Schaile D. and Verzegnassi C., *Z. Phys. C*, **56** 289 (1992).
- [78] Layssac J., Renard F.M. and Verzegnassi C., *Phys. Rev. D*, **48** (1993) 4037; **49** (1994) R2143;  
Chivukula R.S., Renard F.M. and Verzegnassi C., PM/97-27, hep-ph/9708351.
- [79] Fujii K., talk presented at *2nd KEK Topical Conf. on  $e^+e^-$  Collision Physics*, Tsukuba, Japan, Nov 26 - 29, 1991; published in KEK  $e^+e^-$  1991, p.469.
- [80] Miyamoto A., in [8], p.141.

- [81] Peskin M.E. and Schoeder D.V., *An Introduction to Quantum Field Theory*, (Addison-Wesley, Reading, 1995).
- [82] Chiappetta P. and Feruglio F., *Phys. Lett. B*, **213** (1988) 95.
- [83] Layssac J., Moulataka G. and Renard F.M., *Int. J. Mod. Phys. A*, **8** (1993) 3285.
- [84] Casalbuoni R., De Curtis S., Dominici D., Feruglio F. and Gatto R., in [10], p. 513.
- [85] Djouadi A., Leike A., Riemann T., Schaile D. and Verzegnassi C., in [10], p. 491.
- [86] Iddir F., Le Yaouanc A., Oliver L., Pène O. and Raynal J.-C., *Phys. Rev. D*, **41** (1990) 22.
- [87] Frank M., Mättig P., Settles R. and Zeuner W., in [10], p. 223.
- [88] Barklow T.L., in [7], p. 423;  
 Barklow T.L., in *Proceedings of the 8th Meeting of Division of Particles and Fields of the APS*, Albuquerque, New Mexico, August 2-6, 1994, p.1236;  
 Barklow T.L., in [9], p. 105.
- [89] Bernrheuter W. and Schröder T., *Z. Phys. C*, **62** (1994) 615.
- [90] Giudice G.F. et al, HEP-9602207, Feb 1996, hep-ph/9602207, in *Proceedings of the CERN Workshop on LEP II Physics*, eds. G.Altarelli et al, CERN 96-01 Vol.1 (1996).
- [91] Peskin M.E., in Seiden A., *Physics in Collision 4*, (Edition Frontières, Paris), 1984.
- [92] Miyamoto A., Hikasa K. and Izubuchi T., *Proceedings of  $e^+e^-$ ,  $e^-\gamma$  and  $\gamma\gamma$  collisions at linear accelerators*, INS-J-181, May 1985, p.272.
- [93] Hagiwara K., Peccei R.D., Zeppenfeld D. and Hikasa K., *Nucl.Phys. B*, **282** (1987) 253.
- [94] Gounaris G., Kneur J.L., Layssac J., Moulataka G., Renard F.M. and Schildknecht D., in [10], vol. B, p. 735.
- [95] Boudjema F., in [8] p.712, in [11] p.177.
- [96] Abe F. et al, *Phys. Rev. Lett.*, **74** (1995) 1936; *ibidem*, **75** (1995) 1018.
- [97] Abachi S. et al, *Phys. Rev. Lett.*, **75** (1995) 1034; *ibidem*, **75** (1995) 1024.
- [98] Ajaltouni Z., in *Proceedings of the CERN Workshop on LEP II Physics*, eds. G.Altarelli et al, CERN 96-01 Vol.1 p.525 (1996).
- [99] Barklow T.L., in [7] p.423.



- [100] Bilenky M., Schildknecht D., Kneur J.-L. and Renard F.M., in [11], p. 187.
- [101] Bélanger G. and Boudjema F., in [11] p.207;  
Baillargeon M. et al, in [12], p. 255.
- [102] Andreev V.V., Pankov A.A. and Paver N., *Phys. Rev. D*, **53** (1996) 2390.
- [103] Casalbuoni R., De Curtis S. and Guetta D., *Phys. Rev. D*, **55** (1997) 4203;
- [104] Barklow T.L. et al, to appear in *Proceedings of the 1996 DPF/DPB Summer Study on New Directions for High Energy Physics*, Snowmass, Colorado, Jun. 25 - Jul. 12, 1996, hep-ph/9611454, MADPH-96-975, SLAC-PUB-7366, UB-HET-96-05, UM-HE-96-26.
- [105] Gunion J.F. and Tofighi-Niaki A., *Phys. Rev. D*, **36** (1987) 2671; *ibid* **38** (1988) 1433.
- [106] Hagiwara K., Kanzaki J. and Murayama H., DTP-91-18, Mar 1991.
- [107] Kurihara Y. and Najima R., *Phys. Lett. B*, **301** (1993) 292.
- [108] Casalbuoni R., De Curtis S., Chiappetta P., Dominici D., Deandrea A. and Gatto R., in [8] p.887.
- [109] Casalbuoni R., Chiappetta P., De Curtis S., Dominici D. and Gatto R., in [11], p. 367.
- [110] Kilian W., DESY preprint, hep-ph/9609334;  
Boos E., He H.-J., Kilian W., Pukhov A., Yuan C.-P. and Zerwas P.M., *Phys. Rev. D*, **57** (1997) 1553.
- [111] Peskin M.E., Lectures given at *22nd INS International Symposium on Physics with High Energy Colliders*, Tokyo, Japan, 8-10 Mar 1994, p. 439.
- [112] Kuhlman S. et al, *Physics and Technology of the Next Linear Collider*, BNL52-502, A Report Submitted to Snowmass 96 by the NLC-zeroth Order Design Group and the NLC Working Group.
- [113] Barklow T.L. et al, SLAC-PUB-7397, CLNS 97/1473, hep-ph/9704217, Working Group Summary Report to be published on *Proceedings of the 1996 DPF/DPB Summer Study on New Directions for High Energy Physics*, Snowmass, Colorado, Jun. 25 - Jul. 12, 1996.
- [114] Pelaez J.R., to be published on *Proceedings of the 1996 DPF/DPB Summer Study on New Directions for High Energy Physics*, Snowmass, Colorado, Jun. 25 - Jul. 12, 1996;  
Dobado A., Herrero M.J., Pelaez J.R., Ruiz Morales E. and Urdiales M.T., *Phys. Lett. B* **352** (1995) 400.

- [115] CMS Collaboration, CERN report CERN/LHCC/94-38.
- [116] Casalbuoni R., Deandrea A., De Curtis S., Dominici D. and Gatto R., UGVA-DPT-1997-08-986, to be published on the *Proceedings Joint ECFA / DESY Study: Physics and Detectors for a Linear Collider*, Hamburg, Germany, Nov. 20-22, 1996, hep-ph/9708287.
- [117] Casalbuoni R., Chiappetta P., De Curtis S., Feruglio F., Gatto R., Mele B. and Terron J., *Phys. Lett. B*, **249**, 130 (1990);  
 Dobado A., Herrero M.J. and Terron J., *Z. Phys. C*, **50**, 205 (1991); *ibidem* 465 (1991);  
 De Curtis S., in *Proceedings of the XI Symposium on Hadron Collider Physics*, eds. Bisello D., Busetto G. and Stanco L., (World Scientific, Singapore, 1997), p. 334.
- [118] ATLAS Collaboration, CERN report CERN/LHCC/94-43.
- [119] Casalbuoni R., Chiappetta P., Cousinou M.C., De Curtis S., Feruglio F. and Gatto R., *Phys. Lett. B*, **253** (1991) 275, and in *Proceedings of Large Hadron Collider Workshop*, eds. Jarlskog G. and Rein D., p.731.
- [120] Casalbuoni R., Chiappetta P., Deandrea A., De Curtis S., Dominici D. and Gatto R., *Z. Phys. C*, **65** (1995) 327.
- [121] Lubicz V. and Santorelli P., *Nucl. Phys. B*, **460** (1996) 3.
- [122] Cleza Montalvo J.E. and Eboli O.J.P., *Phys. Rev. D*, **47** (1993) 1889.
- [123] Rückl R., Settles R. and Spiesberger H., in *DESY-ECFA Conceptual LC Design Report*.